Developed at the request of:

Department of Energy & Climate Change

Research conducted by:

Met Office Hadley Centre

The University of Nottingham
UNITED KINGDOM · CHINA · MALAYSIA

Walker Institute

Centre for Ecology & Hydrology
Natural Environment Research Council

University of Leeds

Tyndall Centre for Climate Change Research

Climate: Observations, projections and impacts

Kenya

We have reached a critical year in our response to climate change. The decisions that we made in Cancún put the UNFCCC process back on track, saw us agree to limit temperature rise to 2 °C and set us in the right direction for reaching a climate change deal to achieve this. However, we still have considerable work to do and I believe that key economies and major emitters have a leadership role in ensuring a successful outcome in Durban and beyond.

To help us articulate a meaningful response to climate change, I believe that it is important to have a robust scientific assessment of the likely impacts on individual countries across the globe. This report demonstrates that the risks of a changing climate are wide-ranging and that no country will be left untouched by climate change.

I thank the UK's Met Office Hadley Centre for their hard work in putting together such a comprehensive piece of work. I also thank the scientists and officials from the countries included in this project for their interest and valuable advice in putting it together. I hope this report will inform this key debate on one of the greatest threats to humanity.

The Rt Hon. Chris Huhne MP, Secretary of State for Energy and Climate Change

There is already strong scientific evidence that the climate has changed and will continue to change in future in response to human activities. Across the world, this is already being felt as changes to the local weather that people experience every day.

Our ability to provide useful information to help everyone understand how their environment has changed, and plan for future, is improving all the time. But there is still a long way to go. These reports – led by the Met Office Hadley Centre in collaboration with many institutes and scientists around the world – aim to provide useful, up to date and impartial information, based on the best climate science now available. This new scientific material will also contribute to the next assessment from the Intergovernmental Panel on Climate Change.

However, we must also remember that while we can provide a lot of useful information, a great many uncertainties remain. That's why I have put in place a long-term strategy at the Met Office to work ever more closely with scientists across the world. Together, we'll look for ways to combine more and better observations of the real world with improved computer models of the weather and climate; which, over time, will lead to even more detailed and confident advice being issued.

Julia Slingo, Met Office Chief Scientist

Introduction

Understanding the potential impacts of climate change is essential for informing both adaptation strategies and actions to avoid dangerous levels of climate change. A range of valuable national studies have been carried out and published, and the Intergovernmental Panel on Climate Change (IPCC) has collated and reported impacts at the global and regional scales. But assessing the impacts is scientifically challenging and has, until now, been fragmented. To date, only a limited amount of information about past climate change and its future impacts has been available at national level, while approaches to the science itself have varied between countries.

In April 2011, the Met Office Hadley Centre was asked by the United Kingdom's Secretary of State for Energy and Climate Change to compile scientifically robust and impartial information on the physical impacts of climate change for more than 20 countries. This was done using a consistent set of scenarios and as a pilot to a more comprehensive study of climate impacts. A report on the observations, projections and impacts of climate change has been prepared for each country. These provide up to date science on how the climate has already changed and the potential consequences of future changes. These reports complement those published by the IPCC as well as the more detailed climate change and impact studies published nationally.

Each report contains:

- A description of key features of national weather and climate, including an analysis of new data on extreme events.
- An assessment of the extent to which increases in greenhouse gases and aerosols in the atmosphere have altered the probability of particular seasonal temperatures compared to pre-industrial times, using a technique called 'fraction of attributable risk.'
- A prediction of future climate conditions, based on the climate model projections used in the Fourth Assessment Report from the IPCC.
- The potential impacts of climate change, based on results from the UK's Avoiding Dangerous Climate Change programme (AVOID) and supporting literature. For details visit: http://www.avoid.uk.net

The assessment of impacts at the national level, both for the AVOID programme results and the cited supporting literature, were mostly based on global studies. This was to ensure consistency, whilst recognising that this might not always provide enough focus on impacts of most relevance to a particular country. Although time available for the project was short, generally all the material available to the researchers in the project was used, unless there were good scientific reasons for not doing so. For example, some impacts areas were omitted, such as many of those associated with human health. In this case, these impacts are strongly dependant on local factors and do not easily lend themselves to the globally consistent framework used. No attempt was made to include the effect of future adaptation actions in the assessment of potential impacts. Typically, some, but not all, of the impacts are avoided by limiting global average warming to no more than 2 °C.

The Met Office Hadley Centre gratefully acknowledges the input that organisations and individuals from these countries have contributed to this study. Many nations contributed references to the literature analysis component of the project and helped to review earlier versions of these reports.

We welcome feedback and expect these reports to evolve over time. For the latest version of this report, details of how to reference it, and to provide feedback to the project team, please see the website at www.metoffice.gov.uk/climate-change/policy-relevant/obs-projections-impacts

In the longer term, we would welcome the opportunity to explore with other countries and organisations options for taking forward assessments of national level climate change impacts through international cooperation.

Summary

Climate observations

- Widespread warming has been observed over Kenya since 1960.
- There is little precipitation data available for Kenya but there is some limited evidence for decreasing precipitation between 1960 and 2003, the period for which some data is available.

Climate change projections

- For the A1B emissions scenario projections for temperature increases over Kenya, of up to around 3°C, show good agreement between the CMIP3 ensemble members.
- The CMIP3 model ensemble projects strong precipitation increases over East Africa, in particular Kenya, with increases of over 20% projected with strong agreement across the CMIP3 models.

Climate change impacts projections

Crop yields

- The majority of global- and regional-scale studies included here generally project yield declines with climate change for the country's most important staple crops; maize and beans.
- National-scale studies highlight the importance of water storage in ameliorating and managing the impact of future climate change on the country's crops.

Food security

- Kenya is currently a country of moderately high levels of undernourishment. Several global-scale studies project that Kenya could face increasingly serious food security issues over the next 40 years.

Water stress and drought

- Recent analysis of Kenya's current water resources has shown it is exposed to a high water security threat across its entire area.
- Future water availability is uncertain, with potential increases in annual run-off masking overall reductions in water availability during certain periods, while studies neglect the lack of infrastructure to store water.
- Large uncertainties remain in global-, regional- and national-scale projections of future water stress and drought for the country, and as such, knowledge is little improved beyond that reported in the IPCC AR4.
- Simulations from the AVOID programme project that climate change generally has a minor impact on water stress beyond 2030 in Kenya, and that some parts of the country may experience a decrease with climate change from 2050 onward.

Pluvial flooding and rainfall

- The IPCC AR4 noted potential increases in mean precipitation across East Africa, especially in summer.
- Some recent work has contradicted this, suggesting the potential for decreased summer rainfall over Kenya in the future.

Fluvial flooding

- A number of global-scale and catchment-scale assessments are consistent in indicating that flood magnitudes in Kenya could increase with climate change.
- Simulations by the AVOID programme support this, with a large majority of the models showing a tendency for (sometimes very large) increases in flood risk, particularly later in the century and in the A1B scenario.

Tropical cyclones

- Kenya is occasionally affected by tropical cyclones moving westward from the Indian Ocean. There is considerable uncertainty in projections of overall Indian Ocean cyclone frequency and intensity.

- Furthermore, there is large uncertainty in projections of the tracks of these cyclones toward a particular country.

- Uncertainty in projections means that it is not possible to robustly state whether cyclone damages in Kenya may increase or decrease with climate change.

Coastal regions

- A recent study provides new knowledge relative to the IPCC AR4, for coastal impacts in Kenya. A 10% intensification of the current 1-in-100-year storm surge combined with a 1m Sea Level Rise (SLR) could affect around 42% of coastal total land, 22% of coastal agricultural land, 32% of coastal GDP, and 39% of coastal urban areas.

- Research presented in the first national communication of Kenya to the Conference of the Parties to the United Nations Framework Convention on Climate Change (UNFCC) also suggests that Kenya is highly vulnerable to SLR, and that impacts could be severe, especially in the Mombasa district.

Table of Contents

Chapter 1 – Climate Observations

Rationale

Figure 1. *Location of boxes for the regional average time series (red dashed box) in Figures 3 and 4.*

Present day weather and climate play a fundamental role in the day to day running of society. Seasonal phenomena may be advantageous and depended upon for sectors such as farming or tourism. Other events, especially extreme ones, can sometimes have serious negative impacts posing risks to life and infrastructure and significant cost to the economy. Understanding the frequency and magnitude of these phenomena, when they pose risks or when they can be advantageous and for which sectors of society, can significantly improve societal resilience. In a changing climate it is highly valuable to understand possible future changes in both potentially hazardous events and those reoccurring seasonal events that are depended upon by sectors such as agriculture and tourism. However, in order to put potential future changes in context, the present day must first be well understood both in terms of common seasonal phenomena and extremes.

The purpose of this chapter is to summarise the weather and climate from 1960 to present day. This begins with a general climate overview including an up to date analysis of changes in surface mean temperature. These changes may be the result of a number of factors including climate change, natural variability and changes in land use. There is then a focus on extremes of temperature and precipitation selected from 2000 onwards, reported in the World Meteorological Organization (WMO) Annual Statement on the Status of the Global Climate and/or the Bulletin of the American Meteorological Society (BAMS) State of the Climate reports. This is followed by a discussion of changes in moderate extremes from 1960 onwards using the HadEX extremes database (Alexander et al. 2006) which categorises extremes of temperature and precipitation. These are core climate variables which have received significant effort from the climate research community in terms of data acquisition and processing and for which it is possible to produce long high quality records for monitoring. The work presented here is the foundation of future plans to systematically address the region's present and projected future weather and climate, and the associated impacts.

The methodology section that follows provides details of the data shown here and of the scientific analyses underlying the discussions of changes in the mean temperature and in temperature and precipitation extremes.

Climate overview

Kenya is an equatorial country in East Africa which lies between 5°N and 5°S. It has a very diverse relief with a short, low coastal plain on the Indian Ocean shore, extensive inland plateaux regions between 1000m and 1500m, and several mountain ranges and peaks such as Mount Kenya, which rises to 5200m and has a permanent snow-cap.

Because of the reduction of temperature with altitude, temperatures over much of Kenya are subtropical or temperate. The equatorial situation means that there is a very limited annual variation in temperature. Nairobi, in the southern inland highlands at 1800m altitude, has an annual mean temperature of 18°C, with a peak of 19°C in March and a low of 15°C in July. Kisuma, near the shores of Lake Victoria in the west at 1350m altitude, has an annual mean temperature of 26°C. Only the coastal lowlands experience the constant high temperatures and humidity associated with equatorial latitudes, although daytime sea breezes have a cooling effect. Mombasa has an annual mean temperature of 26°C. The northern part of Kenya is also hot throughout the year, but with lower humidity; Lodwar in the north-west has an annual mean temperature of 29°C.

The inter-tropical convergence zone (ITCZ) crosses rather quickly in April and October, with southerly winds blowing towards it from May to September and northerly winds from November to March. Hence, moisture from the sea remains near the coastline and elsewhere, winds usually have a long land track, reducing rainfall. However, Lake Victoria, a huge ‘inland sea’ on the western border, provides a source of moisture for local increase in rainfall and overnight thunderstorms. Kisumu has average annual rainfall of 1390 mm. Most areas of Kenya have a double rainy season between March and May and October to December as the ITCZ passes over, with two intervening dry seasons. The annual average rainfall at Nairobi is 1020 mm and at Mombasa 1060 mm. Although both of these have the double rainy season, the most rainfall is provided by the March to May period (this is also true of Kisumu). Northern Kenya has an arid climate with very low rainfall. Average annual amounts are generally below 500 mm, and in some places below 200 mm. Lodwar, for example, receives only 190 mm on average, with March to May again the wettest months.

Inter-annual variability of rainfall has a major impact in Kenya. Flooding can be caused by heavy rains in the rainy seasons. The failure of rains to arrive leads to periods of severe drought, especially in the arid and semi-arid regions of northern and eastern Kenya.

Analysis of long-term features in the mean temperature

CRUTEM3 data (Brohan et al., 2006) have been used to provide an analysis of mean temperatures from 1960 to 2010 over Kenya using the median of pairwise slopes method to fit the trend (Sen, 1968; Lanzante, 1996). The methods are fully described in the methodology section. In agreement with increasing global average temperatures (Sánchez-Lugo et al. 2011), there is a warming signal for temperature as shown in Figure 2. For the southern region confidence in the warming signal is higher in that the 5^{th} to 95^{th} percentiles of the slopes are of the same sign. The signal is similar for both the cooler months (June to August) and hotter months (December to January). Regionally averaged trends (over grid boxes included in the red dashed box in Figure 1) show warming with higher confidence. For the hotter months (DJF) the trend is 0.29 ^{o}C per decade (5^{th} to 95^{th} percentile of slopes: 0.19 to 0.38 ^{o}C per decade) and for the cooler months (JJA) the trend is 0.25 ^{o}C per decade (5^{th} to 95^{th} percentile of slopes: 0.19 to 0.32 ^{o}C per decade).

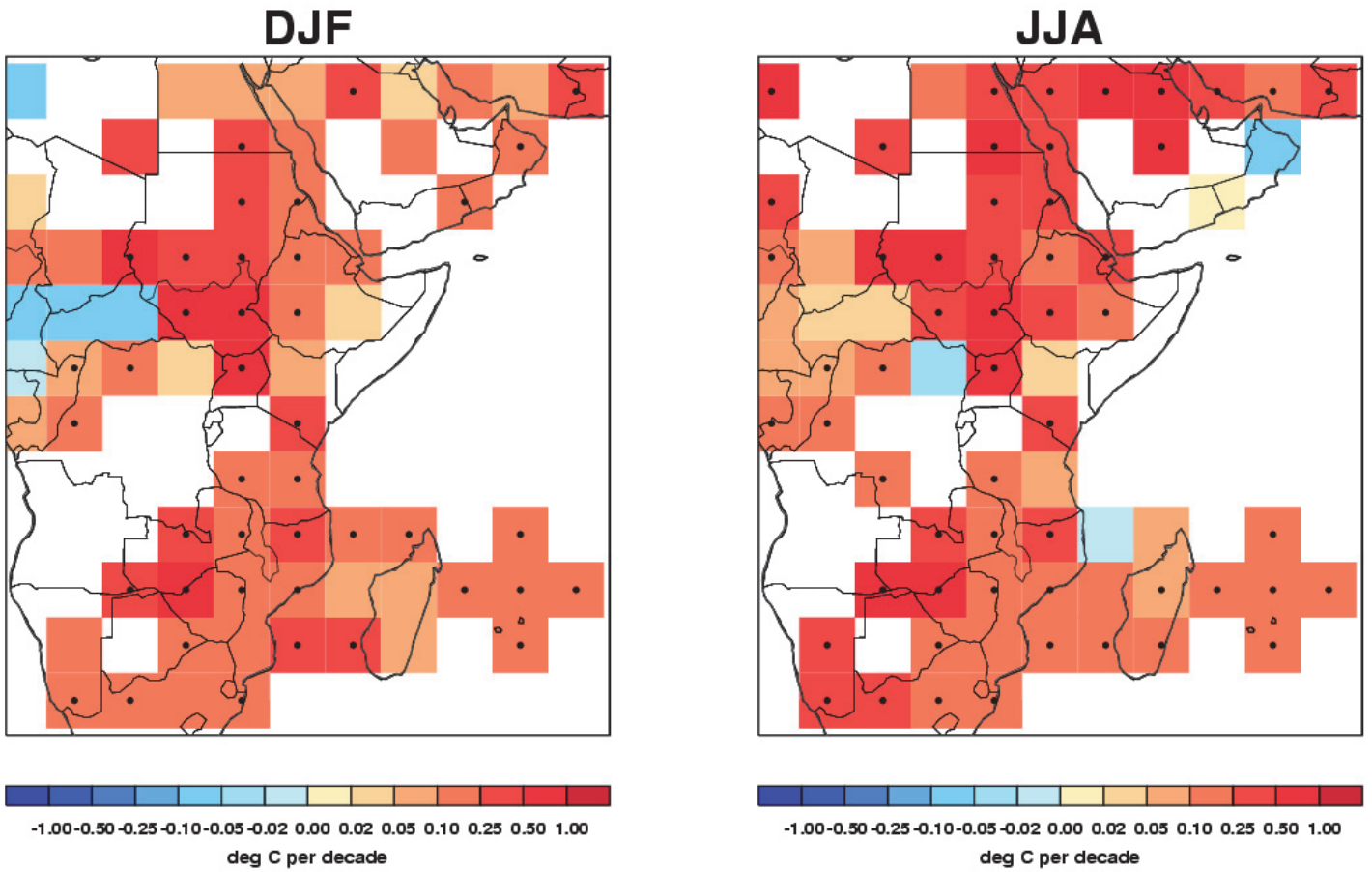

Figure 2. *Decadal trends in seasonally averaged temperatures for Kenya and the surrounding area over the period 1960 to 2010. Monthly mean anomalies from CRUTEM3 (Brohan et al. 2006) are averaged over each 3 month season (December-January-February – DJF and June-July-August – JJA). Trends are fitted using the median of pairwise slopes method (Sen 1968, Lanzante 1996). There is higher confidence in the trends shown if the 5th to 95th percentiles of the pairwise slopes do not encompass zero because here the trend is considered to be significantly different from a zero trend (no change). This is shown by a black dot in the centre of the respective grid box.*

Temperature extremes

Both hot and cold temperature extremes can place many demands on society. While seasonal changes in temperature are normal and indeed important for a number of societal sectors (e.g. tourism, farming etc.), extreme heat or cold can have serious negative impacts. Importantly, what is 'normal' for one region may be extreme for another region that is less well adapted to such temperatures.

Most of Kenya experiences a small annual range of temperatures, and most notable extreme events are linked to the rainfall cycles. No significant extreme temperature event since 2000 was reported in WMO Statements on Status of the Global Climate and/or BAMS State of the Climate reports.

Analysis of long-term features in moderate temperature extremes

HadEX extremes indices (Alexander et al. 2006) are used here for Kenya from 1960 to 2003 using daily maximum and minimum temperatures. However, as there were no temperature data available for Kenya, spatial coverage comes from interpolation from neighbouring countries where data are also sparse. Here we discuss changes in the frequency of cool days and nights and warm days and nights which are moderate extremes. Cool days/nights are defined as being below the 10^{th} percentile of daily maximum/minimum temperature and warm days/nights are defined as being above the 90^{th} percentile of the daily maximum/minimum temperature. The methods are fully described in the methodology section.

The trend towards fewer cool nights and days and more warm nights and days is spatially consistent and in agreement with the predominant pattern of increasing mean temperatures. All grid boxes show higher confidence in the signal. The data presented here are annual totals, averaged across all seasons, and so direct interpretation in terms of seasonal heat waves and cold snaps is not possible. Care should be taken on interpretation of the trends as they are clearly influenced by the latter section of the time series - for warm nights at least this does appear to be quite different from the earlier period. Data in-homogeneity cannot be ruled out here.

Night-time temperatures (daily minima) show widespread decreases in the frequency of cool nights and increases in the frequency of warm nights with high confidence throughout

(Figure 3 a,b,c,d). Regional averages show high confidence in a signal of fewer cool nights and more warm nights. However, the temporal coverage, even for the regional average, is incomplete.

Daytime temperatures (daily maxima) show widespread decreases in the frequency of cool days and increases in the frequency of warm days with high confidence throughout (Figure 3 a,b,c,d). Regional averages show high confidence in a signal of fewer cool days and more warm days. However, as with night-time temperatures, the temporal coverage is incomplete.

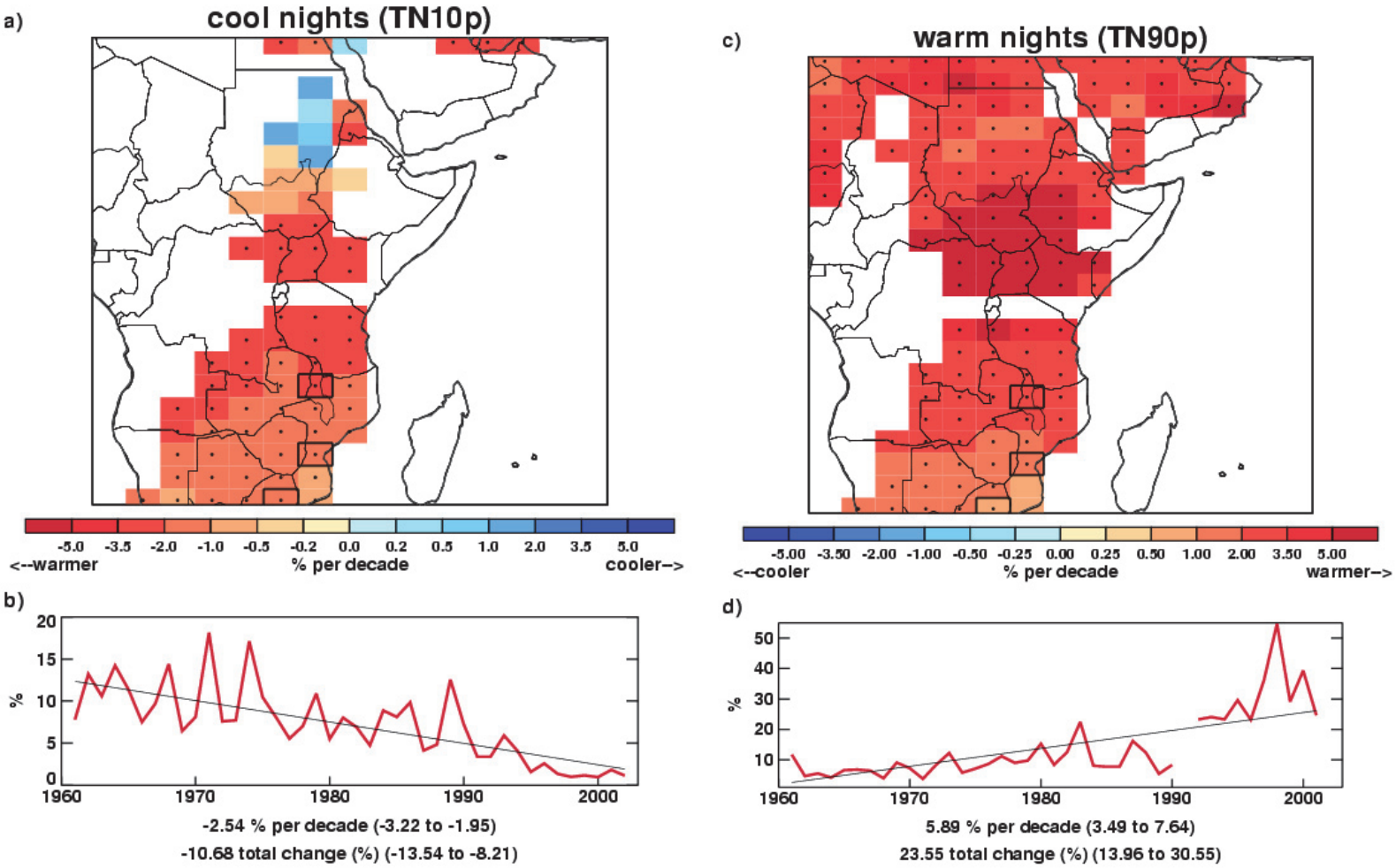
a)
cool nights (TN10p)
-5.0 -3.5 -2.0 -1.0 -0.5 -0.2 0.0 0.2 0.5 1.0 2.0 3.5 5.0
<--warmer
% per decade
cooler-->
b)
20
15
10
5
0
%
1960
1970
1980
1990
2000
-2.54 % per decade (-3.22 to -1.95)
-10.68 total change (%) (-13.54 to -8.21)
c)
warm nights (TN90p)
-5.00 -3.50 -2.00 -1.00 -0.50 -0.25 0.00 0.25 0.50 1.00 2.00 3.50 5.00
<--cooler
% per decade
warmer-->
d)
50
40
30
20
10
%
1960
1970
1980
1990
2000
5.89 % per decade (3.49 to 7.64)
23.55 total change (%) (13.96 to 30.55)

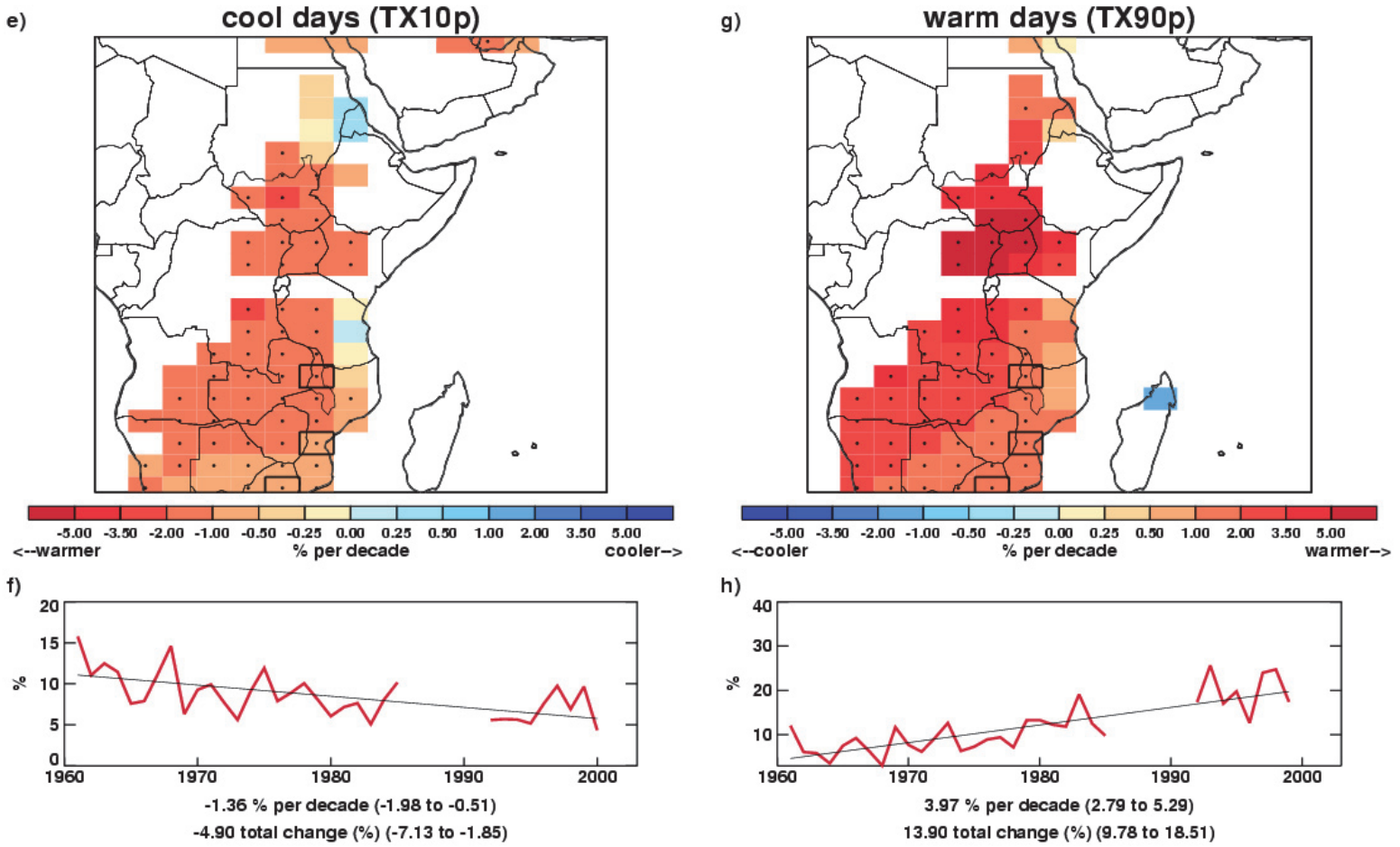

Figure 3. *Percentage change in cool nights (a,b), warm nights (c,d), cool days (e,f) and warm days (g,h) for Kenya over the period 1960 to 2003 relative to 1961-1990 from HadEX (Alexander et al. 2006). a,c,e,g) Grid box decadal trends. Grid boxes outlined in solid black contain at least 3 stations and so are likely to be more representative of the wider grid-box. Trends are fitted using the median of pairwise slopes method (Sen 1968, Lanzante 1996). Higher confidence in a long-term trend is shown by a black dot if the 5th to 95th percentile slopes are of the same sign. Differences in spatial coverage occur because each index has its own decorrelation length scale (see the methodology section). b,d,f,h) Area averaged annual time series for 31.875 to 43.125 ^{o} E, 6.25 ^{o} N to 6.25 ^{o} S as shown in the red box in Figure 1. Trends are fitted as described above. The decadal trend and its 5th to 95th percentile pairwise slopes are shown as well as the change over the period for which there is data. All the trends have higher confidence that they are different from zero as their 5th to 95th percentile slopes are of the same sign.*

Precipitation extremes

Precipitation extremes, either excess or deficit, can be hazardous to human health, societal infrastructure, and livestock and agriculture. While seasonal fluctuations in precipitation are normal and indeed important for a number of societal sectors (e.g. tourism, farming etc.), serious negative impacts can arise from flooding or drought. These are complex phenomena and often the result of accumulated excesses or deficits or other compounding factors such as high tides/storm surges or changes in land use. The analysis section below deals purely with precipitation amounts.

Table 1 shows selected extreme events since 2000 that are reported in WMO Statements on Status of the Global Climate and/or BAMS State of the Climate reports. Two events, the drought during 2005-2006, and flooding during October-November 2006, are highlighted below as examples of recent extreme precipitation events that affected Kenya.

Year	Month	Event	Details	Source
2000		Dry		BAMS (Lawrimore et al, 2001)
2003		Wet	Wettest conditions in 70 years in some areas	WMO (2004)
2003-2005		Drought	Only 50% of rainfall for SE Kenya over 2003-4; drought persisted into 2005.	WMO (2006)
2005-2006		Drought	Long term drought continued	WMO (2007)
2006	Oct-Nov	Flooding		WMO (2007)
2009		Drought		WMO (2010)
2010	Early in year	Flooding	Weeks of heavy rainfall; worst floods in more than a decade	WMO (2011)

***Table 1**. Selected extreme precipitation events reported in WMO Statements on Status of the Global Climate and/or BAMS State of the Climate reports since 2000*

Recent extreme precipitation events

Drought, 2005 - 2006

In 2005-2006 Kenya faced a serious humanitarian crisis following the failure of several cycles of rain, particularly the October to December short rains in 2005 (Oludhe et al., 2006). 3.5 million people were affected by the drought and required humanitarian assistance. The worst affected communities were the pastoralists in the northeast of Kenya, where in some areas 70% of the livestock died. As a consequence, a high number of pastoralists moved to settlements closer to urban areas, increasing significantly household vulnerability and dependence on food aid (CERF, 2006).

Almost 10% of the population required food aid over the next six months which led the Kenyan Government to appeal for $150 million to feed the hungry (FAO, 2006). Between March-December 2006, the United Nations Central Emergency Response Fund provided aid costing over US $ 27 million to Kenya's worst affected sectors including food, health, agriculture, water and sanitation (CERF, 2006).

Flooding, October - November 2006

In the "short rains" season (October to December) of 2006, a long-lasting drought in the Greater Horn of Africa ended with heavy rainfall and reports of the worst flooding in 50 years. The worst-hit areas were in Ethiopia, Kenya, and Somalia, where some stations received more than six times their average monthly rainfall. Flood waters from the Juba River in Somalia and the Tana River in Kenya combined to inundate a large region of northeastern Kenya (Bell et al., 2007). Damage in the three nations was exacerbated by the fact that they were still recovering from a scorching drought (above) that had parched soil, leaving the earth unable to absorb the rain water.

Approximately 60,000 people were displaced in the coastal, western and eastern provinces of Kenya, and the resultant cramped living conditions and lack of water and sanitation, meant that many were left at risk from diseases such as cholera, measles and malaria (OCHA, 2006). The World Health Organization (WHO) reported that in Garissa district, one of the worst affected regions, the number of medical consultations tripled compared to the pre-flood period. The three leading reasons for consultations were diarrhoeal diseases, malaria and acute respiratory infections. Outbreaks of cholera, with deaths, were reported in Moyale, Mombasa and Kwale (OCHA, 2006)

The floods also destroyed and damaged considerable quantities of crops and farmland, provoking fears of renewed food insecurity in the affected regions over the months to come. Access from aid and health workers was also made difficult as the rains caused severe blockages to infrastructure

networks and destroyed several bridges. People in cut-off communities were increasingly vulnerable, and food prices for basic commodities increased, in some cases by over 200 % (OCHA, 2006)

Analysis of long-term features in precipitation

HadEX extremes indices (Alexander et al. 2006) are used here for Kenya from 1960 to 2003 using daily precipitation totals. Here we discuss changes in the annual total precipitation. The methods are fully described in the methodology section.

There are few precipitation data available for Kenya and so spatial coverage is limited. Also, the decorrelation length scales for precipitation over this region are short, and hence, very little can be said about precipitation between 1960 and 2003 (Figure 4). Furthermore, the small numbers of stations present in most grid-boxes means that even if there is high confidence in the signals shown, uncertainty in the signal over the wider grid-box is large.

There is a mixed signal for total annual precipitation with high confidence in decreasing precipitation totals for one grid-box. Regional averages are inconclusive.

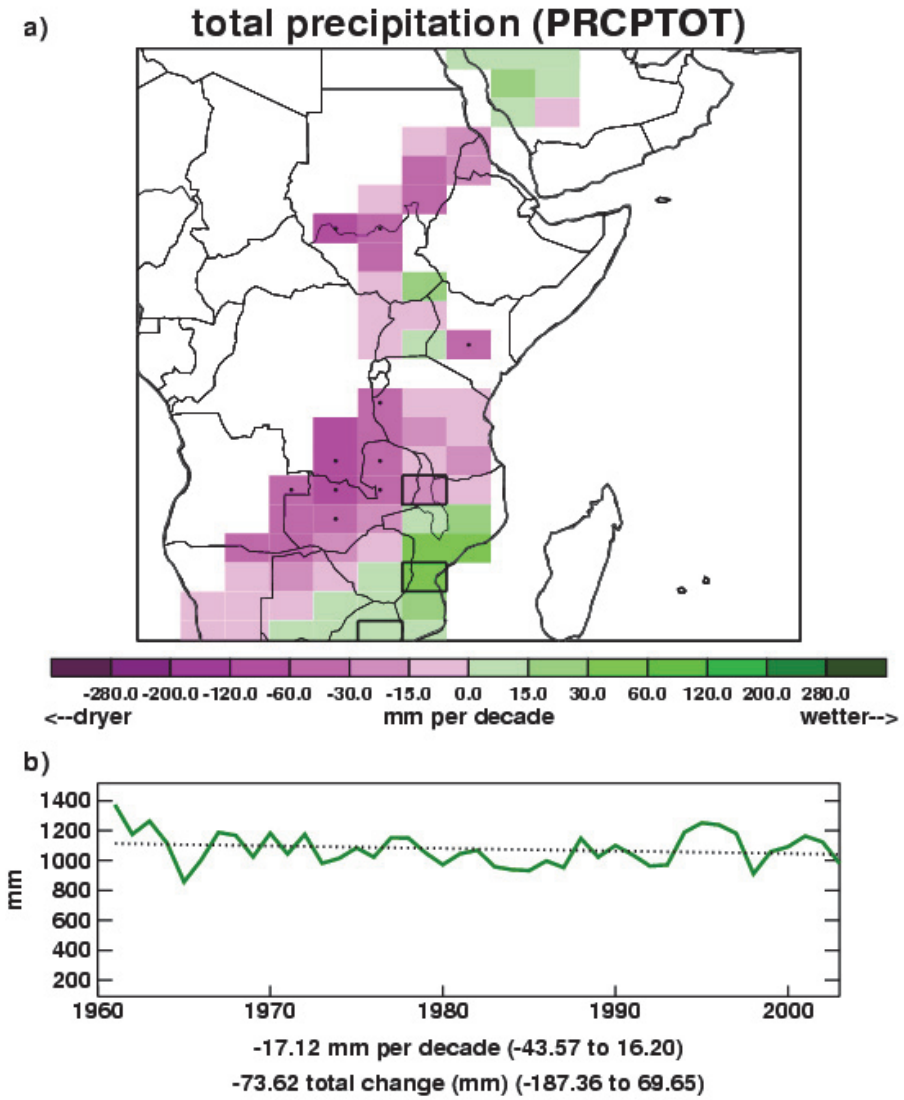

Figure 4. *Total annual precipitation for Kenya over the period 1960 to 2003 relative to 1961-1990 from HadEX (Alexander et al. 2006). a) Decadal trends as described in Figure 3. b) Area average annual time series for 31.875 to 43.125 ^{o} E, 6.25 ^{o} N to 6.25 ^{o} S as described in Figure 3. There is lower confidence that the trend for the total precipitation is different from zero, and hence it is marked with a dotted line.*

Summary

The main features seen in observed climate over Kenya from this analysis are:

- Widespread warming has been observed over Kenya since 1960.
- There is little precipitation data available for Kenya but there is some limited evidence for decreasing precipitation between 1960 and 2003, the period for which some data is available.

Methodology annex

Recent, notable extremes

In order to identify what is meant by ‘recent’ events the authors have used the period since 1994, when WMO Status of the Global Climate statements were available to the authors. However, where possible, the most notable events during the last 10 years have been chosen as these are most widely reported in the media, remain closest to the forefront of the memory of the country affected, and provide an example likely to be most relevant to today’s society. By ‘notable’ the authors mean any event which has had significant impact either in terms of cost to the economy, loss of life, or displacement and long term impact on the population. In most cases the events of largest impact on the population have been chosen, however this is not always the case.

Tables of recent, notable extreme events have been provided for each country. These have been compiled using data from the World Meteorological Organisation (WMO) Annual Statements on the Status of the Global Climate. This is a yearly report which includes contributions from all the member countries, and therefore represents a global overview of events that have had importance on a national scale. The report does not claim to capture all events of significance, and consistency across the years of records available is variable. However, this database provides a concise yet broad account of extreme events per country. This data is then supplemented with accounts from the monthly National Oceanic and Atmospheric Administration (NOAA) State of the Climate reports which outline global extreme events of meteorological significance.

We give detailed examples of heat, precipitation and storm extremes for each country where these have had significant impact. Where a country is primarily affected by precipitation or heat extremes this is where our focus has remained. An account of the impact on human life, property and the economy has been given, based largely on media reporting of events, and official reports from aid agencies, governments and meteorological organisations. Some data has also been acquired from the Centre for Research on Epidemiological Disasters (CRED) database on global extreme events. Although media reports are unlikely to be completely accurate, they do give an indication as to the perceived impact of an extreme event, and so are useful in highlighting the events which remain in the national psyche.

Our search for data has not been exhaustive given the number of countries and events included. Although there are a wide variety of sources available, for many events, an official account is not available. Therefore figures given are illustrative of the magnitude of impact only (references are included for further information on sources). It is also apparent that the reporting of extreme events

varies widely by region, and we have, where possible, engaged with local scientists to better understand the impact of such events.

The aim of the narrative for each country is to provide a picture of the social and economic vulnerability to the current climate. Examples given may illustrate the impact that any given extreme event may have and the recovery of a country from such an event. This will be important when considering the current trends in climate extremes, and also when examining projected trends in climate over the next century.

Observational record

In this section we outline the data sources which were incorporated into the analysis, the quality control procedure used, and the choices made in the data presentation. As this report is global in scope, including 23 countries, it is important to maintain consistency of methodological approach across the board. For this reason, although detailed datasets of extreme temperatures, precipitation and storm events exist for various countries, it was not possible to obtain and incorporate such a varied mix of data within the timeframe of this project. Attempts were made to obtain regional daily temperature and precipitation data from known contacts within various countries with which to update existing global extremes databases. No analysis of changes in storminess is included as there is no robust historical analysis of global land surface winds or storminess currently available.

Analysis of seasonal mean temperature

Mean temperatures analysed are obtained from the CRUTEM3 global land-based surface-temperature data-product (Brohan et al. 2006), jointly created by the Met Office Hadley Centre and Climatic Research Unit at the University of East Anglia. CRUTEM3 comprises of more than 4000 weather station records from around the world. These have been averaged together to create 5° by 5° gridded fields with no interpolation over grid boxes that do not contain stations. Seasonal averages were calculated for each grid box for the 1960 to 2010 period and linear trends fitted using the median of pairwise slopes (Sen 1968; Lanzante 1996). This method finds the slopes for all possible pairs of points in the data, and takes their median. This is a robust estimator of the slope which is not sensitive to outlying points. High confidence is assigned to any trend value for which the 5^{th} to 95^{th} percentiles of the pairwise slopes are of the same sign as the trend value and thus inconsistent with a zero trend.

Analysis of temperature and precipitation extremes using indices

In order to study extremes of climate a number of indices have been created to highlight different aspects of severe weather. The set of indices used are those from the World Climate Research

Programme (WCRP) Climate Variability and Predictability (CLIVAR) Expert Team on Climate Change Detection and Indices (ETCCDI). These 27 indices use daily rainfall and maximum and minimum temperature data to find the annual (and for a subset of the indices, monthly) values for, e.g., the 'warm' days where daily maximum temperature exceeds the 90th percentile maximum temperature as defined over a 1961 to 1990 base period. For a full list of the indices we refer to the website of the ETCCDI (http://cccma.seos.uvic.ca/ETCCDI/index.shtml).

Index	Description	Shortname	Notes
Cool night frequency	Daily minimum temperatures lower than the 10th percentile daily minimum temperature using the base reference period 1961-1990	TN10p	---
Warm night frequency	Daily minimum temperatures higher than the 90th percentile daily minimum temperature using the base reference period 1961-1990	TN90p	---
Cool day frequency	Daily maximum temperatures lower than the 10th percentile daily maximum temperature using the base reference period 1961-1990	TX10p	---
Warm day frequency	Daily maximum temperatures higher than the 90th percentile daily maximum temperature using the base reference period 1961-1990	TX90p	---
Dry spell duration	Maximum duration of continuous days within a year with rainfall <1mm	CDD	Lower data coverage due to the requirement for a 'dry spell' to be at least 6 days long resulting in intermittent temporal coverage
Wet spell duration	Maximum duration of continuous days with rainfall >1mm for a given year	CWD	Lower data coverage due to the requirement for a 'wet spell' to be at least 6 days long resulting in intermittent temporal coverage
Total annual precipitation	Total rainfall per year	PRCPTOT	---

Table 2. *Description of ETCCDI indices used in this document.*

A previous global study of the change in these indices, containing data from 1951-2003 can be found in Alexander et al. 2006, (HadEX; see http://www.metoffice.gov.uk/hadobs/hadex/). In this work we aimed to update this analysis to the present day where possible, using the most recently available data. A subset of the indices is used here because they are most easily related to extreme climate events (Table 2).

Use of HadEX for analysis of extremes

The HadEX dataset comprises all 27 ETCCDI indices calculated from station data and then smoothed and gridded onto a 2.5° x 3.75° grid, chosen to match the output from the Hadley Centre suite of climate models. To update the dataset to the present day, indices are calculated from the individual station data using the RClimDex/FClimDex software; developed and maintained on behalf of the ETCCDI by the Climate Research Branch of the Meteorological Service of Canada. Given the timeframe of this project it was not possible to obtain sufficient station data to create updated HadEX indices to present day for a number of countries: Brazil; Egypt; Indonesia; Japan (precipitation only); South Africa; Saudi Arabia; Peru; Turkey; and Kenya. Indices from the original HadEX data-product are used here to show changes in extremes of temperature and precipitation from 1960 to 2003. In some cases the data end prior to 2003. Table 3 summarises the data used for each country. Below, we give a short summary of the methods used to create the HadEX dataset (for a full description see Alexander et al. 2006).

To account for the uneven spatial coverage when creating the HadEX dataset, the indices for each station were gridded, and a land-sea mask from the HadCM3 model applied. The interpolation method used in the gridding process uses a decorrelation length scale (DLS) to determine which stations can influence the value of a given grid box. This DLS is calculated from the e-folding distance of the individual station correlations. The DLS is calculated separately for five latitude bands, and then linearly interpolated between the bands. There is a noticeable difference in spatial coverage between the indices due to these differences in decorrelation length scales. This means that there will be some grid-box data where in fact there are no stations underlying it. Here we apply black borders to grid-boxes where at least 3 stations are present to denote greater confidence in representation of the wider grid-box area there. The land-sea mask enables the dataset to be used directly for model comparison with output from HadCM3. It does mean, however, that some coastal regions and islands over which one may expect to find a grid-box are in fact empty because they have been treated as sea

Data sources used for updates to the HadEX analysis of extremes

We use a number of different data sources to provide sufficient coverage to update as many countries as possible to present day. These are summarised in Table 3. In building the new datasets we have tried to use exactly the same methodology as was used to create the original HadEX to retain consistency with a product that was created through substantial international effort and widely used, but there are some differences, which are described in the next section.

Wherever new data have been used, the geographical distributions of the trends were compared to those obtained from HadEX, using the same grid size, time span and fitting method. If the pattern

of the trends in the temperature or precipitation indices did not match that from HadEX, we used the HadEX data despite its generally shorter time span. Differences in the patterns of the trends in the indices can arise because the individual stations used to create the gridded results are different from those in HadEX, and the quality control procedures used are also very likely to be different. Countries where we decided to use HadEX data despite the existence of more recent data are Egypt and Turkey.

GHCND:

The Global Historical Climate Network Daily data has near-global coverage. However, to ensure consistency with the HadEX database, the GHCND stations were compared to those stations in HadEX. We selected those stations which are within 1500m of the stations used in the HadEX database and have a high correlation with the HadEX stations. We only took the precipitation data if its r>0.9 and the temperature data if one of its r-values >0.9. In addition, we required at least 5 years of data beyond 2000. These daily data were then converted to the indices using the *fclimdex* software

ECA&D and SACA&D:

The European Climate Assessment and Dataset and the Southeast Asian Climate Assessment and Dataset data are pre-calculated indices comprising the core 27 indices from the ETCCDI as well as some extra ones. We kindly acknowledge the help of Albert Klein Tank, the KNMI[1] and the BMKG[2] for their assistance in obtaining these data.

Mexico:

The station data from Mexico has been kindly supplied by the SMN[3] and Jorge Vazquez. These daily data were then converted to the required indices using the *Fclimdex* software. There are a total of 5298 Mexican stations in the database. In order to select those which have sufficiently long data records and are likely to be the most reliable ones we performed a cross correlation between all stations. We selected those which had at least 20 years of data post 1960 and have a correlation with at least one other station with an *r*-value >0.95. This resulted in 237 stations being selected for further processing and analysis.

[1] Koninklijk Nederlands Meteorologisch Instituut – The Royal Netherlands Meteorological Institute

[2] Badan Meteorologi, Klimatologi dan Geofisika – The Indonesian Meteorological, Climatological and Geophysical Agency

[3] Servicio Meteorológico Nacional de México – The Mexican National Meteorological Service

Indian Gridded:

The India Meteorological Department provided daily gridded data (precipitation 1951-2007, temperature 1969-2009) on a 1° x 1° grid. These are the only gridded daily data in our analysis. In order to process these in as similar a way as possible the values for each grid were assumed to be analogous to a station located at the centre of the grid. We keep these data separate from the rest of the study, which is particularly important when calculating the decorrelation length scale, which is on the whole larger for these gridded data.

Country	**Region box** (red dashed boxes in Fig. 1 and on each map at beginning of chapter)	**Data source** (T = temperature, P = precipitation)	**Period of data coverage** (T = temperature, P = precipitation)	**Indices included** (see Table 2 for details)	**Temporal resolution available**	**Notes**
Argentina	73.125 to 54.375 ° W, 21.25 to 56.25 ° S	Matilde Rusticucci (T,P)	1960-2010 (T,P)	TN10p, TN90p, TX10p, TX90p, PRCPTOT, CDD, CWD	annual	
Australia	114.375 to 155.625 ° E, 11.25 to 43.75 ° S	GHCND (T,P)	1960-2010 (T,P)	TN10p, TN90p, TX10p, TX90p, PRCPTOT, CDD, CWD	monthly, seasonal and annual	Land-sea mask has been adapted to include Tasmania and the area around Brisbane
Banglades h	88.125 to 91.875 ° E, 21.25 to 26.25 ° N	Indian Gridded data (T,P)	1960-2007 (P), 1970-2009 (T)	TN10p, TN90p, TX10p, TX90p, PRCPTOT, CDD, CWD	monthly, seasonal and annual	Interpolated from Indian Gridded data
Brazil	73.125 to 31.875 ° W, 6.25 ° N to 33.75 ° S	HadEX (T,P)	1960-2000 (P) 2002 (T)	TN10p, TN90p, TX10p, TX90p, PRCPTOT, CDD, CWD	annual	Spatial coverage is poor
China	73.125 to 133.125 ° E, 21.25 to 53.75 ° N	GHCND (T,P)	1960-1997 (P) 1960-2003 (T_{min}) 1960-2010 (T_{max})	TN10p, TN90p, TX10p, TX90p, PRCPTOT, CDD, CWD	monthly, seasonal and annual	Precipitation has very poor coverage beyond 1997 except in 2003-04, and no data at all in 2000-02, 2005-11
Egypt	24.375 to 35.625 ° E, 21.25 to 31.25 ° N	HadEX (T,P)	No data	TN10p, TN90p, TX10p, TX90p, PRCPTOT,	annual	There are no data for Egypt so all grid-box values have been interpolated from stations in Jordan, Israel, Libya and Sudan
France	5.625 ° W to 9.375 ° E, 41.25 to 51.25 ° N	ECA&D (T,P)	1960-2010 (T,P)	TN10p, TN90p, TX10p, TX90p, PRCPTOT, CDD, CWD	monthly, seasonal and annual	

Germany	5.625 to 16.875 ° E, 46.25 to 56.25 ° N	ECA&D (T,P)	1960-2010 (T,P)	TN10p, TN90p, TX10p, TX90p, PRCPTOT, CDD, CWD	monthly, seasonal and annual	
India	69.375 to 99.375 ° E, 6.25 to 36.25 ° N	Indian Gridded data (T,P)	1960-2003 (P), 1970-2009 (T)	TN10p, TN90p, TX10p, TX90p, PRCPTOT, CDD, CWD	monthly, seasonal and annual	
Indonesia	95.625 to 140.625 ° E, 6.25 ° N to 11.25 ° S	HadEX (T,P)	1968-2003 (T,P)	TN10p, TN90p, TX10p, TX90p, PRCPTOT,	annual	Spatial coverage is poor
Italy	5.625 to 16.875 ° E, 36.25 to 46.25 ° N	ECA&D (T,P)	1960-2010 (T,P)	TN10p, TN90p, TX10p, TX90p, PRCPTOT, CDD, CWD	monthly, seasonal and annual	Land-sea mask has been adapted to improve coverage of Italy
Japan	129.375 to 144.375 ° E, 31.25 to 46.25 ° N	HadEX (P) GHCND (T)	1960-2003 (P) 1960-2000 (T_{min}) 1960-2010 (T_{max})	TN10p, TN90p, TX10p, TX90p, PRCPTOT,	monthly, seasonal and annual (T), annual (P)	
Kenya	31.875 to 43.125 ° E, 6.25 ° N to 6.25 ° S	HadEX (T,P)	1960-1999 (P)	TN10p, TN90p, TX10p, TX90p, PRCPTOT	annual	There are no temperature data for Kenya and so grid-box values have been interpolated from neighbouring Uganda and the United Republic of Tanzania. Regional averages include grid-boxes from outside Kenya that enable continuation to 2003
Mexico	118.125 to 88.125 ° W, 13.75 to 33.75 ° N	Raw station data from the Servicio Meteorológico Nacional (SMN) (T,P)	1960-2009 (T,P)	TN10p, TN90p, TX10p, TX90p, PRCPTOT, CDD, CWD	monthly, seasonal and annual	237/5298 stations selected. Non uniform spatial coverage. Drop in T and P coverage in 2009.

Peru	84.735 to 65.625 ° W, 1.25 ° N to 18.75 ° S	HadEX (T,P)	1960-2002 (T,P)	TN10p, TN90p, TX10p, TX90p, PRCPTOT, CDD, CWD	annual	Intermittent coverage in TX90p, CDD and CWD
Russia	West Russia 28.125 to 106.875 ° E, 43.75 to 78.75 ° N, East Russia 103.125 to 189.375 ° E, 43.75 to 78.75 ° N	ECA&D (T,P)	1960-2010 (T,P)	TN10p, TN90p, TX10p, TX90p, PRCPTOT, CDD, CWD	monthly, seasonal and annual	Country split for presentation purposes only.
Saudi Arabia	31.875 to 54.375 ° E, 16.25 to 33.75 ° N	HadEX (T,P)	1960-2000 (T,P)	TN10p, TN90p, TX10p, TX90p, PRCPTOT	annual	Spatial coverage is poor
South Africa	13.125 to 35.625 ° W, 21.25 to 36.25 ° S	HadEX (T,P)	1960-2000 (T,P)	TN10p, TN90p, TX10p, TX90p, PRCPTOT, CDD, CWD	annual	---
Republic of Korea	125.625 to 129.375 ° E, 33.75 to 38.75 ° N	HadEX (T,P)	1960-2003 (T,P)	TN10p, TN90p, TX10p, TX90p, PRCPTOT, CDD	annual	There are too few data points for CWD to calculate trends or regional timeseries
Spain	9.375 ° W to 1.875 ° E, 36.25 to 43.75 ° N	ECA&D (T,P)	1960-2010 (T,P)	TN10p, TN90p, TX10p, TX90p, PRCPTOT, CDD, CWD	monthly, seasonal and annual	
Turkey	24.375 to 46.875 ° E, 36.25 to 43.75 ° N	HadEX (T,P)	1960-2003 (T,P)	TN10p, TN90p, TX10p, TX90p, PRCPTOT, CDD, CWD	annual	Intermittent coverage in CWD and CDD with no regional average beyond 2000

United Kingdom	9.375 ° W to 1.875 ° E, 51.25 to 58.75 ° N	ECA&D (T,P)	1960-2010 (T,P)	TN10p, TN90p, TX10p, TX90p, PRCPTOT, CDD, CWD	monthly, seasonal and annual	
United States of America	125.625 to 65.625 ° W, 23.75 to 48.75 ° N	GHCND (T,P)	1960-2010 (T,P)	TN10p, TN90p, TX10p, TX90p, PRCPTOT, CDD, CWD	monthly, seasonal and annual	

Table 3. *Summary of data used for each country*

Quality control and gridding procedure used for updates to the HadEX analysis of extremes

In order to perform some basic quality control checks on the index data, we used a two-step process on the indices. Firstly, internal checks were carried out, to remove cases where the 5 day rainfall value is less than the 1 day rainfall value, the minimum T_min is greater than the minimum T_max and the maximum T_min is greater than the maximum T_max. Although these are physically impossible, they could arise from transcription errors when creating the daily dataset, for example, a misplaced minus sign, an extra digit appearing in the record or a column transposition during digitisation. During these tests we also require that there are at least 20 years of data in the period of record for the index for that station, and that some data is found in each decade between 1961 and 1990, to allow a reasonable estimation of the climatology over that period.

Weather conditions are often similar over many tens of kilometres and the indices calculated in this work are even more coherent. The correlation coefficient between each station-pair combination in all the data obtained is calculated for each index (and month where appropriate), and plotted as a function of the separation. An exponential decay curve is fitted to the data, and the distance at which this curve has fallen by a factor $1/e$ is taken as the decorrelation length scale (DLS). A DLS is calculated for each dataset separately. For the GHCND, a separate DLS is calculated for each hemisphere. We do not force the fitted decay curve to show perfect correlation at zero distance, which is different to the method employed when creating HadEX. For some of the indices in some countries, no clear decay pattern was observed in some data sets or the decay was so slow that no value for the DLS could be determined. In these cases a default value of 200km was used.

We then perform external checks on the index data by comparing the value for each station with that of its neighbours. As the station values are correlated, it is therefore likely that if one station measures a high value for an index for a given month, its neighbours will also be measuring high. We exploit this coherence to find further bad values or stations as follows. Although raw precipitation data shows a high degree of localisation, using indices which have monthly or annual resolution improves the coherence across wider areas and so this neighbour checking technique is a valid method of finding anomalous stations.

We calculate a climatology for each station (and month if appropriate) using the mean value for each index over the period 1961-1990. The values for each station are then anomalised using this climatology by subtracting this mean value from the true values, so that it is clear if the station values are higher or lower than normal. This means that we do not need to take

differences in elevation or topography into account when comparing neighbours, as we are not comparing actual values, but rather deviations from the mean value.

All stations which are within the DLS distance are investigated and their anomalised values noted. We then calculate the weighted median value from these stations to take into account the decay in the correlation with increasing distance. We use the median to reduce the sensitivity to outliers.

If the station value is greater than 7.5 median-absolute-deviations away from the weighted median value (this corresponds to about 5 standard deviations if the distribution is Gaussian, but is a robust measure of the spread of the distribution), then there is low confidence in the veracity of this value and so it is removed from the data.

To present the data, the individual stations are gridded on a 3.75^{o} x 2.5^{o} grid, matching the output from HadCM3. To determine the value of each grid box, the DLS is used to calculate which stations can reasonably contribute to the value. The value of each station is then weighted using the DLS to obtain a final grid box value. At least three stations need to have valid data and be near enough (within 1 DLS of the gridbox centre) to contribute in order for a value to be calculated for the grid point. As for the original HadEX, the HadCM3 land-sea mask is used. However, in three cases the mask has been adjusted as there are data over Tasmania, eastern Australia and Italy that would not be included otherwise (Figure 5).

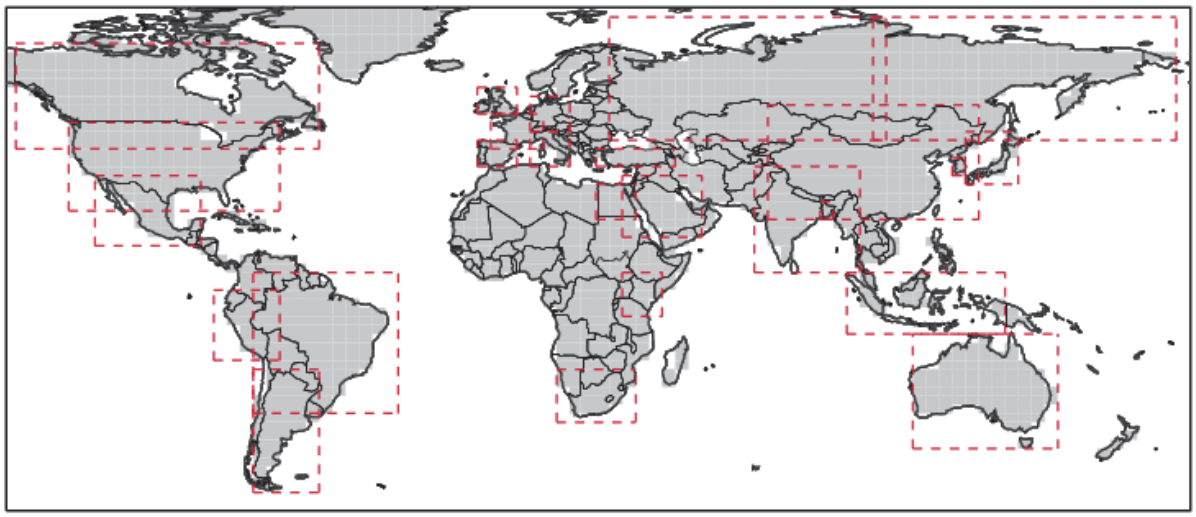

Figure 5. *Land-sea mask used for gridding the station data and regional areas allocated to each country as described in Table 3.*

Presentation of extremes of temperature and precipitation

Indices are displayed as regional gridded maps of decadal trends and regional average time-series with decadal trends where appropriate. Trends are fitted using the median of pairwise slopes method (Sen 1968, Lanzante 1996). Trends are considered to be significantly different from a zero trend if the 5th to 95th percentiles of the pairwise slopes do not encompass zero. This is shown by a black dot in the centre of the grid-box or by a solid line on time-series plots. This infers that there is high confidence in the sign (positive or negative) of the sign. Confidence in the trend magnitude can be inferred by the spread of the 5th to 95th percentiles of the pairwise slopes which is given for the regional average decadal trends. Trends are only calculated when there are data present for at least 50% of years in the period of record and for the updated data (not HadEX) there must be at least one year in each decade.

Due to the practice of data-interpolation during the gridding stage (using the DLS) there are values for some grid boxes when no actually station lies within the grid box. There is more confidence in grid boxes for which there are underlying data. For this reason, we identify those grid boxes which contain at least 3 stations by a black contour line on the maps. The DLS differs with region, season and index which leads to large differences in the spatial coverage. The indices, by their nature of being largely threshold driven, can be intermittent over time which also effects spatial and temporal coverage (see Table 2).

Each index (and each month for the indices for which there is monthly data) has a different DLS, and so the coverage between different indices and datasets can be different. The restrictions on having at least 20 years of data present for each input station, at least 50% of years in the period of record and at least one year in each decade for the trending calculation, combined with the DLS, can restrict the coverage to only those regions with a dense station network reporting reliably.

Each country has a rectangular region assigned as shown by the red dashed box on the map in Figure 1 and listed in Table 2, which is used for the creation of the regional average. This is sometimes identical to the attribution region shown in grey on the map in Figure 1. This region is again shown on the maps accompanying the time series of the regional averages as a reminder of the region and grid boxes used in the calculation. Regional averages are created by weighting grid box values by the cosine of their grid box centre latitude. To ensure consistency over time a regional average is only calculated when there are a sufficient number of grid boxes present. The full-period median number of grid-boxes present is calculated. For regions with a median of more than six grid-boxes there must be at least 80%

of the median number of grid boxes present for any one year to calculate a regional average. For regions with six or fewer median grid boxes this is relaxed to 50%. These limitations ensure that a single station or grid box which has a longer period of record than its neighbours cannot skew the timeseries trend. So sometimes there may be grid-boxes present but no regional average time series. The trends for the regional averages are calculated in the same way as for the individual grid boxes, using the median of pairwise slopes method (Sen 1968, Lanzante 1996). Confidence in the trend is also determined if the 5^{th} to 95^{th} percentiles of the pairwise slopes are of the same sign and thus inconsistent with a zero trend. As well as the trend in quantity per decade, we also show the full change in the quantity from 1960 to 2010 that this fitted linear trend implies.

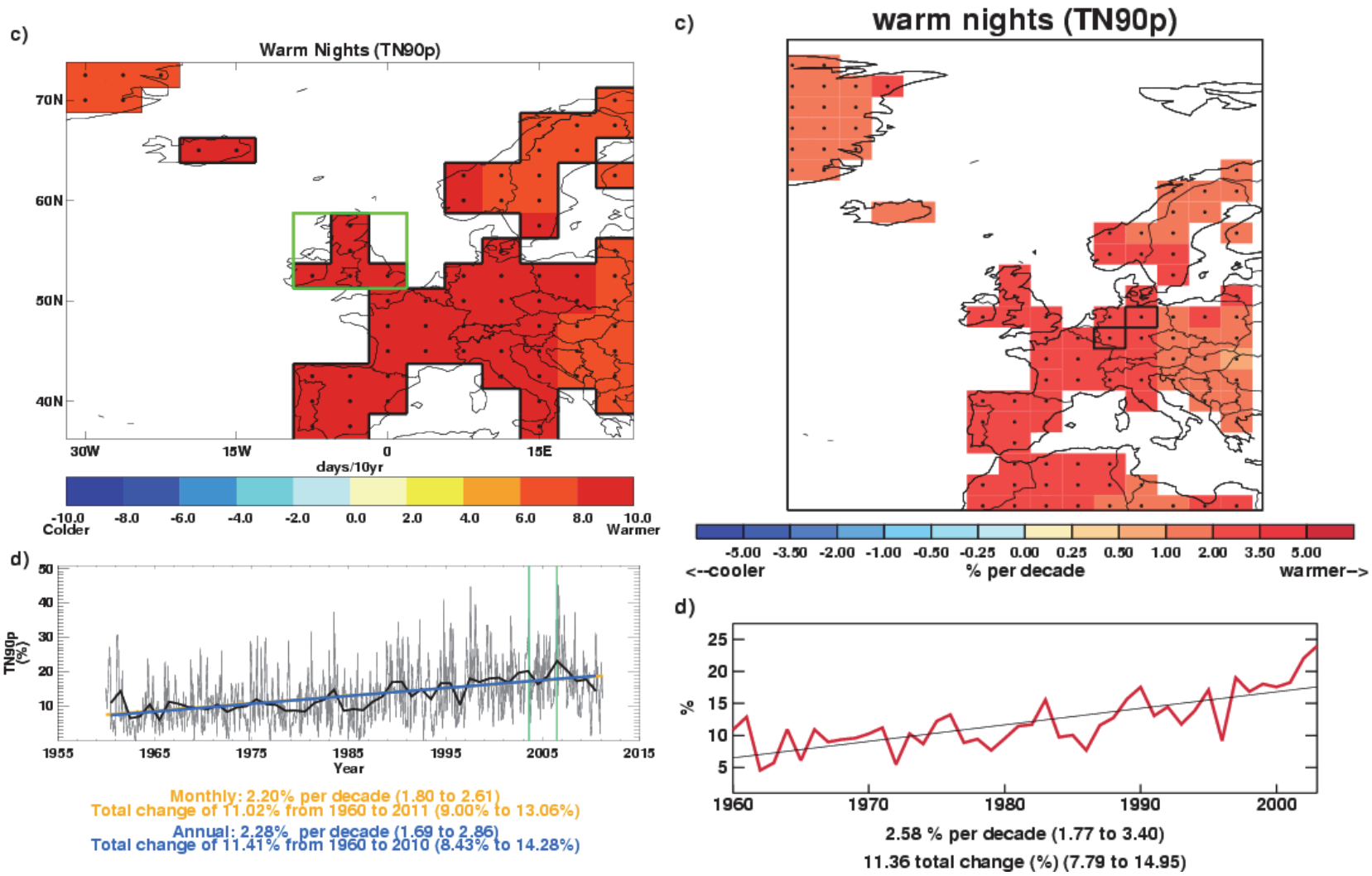

Figure 6. *Examples of the plots shown in the data section. Left: From ECA&D data between 1960-2010 for the number of warm nights, and Right: from HadEX data (1960-2003) for the total precipitation. A full explanation of the plots is given in the text below.*

The results are presented in the form of a map and a time series for each country and index. The map shows the grid box decadal trend in the index over the period for which there are data. High confidence, as determined above, is shown by a black dot in the grid box centre. To show the variation over time, the values for each year (and month if available) are shown in a time series for a regional average. The values of the indices have been normalised to a base period of 1961-1990 (except the Indian gridded data which use a 1971 to 1990 period), both in HadEX and in the new data acquired for this project. Therefore, for example, the percentage of nights exceeding the 90th percentile for a temperature is 10% for that period.

There are two influences on whether a grid box contains a value or not – the land-sea mask, and the decorrelation length scale. The land-sea mask is shown in Figure 5. There are grid boxes which contain some land but are mostly sea and so are not considered. The decorrelation length scale sets the maximum distance a grid box can be from stations before no value is assigned to it. Grid boxes containing three or more stations are highlighted by a thick border. This indicates regions where the value shown is likely to be more representative of the grid box area mean as opposed to a single station location.

On the maps for the new data there is a box indicating which grid boxes have been extracted to calculate the area average for the time series. This box is the same as shown in Figure 1 at the beginning of each country's document. These selected grid boxes are combined using area (cosine) weighting to calculate the regional average (both annual [thick lines] and monthly [thin lines] where available). Monthly (orange) and annual (blue) trends are fitted to these time series using the method described above. The decadal trend and total change over the period where there are data are shown with 5th to 95th percentile confidence intervals in parentheses. High confidence, as determined above, is shown by a solid line as opposed to a dotted one. The green vertical lines on the time series show the dates of some of the notable events outlined in each section.

Attribution

Regional distributions of seasonal mean temperatures in the 2000s are computed with and without the effect of anthropogenic influences on the climate. The analysis considers temperatures averaged over the regions shown in Figure 7. These are also identified as grey boxes on the maps in Figure 1. The coordinates of the regions are given in Table 4. The methodology combines information from observations and model simulations using the approach originally introduced in Christidis et al., 2010 and later extended in Christidis et al., 2011, where more details can be found. The analysis requires spatial scales greater than about 2,500 km and for that reason the selected regions (Fig.7 and Table 4) are often larger

than individual countries, or include several smaller countries in a single region (for example UK, Germany and France are grouped in one region).

Observations of land temperature come from the CRUTEM3 gridded dataset (Brohan et al., 2006) and model simulations from two coupled GCMs, namely the Hadley Centre HadGEM1 model (Martin et al., 2006) and version 3.2 of the MIROC model (K-1 Developers, 2004). The use of two GCMs helps investigate the sensitivity of the results to the model used in the analysis. Ensembles of model simulations from two types of experiments are used to partition the temperature response to external forcings between its anthropogenic and natural components. The first experiment (ALL) simulates the combined effect of natural and anthropogenic forcings on the climate system and the second (ANTHRO) includes anthropogenic forcings only. The difference of the two gives an estimate of the effect of the natural forcings (NAT). Estimates of the effect of internal climate variability are derived from long control simulations of the unforced climate. Distributions of the regional summer mean temperature are computed as follows:

a) A global optimal fingerprinting analysis (Allen and Tett, 1999; Allen and Stott, 2003) is first carried out that scales the global simulated patterns (fingerprints) of climate change attributed to different combinations of external forcings to best match them to the observations. The uncertainty in the scaling that originates from internal variability leads to samples of the scaled fingerprints, i.e. several realisations that are plausibly consistent with the observations. The 2000-2009 decade is then extracted from the scaled patterns and two samples of the decadal mean temperature averaged over the reference region are then computed with and without human influences, which provide the Probability Density Functions (PDFs) of the decadal mean temperature attributable to ALL and NAT forcings.

b) Model-derived estimates of noise are added to the distributions to take into account the uncertainty in the simulated fingerprints.

c) In the same way, additional noise from control model simulations is introduced to the distributions to represent the effect of internal variability in the annual values of the seasonal mean temperatures. The result is a pair of estimated distributions of the annual values of the seasonal mean temperature in the region with and without the effect of human activity on the climate. The temperatures throughout the analysis are expressed as anomalies relative to period 1961-1990.

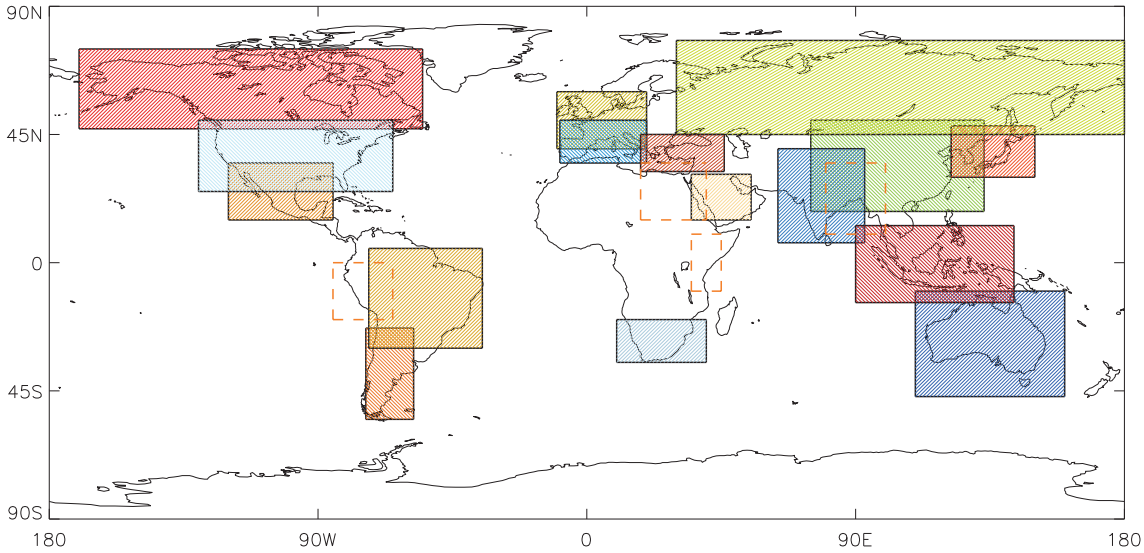

Figure 7. *The regions used in the attribution analysis. Regions marked with dashed orange boundaries correspond to non-G20 countries that were also included in the analysis.*

Region	Region Coordinates
Argentina	74-58W, 55-23S
Australia	110-160E, 47-10S
Bangladesh	80-100E, 10-35N
Brazil	73-35W, 30S-5N
Canada-Alaska	170-55W, 47-75N
China	75-133E, 18-50N
Egypt	18-40E, 15-35N
France-Germany-UK	10W-20E, 40-60N
India	64-93E, 7-40N
Indonesia	90-143E, 14S-13N
Italy-Spain	9W-20E, 35-50N
Japan-Republic of Korea	122-150E, 30-48N
Kenya	35-45E, 10S-10N
Mexico	120-85W, 15-35N
Peru	85-65W, 20-0S
Russia	30-185E, 45-78N
Saudi Arabia	35-55E, 15-31N
South Africa	10-40E, 35-20S
Turkey	18-46E, 32-45N

Table 4. *The coordinates of the regions used in the attribution analysis.*

References

ALEXANDER, L. V., ZHANG. X., PETERSON, T. C., CAESAR, J., GLEASON, B., KLEIN TANK, A. M. G., HAYLOCK, M., COLLINS, D., TREWIN, B., RAHIMZADEH, F., TAGIPOUR, A., RUPA KUMAR, K., REVADEKAR, J., GRIFFITHS, G., VINCENT, L., STEPHENSON, D. B., BURN, J., AGUILAR, E., BRUNET, M., TAYLOR, M., NEW, M., ZHAI, P., RUSTICUCCI, M. AND VAZQUEZ-AGUIRRE, J. L. 2006. Global observed changes in daily climate extremes of temperature and precipitation. *J. Geophys. Res*. 111, D05109. doi:10.1029/2005JD006290.

ALLEN, M. R., TETT S. F. B. 1999. Checking for model consistency in optimal fingerprinting. Clim Dyn 15: 419-434

ALLEN M. R., STOTT P. A. 2003. Estimating signal amplitudes in optimal fingerprinting, part I: theory. Clim Dyn 21: 477-491

BELL, M., OLUDHE, C., AMBENJE, P., NJAU, L., MUMBA, Z., AND KADI, M. 2007. Regional Climates – Eastern Africa in State of the Climate 2006. *Bulletin of the American Meteorological Society* 88 (6), S77-S79].

BROHAN, P., KENNEDY, J.J., HARRIS, I., TETT, S.F.B. AND JONES, P.D. 2006. Uncertainty estimates in regional and global observed temperature changes: a new dataset from 1850. *J. Geophys. Res*. 111, D12106. doi:10.1029/2005JD006548.

CERF (UNITED NATIONS CENTRAL EMERGENCY RESPONSE FUND). 2006. CERF in Kenya 2006. http://ochaonline.un.org/Default.aspx?tabid=1749

CHRISTIDIS N., STOTT. P A., ZWIERS, F. W., SHIOGAMA, H., NOZAWA, T. 2010. Probabilistic estimates of recent changes in temperature: a multi-scale attribution analysis. Clim Dyn 34: 1139-1156

CHRISTIDIS, N., PA STOTT, FW ZWIERS, H SHIOGAMA, T NOZAWA 2011. The contribution of anthropogenic forcings to regional changes in temperature during the last decade. Clim Dyn (submitted)

FAO (FOOD AND AGRICULTURAL ORGANISATION of the UN). 2006. Millions of people are on the brink of starvation in the Horn of Africa http://www.fao.org/newsroom/en/news/2006/1000206/index.html

K-1 MODEL DEVELOPERS (2004) K-1 coupled GCM (MIROC) description, K-1 Tech Rep, H Hasumi and S Emori (eds), Centre for Clim Sys Res, Univ of Tokyo

LANZANTE, J. R. 1996. Resistant, robust and non-parametric techniques for the analysis of climate data: theory and examples, including applications to historical radiosonde station data. *Int. J. Clim*. 16, 1197–226.

LAWRIMORE, J., HALPERT, M., BELL, G., MENNE, M., LYON, B., SCHNELL, R., GLEASON, K., EASTERLING, D., THIAW, W., WRIGHT, W., HEIM, J.R.R., ROBINSON, D. AND ALEXANDER, L. 2001. State of the Climate 2006. *Bulletin of the American Meteorological Society* 82.

MARTIN G.M., RINGER. M. A., POPE V. D., JONES, A., DEARDEN, C., HINTON, T. 2006. The physical properties of the atmosphere in the new Hadley Centre Global Environmental Model (HadGEM1). Part I: Model description and global climatology. J Clim 19: 1274-1301

OCHA (UN OFFICE FOR THE COORDINATION OF HUMANITARIAN AFFAIRS). 2006. Situation Report No. 6 Ref: OCHA/GVA 2006/0258 http://reliefweb.int/node/221316

OLUDHE, C., AMBENJE, P., AND OGALLO, L. 2006. State of the Climate 2005. *Bulletin of the American Meteorological Society* 87 (6), S56-S57].

SANCHEZ-LUGO, A., KENNEDY, J.J. AND BERRISFORD, P. 2011. Global Climate – Surface Temperatures in State of the Climate 2010. *Bulletin of the American Meteorological Society* 92 (6), S36-S37].

SEN, P. K. 1968. Estimates of the regression coefficient based on Kendall's tau. *J. Am. Stat. Assoc*. 63, 1379–89.

WMO WORLD METEOROLOGICAL ORGANIZATION. 2004. Statement on Status of the Global Climate in 2003, WMO-No. 966. http://www.wmo.int/pages/prog/wcp/wcdmp/statement/wmostatement_en.html

WMO WORLD METEOROLOGICAL ORGANIZATION. 2006. Statement on Status of the Global Climate in 2005, WMO-No. 998. http://www.wmo.int/pages/prog/wcp/wcdmp/statement/wmostatement_en.html

WMO WORLD METEOROLOGICAL ORGANIZATION. 2007. Statement on Status of the Global Climate in 2006, WMO-No. 1016. http://www.wmo.int/pages/prog/wcp/wcdmp/statement/wmostatement_en.html

WMO WORLD METEOROLOGICAL ORGANIZATION. 2010. Statement on Status of the Global Climate in 2009, WMO-NO. 1055. http://www.wmo.int/pages/prog/wcp/wcdmp/statement/wmostatement_en.html

WMO WORLD METEOROLOGICAL ORGANIZATION. 2011. Statement on Status of the Global Climate in 2010, WMO-NO. 1074.
http://www.wmo.int/pages/prog/wcp/wcdmp/statement/wmostatement_en.html

Acknowledgements

We thank Lisa Alexander and Markus Donat (University of New South Wales) for their help and advice. We also thank reviewers from Kenya for their advice and input.

Chapter 2 – Climate Change Projections

Introduction

Climate models are used to understand how the climate will evolve over time and typically represent the atmosphere, ocean, land surface, cryosphere, and biogeochemical processes, and solve the equations governing their evolution on a geographical grid covering the globe. Some processes are represented explicitly within climate models, large-scale circulations for instance, while others are represented by simplified parameterisations. The use of these parameterisations is sometimes due to processes taking place on scales smaller than the typical grid size of a climate model (a Global Climate Model (GCM) has a typical horizontal resolution of between 250 and 600km) or sometimes to the current limited understanding of these processes. Different climate modelling institutions use different plausible representations of the climate system, which is why climate projections for a single greenhouse gas emissions scenario differ between modelling institutes. This gives rise to "climate model structural uncertainty".

In response to a proposed activity of the World Climate Research Programme's (WCRP's; http://www.wcrp-climate.org/) Working Group on Coupled Modelling (WGCM), the Program for Climate Model Diagnosis and Intercomparison (PCMDI; http://www-pcmdi.llnl.gov/) volunteered to collect model output contributed by leading climate modelling centres around the world. Climate model output from simulations of the past, present and future climate was collected by PCMDI mostly during the years 2005 and 2006, and this archived data constitutes phase 3 of the Coupled Model Intercomparison Project (CMIP3). In part, the WGCM organised this activity to enable those outside the major modelling centres to perform research of relevance to climate scientists preparing the IPCC Fourth Assessment Report (AR4). This unprecedented collection of recent model output is commonly known as the "CMIP3 multi-model dataset". The GCMs included in this dataset are referred to regularly throughout this review, although not exclusively.

The CMIP3 multi-model ensemble has been widely used in studies of regional climate change and associated impacts. Each of the constituent models was subject to extensive testing by the contributing institute, and the ensemble has the advantage of having been constructed from a large pool of alternative model components, therefore sampling alternative structural assumptions in how best to represent the physical climate system. Being assembled on an opportunity basis, however, the CMIP3 ensemble was not designed to represent model uncertainties in a systematic manner, so it does not, in isolation, support

robust estimates of the risk of different levels of future climate change, especially at a regional level.

Since CMIP3, a new (CMIP5) generation of coupled ocean-atmosphere models has been developed, which is only just beginning to be available and is being used for new projections for the IPCC Fifth Assessment Report (AR5).

These newer models typically feature higher spatial resolution than their CMIP3 counterparts, including in some models a more realistic representation of stratosphere-troposphere interactions. The CMIP5 models also benefit from several years of development in their parameterisations of small scale processes, which, together with resolution increases, are expected to result in a general improvement in the accuracy of their simulations of historical climate, and in the credibility of their projections of future changes. The CMIP5 programme also includes a number of comprehensive Earth System Models (ESMs) which explicitly simulate the earth's carbon cycle and key aspects of atmospheric chemistry, and also contain more sophisticated representations of aerosols compared to CMIP3 models.

The CMIP3 results should be interpreted as a useful interim set of plausible outcomes. However, their neglect of uncertainties, for instance in carbon cycle feedbacks, implies that higher levels of warming outside the CMIP3 envelope cannot be ruled out. In future, CMIP5 coupled model and ESM projections can be expected to produce improved advice on future regional changes. In particular, ensembles of ESM projections will be needed to provide a more comprehensive survey of possible future changes and their relative likelihoods of occurrence. This is likely to require analysis of the CMIP5 multi-model ESM projections, augmented by larger ensembles of ESM simulations in which uncertainties in physical and biogeochemical feedback processes can be explored more systematically, for example via ensembles of model runs in which key aspects of the climate model are slightly adjusted. Note that such an exercise might lead to the specification of wider rather than narrower uncertainties compared to CMIP3 results, if the effects of representing a wider range of earth system processes outweigh the effects of refinements in the simulation of physical atmosphere-ocean processes already included in the CMIP3 models.

Climate projections

The Met Office Hadley Centre is currently producing perturbed parameter ensembles of a single model configuration known as HadCM3C, to explore uncertainties in physical and biogeochemical feedback processes. The results of this analysis will become available in the next year and will supplement the CMIP5 multi-model ESM projections, providing a more comprehensive set of data to help progress understanding of future climate change. However, many of the studies covered in the chapter on climate impacts have used CMIP3 model output. For this reason, and because it is still the most widely used set of projections available, the CMIP3 ensemble output for temperature and precipitation, for the A1B emission scenario, for Kenya and the surrounding region is shown below.

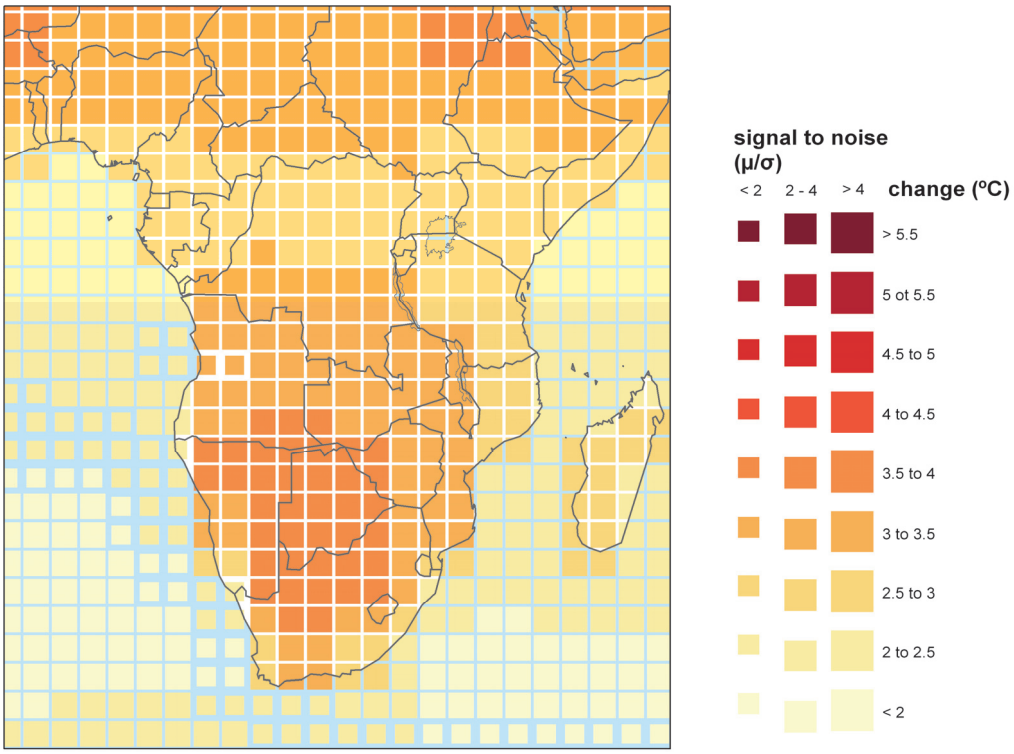

Figure 1. *Percentage change in average annual temperature by 2100 from 1960-1990 baseline climate, averaged over 21 CMIP3 models. The size of each pixel represents the level of agreement between models on the magnitude of the change.*

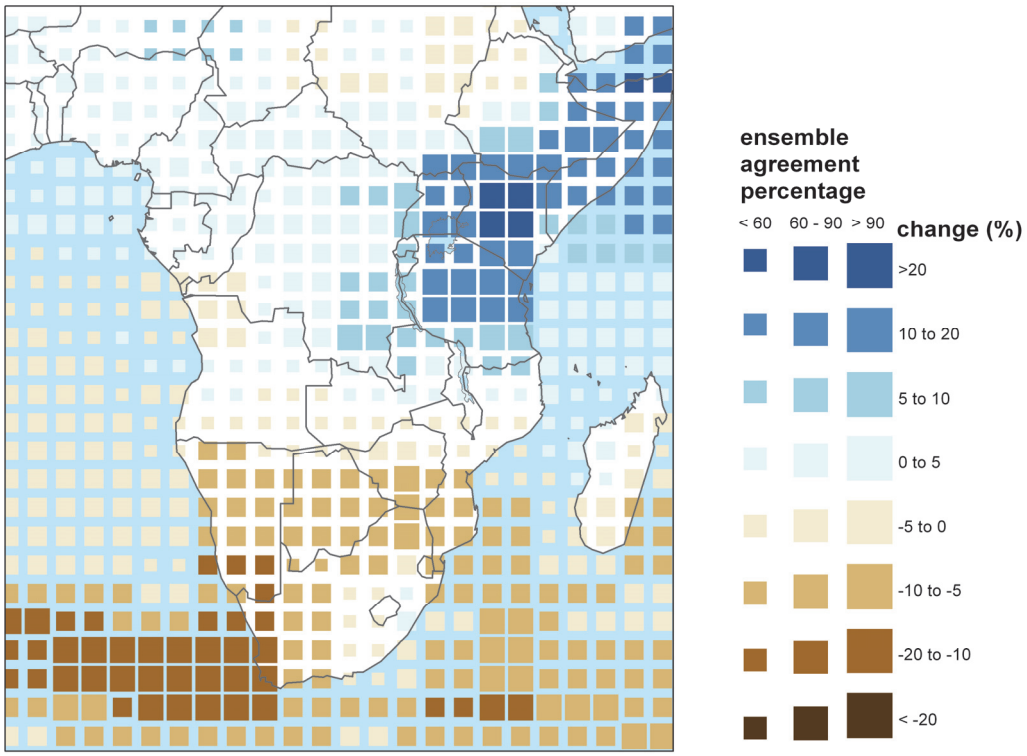

Figure 2. *Percentage change in average annual precipitation by 2100 from 1960-1990 baseline climate, averaged over 21 CMIP3 models. The size of each pixel represents the level of agreement between models on the sign of the change.*

Summary of temperature change in Kenya

Figure 1 shows the percentage change in average annual temperature by 2100 from 1960-1990 baseline climate, averaged over 21 CMIP3 models. All of the models in the CMIP3 ensemble project increased temperatures in the future, but the size of each pixel indicates how well the models agree over the magnitude of the increase.

Projections for temperature increases over Kenya, of up to around 3°C, show good agreement between the ensemble members.

Summary of precipitation change in Kenya

Figure 2 shows the percentage change in average annual precipitation by 2100 from 1960-1990 baseline climate, averaged over 21 CMIP3 models. Unlike for temperature, the models sometimes disagree over whether precipitation is increasing or decreasing over a region, so in this case the size of each pixel indicates the percentage of the models in the ensemble that agree on the sign of the change in precipitation.

The model ensemble projects strong precipitation increases over East Africa, in particular Kenya, with increases of over 20% projected with strong ensemble agreement.

Chapter 3 – Climate Change Impact Projections

Introduction

Aims and approach

This chapter looks at research on a range of projected climate change impacts, with focus on results for Kenya. It includes projections taken from the AVOID programme, for some of the impact sectors.

The aim of this work is to take a 'top down' approach to assessing global impacts studies, both from the literature and from new research undertaken by the AVOID programme. This project covers 23 countries, with summaries from global studies provided for each of these. This global approach allows some level of comparison between countries, whilst presenting information on a scale most meaningful to inform international policy.

The literature covered in this chapter focuses on research published since the Fourth Assessment Report (AR4) of the Intergovernmental Panel on Climate Change (IPCC) and should be read in conjunction with IPCC AR4 WG1 and WG2 reports. For some sectors considered, an absence of research developments since the IPCC AR4, means earlier work is cited as this helps describe the current level of scientific understanding. This report focuses on assessing scientific research about climate change impacts within sectors; it does not present an integrated analysis of climate change adaptation policies.

Some national and sub-national scale literature is reported to a limited extent to provide some regional context.

Impact sectors considered and methods

This report reviews the evidence for the impact of climate change on a number of sectors, for Kenya. The following sectors are considered in turn in this report:

- Crop yields
- Food security
- Water stress and drought
- Pluvial flooding and rainfall

- Fluvial flooding
- Tropical cyclones (where applicable)
- Coastal regions

Supporting literature

Literature searches were conducted for each sector with the Thomson Reuters Web of Science (WoS., 2011) and Google Scholar academic search engines respectively. Furthermore, climate change impact experts from each of the 23 countries reviewed were contacted. These experts were selected through a combination of government nomination and from experts known to the Met Office. They were asked to provide literature that they felt would be of relevance to this review. Where appropriate, such evidence has been included. A wide range of evidence was considered, including; research from international peer-reviewed journal papers; reports from governments, non-governmental organisations, and private businesses (e.g. reinsurance companies), and research papers published in national journals.

For each impact sector, results from assessments that include a global- or regional-scale perspective are considered separately from research that has been conducted at the national- or sub-national-scale. The consideration of global- and regional-scale studies facilitates a comparison of impacts across different countries, because such studies apply a consistent methodology for each country. While results from national- and sub-national-scale studies are not easily comparable between countries, they can provide a level of detail that is not always possible with larger-scale studies. However, the national- and sub-national scale literature included in this project does not represent a comprehensive coverage of regional-based research and cannot, and should not, replace individual, detailed impacts studies in countries. The review aims to present an up-to-date assessment of the impact of climate change on each of the sectors considered.

AVOID programme results

Much of the work in this report is drawn from modelling results and analyses coming out of the AVOID programme. The AVOID programme is a research consortium funded by DECC and Defra and led by the UK Met Office and also comprises the Walker Institute at the University of Reading, the Tyndall Centre represented through the University of East Anglia,

and the Grantham Institute for Climate Change at Imperial College. The expertise in the AVOID programme includes climate change research and modelling, climate change impacts in natural and human systems, socio-economic sciences, mitigation and technology. The unique expertise of the programme is in bringing these research areas together to produce integrated and policy-relevant results. The experts who work within the programme were also well suited to review the literature assessment part of this report. In this report the modelling of sea level rise impacts was carried out for the AVOID programme by the University of Southampton.

The AVOID programme uses the same emissions scenarios across the different impact sectors studied. These are a business as usual (IPCC SRES A1B) and an aggressive mitigation (the AVOID A1B-2016-5-L) scenario. Model output for both scenarios was taken from more than 20 GCMs and averaged for use in the impact models. The impact models are sector specific, and frequently employ further analytical techniques such as pattern scaling and downscaling in the crop yield models.

Data and analysis from AVOID programme research is provided for the following impact sectors:

- Crop yields
- Water stress and drought
- Fluvial flooding
- Coastal regions

Uncertainty in climate change impact assessment

There are many uncertainties in future projections of climate change and its impacts. Several of these are well-recognised, but some are not. One category of uncertainty arises because we don’t yet know how mankind will alter the climate in the future. For instance, uncertainties in future greenhouse gas emissions depends on the future socio-economic pathway, which, in turn, depends on factors such as population, economic growth, technology development, energy demand and methods of supply, and land use. The usual approach to dealing with this is to consider a range of possible future scenarios.

Another category of uncertainties relate to our incomplete understanding of the climate system, or an inability to adequately model some aspects of the system. This includes:

- Uncertainties in translating emissions of greenhouse gases into atmospheric concentrations and radiative forcing. Atmospheric CO_2 concentrations are currently rising at approximately 50% of the rate of anthropogenic emissions, with the remaining 50% being offset by a net uptake of CO_2 into the oceans and land biosphere. However, this rate of uptake itself probably depends on climate, and evidence suggests it may weaken under a warming climate, causing more CO_2 to remain in the atmosphere, warming climate further. The extent of this feedback is highly uncertain, but it not considered in most studies. The phase 3 of the Coupled Model Intercomparison Project (CMIP3), which provided the future climate projections for the IPCC Fourth Assessment Report (AR4), used a single estimate of CO_2 concentration rise for each emissions scenario, so the CMIP3 projections (which were used in most studies presented here, including AVOID) do not account for this uncertainty.

- Uncertainty in climate response to the forcing by greenhouse gases and aerosols. One aspect of this is the response of global mean temperature ("climate sensitivity"), but a more relevant aspect for impacts studies is the response of regional climates, including temperature, precipitation and other meteorological variables. Different climate models can give very different results in some regions, while giving similar results in other regions. Confidence in regional projections requires more than just agreement between models: physical understanding of the relevant atmospheric, ocean and land surface processes is also important, to establish whether the models are likely to be realistic.

- Additional forcings of regional climate. Greenhouse gas changes are not the only anthropogenic driver of climate change; atmospheric aerosols and land cover change are also important, and unlike greenhouse gases, the strength of their influence varies significantly from place to place. The CMIP3 models used in most impacts studies generally account for aerosols but not land cover change.

- Uncertainty in impacts processes. The consequences of a given changes in weather or climatic conditions for biophysical impacts such as river flows, drought, flooding, crop yield or ecosystem distribution and functioning depend on many other processes which are often poorly-understood, especially at large scales. In particular,

the extent to which different biophysical impacts interact with each other has been hardly studied, but may be crucial; for example, impacts of climate change on crop yield may depend not only on local climate changes affecting rain-fed crops, but also remote climate changes affecting river flows providing water for irrigation.

- Uncertainties in non-climate effects of some greenhouse gases. As well as being a greenhouse gas, CO_2 exerts physiological influences on plants, affecting photosynthesis and transpiration. Under higher CO_2 concentrations, and with no other limiting factors, photosynthesis can increase, while the requirements of water for transpiration can decrease. However, while this has been extensively studied under experimental conditions, including in some cases in the free atmosphere, the extent to which the ongoing rise in ambient CO_2 affects crop yields and natural vegetation functioning remains uncertain and controversial. Many impacts projections assume CO_2 physiological effects to be significant, while others assume it to be non-existent. Studies of climate change impacts on crops and ecosystems should therefore be examined with care to establish which assumptions have been made.

In addition to these uncertainties, the climate varies significantly through natural processes from year-to-year and also decade-to-decade, and this variability can be significant in comparison to anthropogenic forcings on shorter timescales (the next few decades) particularly at regional scales. Whilst we can characterise the natural variability it will not be possible to give a precise forecast for a particular year decades into the future.

A further category of uncertainty in projections arises as a result of using different methods to correct for uncertainties and limitations in climate models. Despite being painstakingly developed in order to represent current climate as closely as possible, current climate models are nevertheless subject to systematic errors such as simulating too little or too much rainfall in some regions. In order to reduce the impact of these, '*bias correction*' techniques are often employed, in which the climate model is a source of information on the *change* in climate which is then applied to the observed present-day climate state (rather than using the model's own simulation of the present-day state). However, these bias-corrections typically introduce their own uncertainties and errors, and can lead to inconsistencies between the projected impacts and the driving climate change (such as river flows changing by an amount which is not matched by the original change in precipitation). Currently, this source of uncertainty is rarely considered

When climate change projections from climate models are applied to climate change impact models (e.g. a global hydrological model), the climate model structural uncertainty carries through to the impact estimates. Additional uncertainties include changes in future emissions and population, as well as parameterisations within the impact models (this is rarely considered). Figure 1 highlights the importance of considering climate model structural uncertainty in climate change impacts assessment. Figure 1 shows that for 2°C prescribed global-mean warming, the magnitude of, and sign of change in average annual runoff from present, simulated by an impacts model, can differ depending upon the GCM that provides the climate change projections that drive the impact model. This example also shows that the choice of impact model, in this case a global hydrological model (GHM) or catchment-scale hydrological model (CHM), can affect the magnitude of impact and sign of change from present (e.g. see IPSL CM4 and MPI ECHAM5 simulations for the Xiangxi). To this end, throughout this review, the number of climate models applied in each study reviewed, and the other sources of uncertainty (e.g. emissions scenarios) are noted. Very few studies consider the application of multiple impacts models and it is recommended that future studies address this.

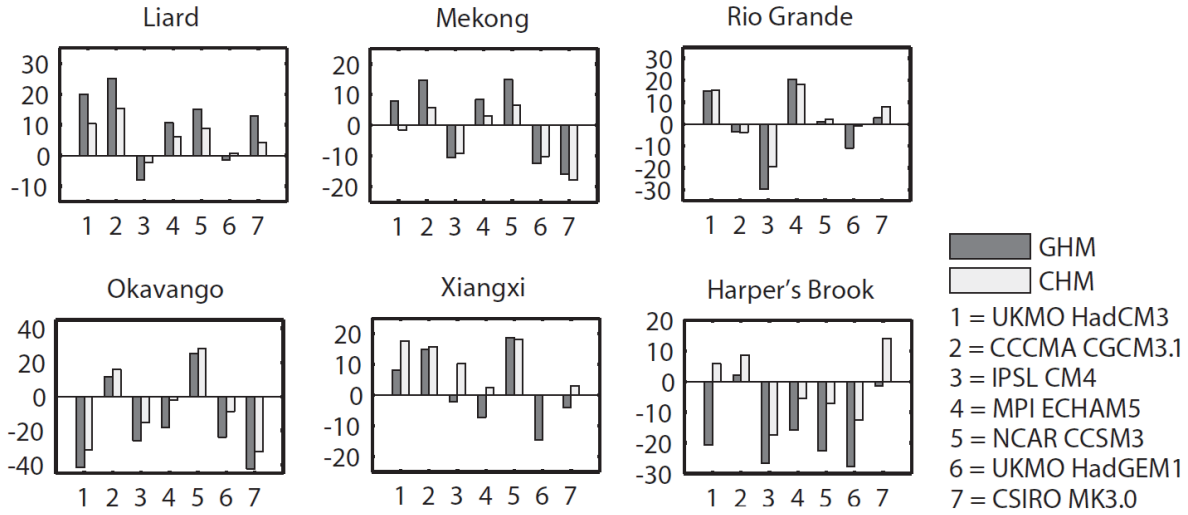

Figure 1. *Change in average annual runoff relative to present (vertical axis; %), when a global hydrological model (GHM) and a catchment-scale hydrological model (CHM) are driven with climate change projections from 7 GCMs (horizontal axis), under a 2°C prescribed global-mean warming scenario, for six river catchments. The figure is from Gosling et al. (2011).*

Uncertainties in the large scale climate relevant to Kenya includes changes in the El Niño-Southern Oscillation (ENSO) which could undergo rapid change with climate change. This could have a serious impact on large-scale atmospheric circulation, rainfall and seasonality in many parts of the world. Latif and Keenlyside (2009) concluded that, at this stage of understanding, it is not known how climate change might affect the tropical Pacific climate

system. None of the global climate models (GCMs) they analysed showed rapid changes in behaviour. However, a threshold of abrupt change cannot be ruled out because whilst the GCMs that Latif and Keenlyside (2009) analysed (the CMIP3 multi-model dataset) are better than the previous generation of models (Reichler and Kim, 2008), these same models all show large biases in simulating the contemporary tropical Pacific, with no consensus on the sign of change in ENSO-like response.

The Indian Ocean Dipole (IOD) is another climate mode which arises from ocean–atmosphere interaction (Saji et al., 1999). The IOD causes inter-annual climate variability in the tropical Indian Ocean, and has both positive and negative phases. During positive IOD events, the East African region receives higher than normal rainfall, while rainfall in Indonesia and Australia is reduced, which can result in severe drought (Saji et al., 1999). There remains high uncertainty as to how the IOD may be affected by climate change.

Summary of findings for each sector

Crop yields

- Quantitative crop yield projections under climate change scenarios for Kenya vary across studies due to the application of different models, assumptions and emissions scenarios.
- However, the majority of global- and regional-scale studies included here generally project yield declines with climate change for the country's most important staple crops; maize and beans.
- National-scale studies highlight the importance of water storage in ameliorating and managing the impact of future climate change on the country's crops.
- Important knowledge gaps and key uncertainties include the quantification of yield increases due to CO_2 fertilisation, quantification of yield reductions due to ozone damage and the extent to which crop diseases might affect crop yields with climate change.

Food security

- Kenya is currently a country with moderately high levels of undernourishment. Several global-scale studies project that Kenya could face increasingly serious food security issues over the next 40 years.
- One study concluded that the national economy of Kenya presents a moderate vulnerability to climate change impacts on fisheries by the 2050s.

Water stress and drought

- Recent analysis of Kenya's current water resources has shown it is exposed to a high water security threat across its entire area.
- Future water availability is uncertain, with potential increases in annual run-off masking overall reductions in water availability during certain periods, while studies neglect the lack of infrastructure to store water.

- Large uncertainties remain in global-, regional- and national-scale projections of future water stress and drought for the country, and as such, knowledge is little improved beyond that reported in the IPCC AR4.

- Simulations from the AVOID programme project that climate change generally has a minor impact on water stress beyond 2030 in Kenya, and that some parts of the country may experience a decrease with climate change from 2050 onward.

Pluvial flooding and rainfall

- The IPCC AR4 noted potential increases in mean precipitation across East Africa, especially in summer.

- Some recent work has contradicted this, suggesting the potential for decreased summer rainfall over Kenya in the future.

Fluvial flooding

- A number of global-scale and catchment-scale assessments are consistent in indicating that flood magnitudes in Kenya could increase with climate change.

- Simulations by the AVOID programme support this, with a large majority of the models showing a tendency for (sometimes very large) increases in flood risk, particularly later in the century and in the A1B scenario.

Tropical cyclones

- There remains large uncertainty in the current understanding of how tropical cyclones might be affected by climate change, as conclusions are based upon a limited number of studies whose projections are from either coarse-resolution global models or from statistical or dynamical downscaling techniques. To this end, caution should be applied in interpreting model-based results, even where the models are in agreement.

- Kenya is occasionally affected by tropical cyclones moving westward from the Indian Ocean. There is considerable uncertainty in projections of overall Indian Ocean cyclone frequency and intensity, however.

- Furthermore, there is large uncertainty in projections of the tracks of these cyclones toward a particular country.
- Uncertainty in projections means that it is not possible to robustly state whether cyclone damages in Kenya may increase or decrease with climate change.

Coastal regions

- A recent study provides new knowledge relative to the IPCC AR4, for coastal impacts in Kenya. A 10% intensification of the current 1-in-100-year storm surge combined with a 1m Sea Level Rise (SLR) could affect around 42% of coastal total land, 22% of coastal agricultural land, 32% of coastal GDP, and 39% of coastal urban areas.
- Research presented in the first national communication of Kenya to the Conference of the Parties to the United Nations Framework Convention on Climate Change (UNFCC) also suggests that Kenya is highly vulnerable to SLR, and that impacts could be severe, especially in the Mombasa district.

Crop yields

Headline

Crop yield projections under climate change scenarios for Kenya vary greatly across studies due to the application of different models, assumptions and emissions scenarios. However, generally, the majority of studies show yield declines with climate change for the most important staple crops; maize and beans. It should be noted that some of the projections presented here are for regions greater than Kenya, e.g. East Africa or Subsaharan Africa (these are highlighted in such cases). Whilst Kenya is included in these regions, it is unclear how representative these simulations are for Kenya alone.

Important knowledge gaps and key uncertainties, which are applicable to Kenya as well as at the global-scale, include; the quantification of yield increases due to CO_2 fertilisation and yield reductions due to ozone damage (Ainsworth and McGrath, 2010, Iglesias et al., 2009), and the extent crop diseases could affect crop yields with climate change (Luck et al., 2011).

Results from the AVOID programme for Kenya indicate that the balance of projected changes in cropland suitability is more towards increased suitability in 2030 and this situation remains the same through the 21st century for the mitigation scenario. However, under A1B the balance shifts to be more even between increasing and decreasing suitability.

Supporting literature

Introduction

The impacts of climate change on crop productivity are highly uncertain due to the complexity of the processes involved. Most current studies are limited in their ability to capture the uncertainty in regional climate projections, and often omit potentially important aspects such as extreme events and changes in pests and diseases. Importantly, there is a lack of clarity on how climate change impacts on drought are best quantified from an agricultural perspective, with different metrics giving very different impressions of future risk. The dependence of some regional agriculture on remote rainfall, snowmelt and glaciers adds to the complexity - these factors are rarely taken into account, and most studies focus solely on the impacts of local climate change on rain-fed agriculture. However, irrigated agricultural land produces approximately 40-45 % of the world's food (Doll and Siebert 2002), and the water for irrigation is often extracted from rivers which can depend on climatic conditions far

from the point of extraction. Hence, impacts of climate change on crop productivity often need to take account of remote as well as local climate changes. Indirect impacts via sea-level rise, storms and diseases have also not been quantified. Perhaps most seriously, there is high uncertainty in the extent to which the direct effects of CO_2 rise on plant physiology will interact with climate change in affecting productivity. Therefore, at present, the aggregate impacts of climate change on large-scale agricultural productivity cannot be reliably quantified (Gornall et al, 2010). This section summarises findings from a range of post IPCC AR4 assessments to inform and contextualise the analysis performed by AVOID programme for this project. The results from the AVOID work are discussed in the next section.

According to the FAO (FAO, 2008), agricultural production in Kenya is highly diverse but maize is the major staple crop (see Table 1). Other important food crops include beans, plantains, pigeon peas, cow peas, sweet potatoes and cassava.

Harvested area (ha)		Quantity (Metric ton)		Value ($1000)	
Maize	1700000	Sugar cane	5110000	Tea	374000
Beans, dry	641000	Maize	2360000	Maize	259000
Pigeon peas	195000	Sweet potatoes	894000	Tomatoes	132000
Tea	157000	Bananas	843000	Plantains	131000
Coffee, green	155000	Plantains	843000	Beans, dry	115000
Cow peas, dry	148000	Cassava	750000	Vegetables fresh (nes)[1]	111000
Wheat	127000	Potatoes	600000	Sugar cane	106000

Table 1. *The top 7 crops by harvested area, quantity and value according to the FAO (2008) in Kenya. Crops that feature in all lists are shaded green; crops that feature in two top 7 lists are shaded amber. Data is from FAO (2008) and has been rounded down to three significant figures.*

A number of global, regional, national and sub-national impact model studies, which include results for some of the main crops in Kenya, have been conducted. They applied a variety of methodological approaches, including using different climate model inputs and treatment of other factors that might affect yield, such as impact of increased CO_2 in the atmosphere on plant growth and adaption of agricultural practises to changing climate conditions. These different models, assumptions and emissions scenarios mean that there are a range of crop yield projections for Kenya. However, the majority of studies explored in this report show that yield declines with climate change for the most important staple crops; maize and beans.

Important knowledge gaps, which are applicable to Kenya as well as at the global-scale, include; the quantification of yield reductions due to ozone damage (Ainsworth and McGrath, 2010, Iglesias et al., 2009), and the extent crop diseases could affect crop yields with climate

change (Luck et al., 2011). Most crop simulation models do not include the direct effect of extreme temperatures on crop development and growth, thus only changes in mean climate conditions are considered to affect crop yields for the studies included here.

Assessments that include a global or regional perspective

Recent Past

Crop yield changes could be due to a variety of factors, which might include, but not be confined to, a changing climate. In order to assess the impact of recent climate change (1980-2008) on wheat, maize, rice and soybean, Lobell et al. (2011) looked at how the overall yield trend in these crops changed in response to changes in climate over the period studied. The study was conducted at the global-scale but national estimates for Kenya were also calculated. Lobell et al. (2011) divided the climate-induced yield trend by the overall yield trend for 1980–2008, to produce a simple metric of the importance of climate relative to all other factors. The ratio produced indicates the influence of climate on the productivity trend overall. So for example a value of –0.1 represents a 10% reduction in yield gain due to climate change, compared to the increase that could have been achieved without climate change, but with technology and other gains. This can also be expressed as 10 years of climate trend being equivalent to the loss of roughly 1 year of technology gains. For Kenya, negative effects on maize and rice yields were estimated relative to what could have been achieved without the climate trends (see Table 2).

Crop	Trend
Maize	-0.2 to -0.1
Rice	-0.2 to -0.1
Wheat	n/a
Soybean	n/a

Table 2. *The estimated net impact of climate trends for 1980-2008 on crop yields. Climate-induced yield trend divided by overall yield trend. 'n/a' infers zero or insignificant crop production or unavailability of data. Data is from Lobell et al. (2011).*

Climate change studies

Included in this section are results from recent studies that have applied climate projections from Global Climate Models (GCMs) to crop yield models to assess the global-scale impact of climate change on crop yields, and which include impact estimates at the national-scale for Kenya.(Iglesias and Rosenzweig, 2009). The process of CO_2 fertilisation of some crops is usually included in climate impact studies of yields. However, other gases can influence crop growth, and are not always included in impact model projections. An example of this is

ozone, (O_3) and so a study which attempts to quantify the potential impact of changes in the atmospheric concentration of this gas is also included Avnery et al., (2011).

In addition to these studies, the AVOID programme analysed the patterns of climate change for 21 GCMs to establish an index of 'climate suitability' of agricultural land. Climate suitability is not directly equivalent to crop yields, but is a means of looking at a standard metric across all countries included in this project, and of assessing the level of agreement on variables that affect crop production between all 21 GCMs.

Iglesias and Rosenzweig (2009) repeated an earlier study presented by Parry et al. (2004) by applying climate projections from the HadCM3 GCM (instead of HadCM2, which was applied by Parry et al. (2004)), under seven SRES emissions scenarios and for three future time periods.This study used consistent crop simulation methodology and climate change scenarios globally, and weighted the model site results by their contribution to regional and national, rain-fed and irrigated production. The study also applied a quantitative estimation of physiological CO_2 effects on crop yields and considered the affect of adaptation by assessing the potential of the country or region to reach optimal crop yield. The results from the study are presented in Table 3 and Table 4. The simulations showed that wheat yields in Kenya increased up to 2020 with climate change but declined thereafter, such that by 2050 and 2080 yield was projected below baseline (1970-2000) levels in 5 and 7 emission scenarios respectively. Maize yield declined steadily with climate change, with yield levels consistently below baseline in all emission scenarios.

Scenario	Year	Wheat	Maize
A1FI	2020	1.40	-1.60
	2050	-4.07	-11.07
	2080	-17.41	-27.41
A2a	2020	2.24	-0.76
	2050	-1.84	-8.84
	2080	-7.79	-18.79
A2b	2020	1.91	-1.09
	2050	0.43	-6.57
	2080	-7.45	-18.45
A2c	2020	2.71	-0.29
	2050	1.39	-5.61
	2080	-6.27	-17.27
B1a	2020	1.78	-1.22
	2050	-0.87	-5.87
	2080	-4.77	-10.77
B2a	2020	0.82	-2.18
	2050	-1.80	-6.80
	2080	-6.77	-13.77
B2b	2020	0.86	-2.14
	2050	-2.99	-7.99
	2080	-4.36	-11.36

Table 3. *Wheat and maize yield changes (%) relative to baseline scenario (1970-2000) for different emission scenarios and future time periods. Some emissions scenarios were run in an ensemble simulation (e.g. A2a, A2b, A2c). Data is from Iglesias and Rosenzweig (2009).*

	Wheat		Maize	
	Up	Down	Up	Down
Baseline to 2020	7	0	0	7
Baseline to 2050	2	5	0	7
Baseline to 2080	0	7	0	7
2020 to 2050	0	7	0	7
2050 to 2080	0	7	0	7

Table 4. *The number of emission scenarios that predict yield gains ("Up") or yield losses ("Down") for wheat and maize between two points in time. Data is from Iglesias and Rosenzweig (2009).*

Elsewhere, several studies have assessed the impact of climate change on a global-scale and include impact estimates for Sub-Saharan Africa or Eastern Africa as a whole (Arnell et al., 2010, Nelson et al., 2009, Tatsumi et al., 2011, Lobell et al., 2008, Fischer et al., 2009, Thornton et al., 2011). Whilst these studies provide a useful indicator of crop yields under climate change for the *region*, it should be noted that the crop yields presented in such cases are not definitive *national* estimates. This is because the yields are averaged over the entire region, which includes other countries as well as Kenya.

Thornton et al. (2011) used an ensemble mean of three emissions scenarios (A2, A1B and B1) and 14 GCMs to run crop simulations for conditions in a 4°C warmer world by 2090, for maize and *Phaseolus* bean. For Eastern Africa a yield loss of 19% and 47% was projected for maize and beans respectively (mean across the 14 GCMs).

Nelson et al. (2009) applied two GCMs in combination with the DSSAT crop model under the SRES A2 emissions scenario to project future yields of rice, maize, soybean, wheat and groundnut with and without CO_2 enrichment, and for rain-fed and irrigated lands, for several regions across the globe. Table 5 represents the results for Sub-Saharan Africa, the IFPRI regional grouping in which Kenya is included. It can be seen that in all cases, increased CO_2 levels were of benefit to all crops simulated, whether rain-fed or irrigated. However the effects of CO_2 fertilisation in the case of rain-fed wheat and rain-fed maize are not projected to be large enough to fully compensate for factors which lead to yield reductions, such as increasing temperatures, out to 2050.

GCM and CO_2 fertilisation	**Rice**		**Maize**		**Soybean**		**Wheat**		**Groundnut**	
	Rf.	Irr.	Rf.	Irr.	Rf.	Irr.	Rf.	Irr.	Rf.	Irr.
CSIRO NoCF	0.1	-11.4	-2.4	0.3	-3.5	4.6	-19.3	0.7	-4.1	-11.5
NCAR NoCF	-0.5	-14.1	-4.6	0.6	-5.8	5.0	-21.9	1.4	-8.6	-11.3
CSIRO CF	8.1	5.7	-0.8	0.5	19.1	17.8	-11.2	7.3	14.2	3.9
NCAR CF	7.3	2.4	-2.7	0.8	17.8	17.8	-15.9	9.7	8.8	4.2

Table 5. *Projected yield changes (%) by 2050 compared to baseline (yields with 2000 climate) using two GCMs with (CF) and without CO_2 fertilisation effect (NoCF). Rain-fed (Rf.) and Irrigated (Irr.) crop lands were assessed separately. Data is from Nelson et al. (2009).*

Tatsumi et al. (2011) applied an improved version of the GAEZ crop model (iGAEZ) to simulate crop yields on a global scale for wheat, potato, cassava, soybean, rice, sweet potato, maize, green beans. The impact of global warming on crop yields from the 1990s to 2090s was assessed by projecting five GCM outputs under the SRES A1B scenario and comparing the results for crop yields as calculated using the iGAEZ model for the period of 1990-1999. The results for Eastern Africa, which includes Kenya, are displayed in Table 6. Wheat, sweet potato, potato and soybean are projected to be negatively affected, with small positive increases seen for green beans, maize and rice, and a larger increase in yield for cassava.

Wheat	Potato	Cassava	Soybean	Rice	Sweet	Maize	Green
-14.6	-17.05	10.49	-12.41	0.92	-15.06	0.43	0.21

Table 6. *Average change in yield (%), during 1990s-2090s in Eastern Africa. Data is from Tatsumi et al. (2011).*

To further quantify the impact of climate change on crops, Arnell et al. (2010) used 5GCMs to assess the effects of different climate scenarios on crop productivity. Specifically, the crop simulation model GLAM-maize was used to simulate the effect of climate change on maize productivity. For Eastern Africa a loss of between 27% and 41% of yield was predicted relative to the baseline (1961-1990) in the absence of adaptation and mitigation strategies. Implementing the mitigation strategy A1B-2016-5-L (a 5%/year reduction in emissions from 2016 onwards to a low emissions floor) reduced the negative impact by approximately 17% and 27% in 2050 and 2100 respectively.

The impact of future climate on crop yields of rain-fed cereals was investigated by Fischer (2009) who projected global 'production potential' changes for 2050 using the GAEZ (Global Agro-Ecological Zones) crops model with climate change scenarios from the HadCM3 and CSIRO GCMs respectively, under SRES A2 emissions. The impact of future climate on crop yields of rain-fed cereals are presented in Table 7 (relative to yield realised under current climate) for Eastern Africa. As with the study by Nelson et al. (2009) CO_2 fertilization was found to offset, but by no means fully compensate for the projected impacts of climate change. Both studies also projected wheat would be the most negatively affected crop.

	CO_2 fert.	2020s		2050s		2080s	
		CSIRO	HADCM3	CSIRO	HADCM3	CSIRO	HADCM3
Rain-fed wheat	Yes	-30	-38	-48	-63	-72	-81
	No	-31	n/a [1]	-50	n/a	-74	n/a
Rain-fed maize	Yes	3	6	4	9	-1	11
	No	1	n/a	0	n/a	-7	n/a
Rain-fed cereals	Yes	n/a	3	n/a	6	n/a	9
	No	n/a	n/a	n/a	n/a	n/a	n/a
Rain-fed sorghum	Yes	4	n/a	4	n/a	-2	n/a
	No	2	n/a	0	n/a	-7	n/a

Table 7. *Impacts of climate change on the production potential of rain-fed cereals in current cultivated land (% change with respect to yield realised under current climate), with two GCMs and with and without CO_2 fertilisation ("CO_2 fert.") under SRES A2 emissions. Data is from Fischer (2009).*

To identify appropriate adaptation priorities Lobell et al. (2008) conducted an analysis of climate risks for the major crops in 12 food-insecure regions. Statistical crop models were

used in combination with climate projections for 2030 from 20 GCMs that have contributed to the World Climate Research Programme's Coupled Model Intercomparison Project phase 3. The results from the study for Eastern Africa, are presented in Figure 2. Lobell et al. (2008) found that in Eastern Africa, climate change had an adverse impact in 2030 on crop yield for cowpeas (at least 95% of projections were associated with yield losses) and to a lesser degree beans and sugar cane (at least 75% of projections were associated with yield losses). Yield increases were projected for barley (at least 95% of projections were associated with yield gains), wheat, groundnut and rice (at least 75% of projections were associated with yield gains).

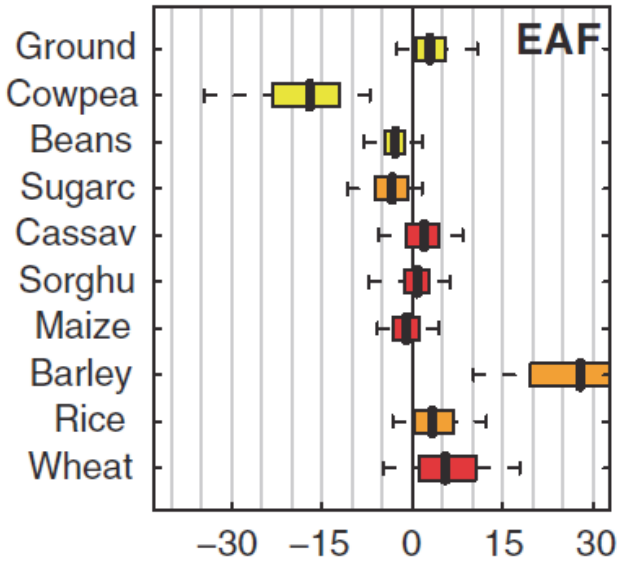

Figure 2. *Probabilistic projections of production impacts in 2030 from climate change (expressed as a percentage of 1998 to 2002 average yields) for Eastern Africa. Red, orange, and yellow indicate a Hunger Importance Ranking of 1 to 30 (more important), 31 to 60 (important), and 61 to 94 (less important), respectively. Dashed lines extend from 5th to 95th percentile of projections, boxes extend from 25th to 75th percentile, and the middle vertical line within each box indicates the median projection. Figure is from Lobell et al. (2008).*

In addition to the studies looking at the effect of changes in climate and CO_2 concentrations on crop yield, Avnery et al. (2011) investigated the effects of ozone surface exposure on crop yield losses for soybeans, maize and wheat under the SRES A2 and B1 scenarios respectively. Two metrics of ozone exposure were investigated; seasonal daytime (08:00-19:59) mean O_3 ("M12") and accumulated O_3 above a threshold of 40 ppbv ("AOT40"). The results for Kenya are presented in Table 8.

	A2		B1	
	M12	AOT40	M12	AOT40
Soybeans	-	-	-	-
Maize	2-4	0-2	2-4	0-2
Wheat	-	-	-	-

Table 8. *National relative crop yield losses (%) for 2030 under A2 and B1 emission scenarios according to the M12 (seasonal daytime (08:00–19:59) mean) and AOT40 (accumulated O_3 above a threshold of 40 ppbv) metrics of O_3 exposure. Data is from Avnery et al. (2011).*

National-scale or sub-national scale assessments

Climate change studies

A study by Cooper et al. (2009) simulated crop yield for short-duration pigeon-pea and maize using historical daily weather data (1959-2004) and crop models under prescribed temperature increase scenarios from +1°C to +5°C. The simulations suggested a linear response of crop yield (reduction) to temperature increase. The simulations for pigeon-pea also suggested that regardless of the sign of precipitation change, temperature increases was always associated with yield loss by reducing time to maturity (see Table 9).

Temperature	Mean rainfall change from current levels			
	0%	+10%	0%	-10%
	Maize	Pigeon-pea		
Current	-	n/a	-	n/a
+1°C	-4.1	3.5	-7.1	-19.4
+2°C	-9.0	-4.0	-13.4	-24.1
+3°C	-14.2	-10.3	-19.0	-29.0
+4°C	-18.8	-16.2	-23.8	-32.8
+5°C	-25.1	-21.6	-28.7	-37.2

Table 9. *Simulated maize and pigeon-pea yield changes (%) relative to mean yield under current climate, as caused by temperature increases alone (maize) or by a combination of temperature increase and rainfall changes (pigeon-pea), at Makindu and Katumani in Kenya respectively.*

While yield losses are possible with climate change, recent work has highlighted the importance of adaptation. Research suggests that not only can water conservation measures have important beneficial impacts on water storage in the soil profile and hence the length of growing period under current climate conditions, they can also play a major role in helping to manage and ameliorate the impact of future climate change (Cooper et al., 2009, van de Steeg et al., 2009, Rao and Okwach, 2005).

AVOID programme results

To further quantify the impact of climate change on crops, the AVOID programme simulated the effect of climate change on the suitability of land for crop cultivation for all countries reviewed in this literature assessment based upon the patterns of climate change from 21 GCMs (Warren et al., 2010). This ensures a consistent methodological approach across all countries and takes consideration of climate modelling uncertainties.

Methodology

The effect of climate change on the suitability of land for crop cultivation is characterised here by an index which defines the percentage of cropland in a region with 1) a decrease in suitability or 2) an increase in suitability. A threshold change of 5% is applied here to characterise decrease or increase in suitability. The crop suitability index is calculated at a spatial resolution of 0.5°x0.5°, and is based on climate and soil properties (Ramankutty et al., 2002). The baseline crop suitability index, against which the future changes are measured, is representative of conditions circa 2000. The key features of the climate for the crop suitability index are temperature and the availability of water for plants. Changes in these were derived from climate model projections of future changes in temperature and precipitation, with some further calculations then being used to estimate actual and potential evapotranspiration as an indicator of water availability. It should be noted that changes in atmospheric CO_2 concentrations can decrease evapotranspiration by increasing the efficiency of water use by plants (Ramankutty et al., 2002), but that aspect of the index was not included in the analysis here. Increased CO_2 can also increase photosynthesis and improve yield to a small extent, but again these effects are not included. Exclusion of these effects may lead to an overestimate of decreases in suitability.

The index here is calculated only for grid cells which contain cropland circa 2000, as defined in the global crop extent data set described by Ramankutty et al. (2008) which was derived from satellite measurements. It is assumed that crop extent does not change over time. The crop suitability index varies significantly for current croplands across the world (Ramankutty et al., 2002), with the suitability being low in some current cropland areas according to this index. Therefore, while climate change clearly has the potential to decrease suitability for cultivation if temperature and precipitation regimes become less favourable, there is also scope for climate change to increase suitability in some existing cropland areas if conditions become more favourable in areas where the suitability index is not at its maximum value of 1. It should be noted that some areas which are not currently croplands may already be

suitable for cultivation or may become suitable as a result of future climate change, and may become used a croplands in the future either as part of climate change adaptation or changes in land use arising for other reasons. Such areas are not included in this analysis.

Crop suitability was estimated under the pattern of climate change from 21 GCMs with two emissions scenarios; 1) SRES A1B and 2) an aggressive mitigation scenario where emissions follow A1B up to 2016 but then decline at a rate of 5% per year thereafter to a low emissions floor (denoted A1B-2016-5-L). The application of 21 GCMs is an attempt to quantify the uncertainty due to climate modelling, although it is acknowledged that only one crop suitability impacts model is applied. Simulations were performed for the years 2030, 2050, 2080 and 2100. The results for Kenya are presented in Figure 3.

Under all the climate projections, some existing cropland areas in Kenya become less suitable for cultivation while other existing cropland areas become more suitable. The areas of increased and decreased suitability differ considerably according to the climate model used. Under both emissions scenarios, the area of current cropland projected to undergo increased suitability ranges from 0% to 75% under both emissions scenarios across the full set of models throughout the 21st century. These results are quite unusual and this signal is not necessarily a result of climate change, and could be a feature associated with the way that the model data was processed, or the fact that the driving GCMs behind the impacts model have a relatively low resolution. For this reason, these results should be treated with caution. The small change after 2030 may be because only current croplands are considered – although over a wider area there may be differences in suitability between different scenarios and different times, this would not appear in the current analysis if such changes occurred outside current cropland areas. By 2030, between 0% and 60% of current cropland areas are projected to undergo a decline in suitability for cultivation under both emissions scenarios. By 2100 this has risen to 0 - 80% under A1B and 0 – 70% under the mitigation scenario

So, for Kenya, the balance of projected changes in cropland suitability is more towards increased suitability in 2030 and this situation remains the same through the 21st century for the mitigation scenario. However, under A1B the balance shifts to be more even between increasing and declining suitability.

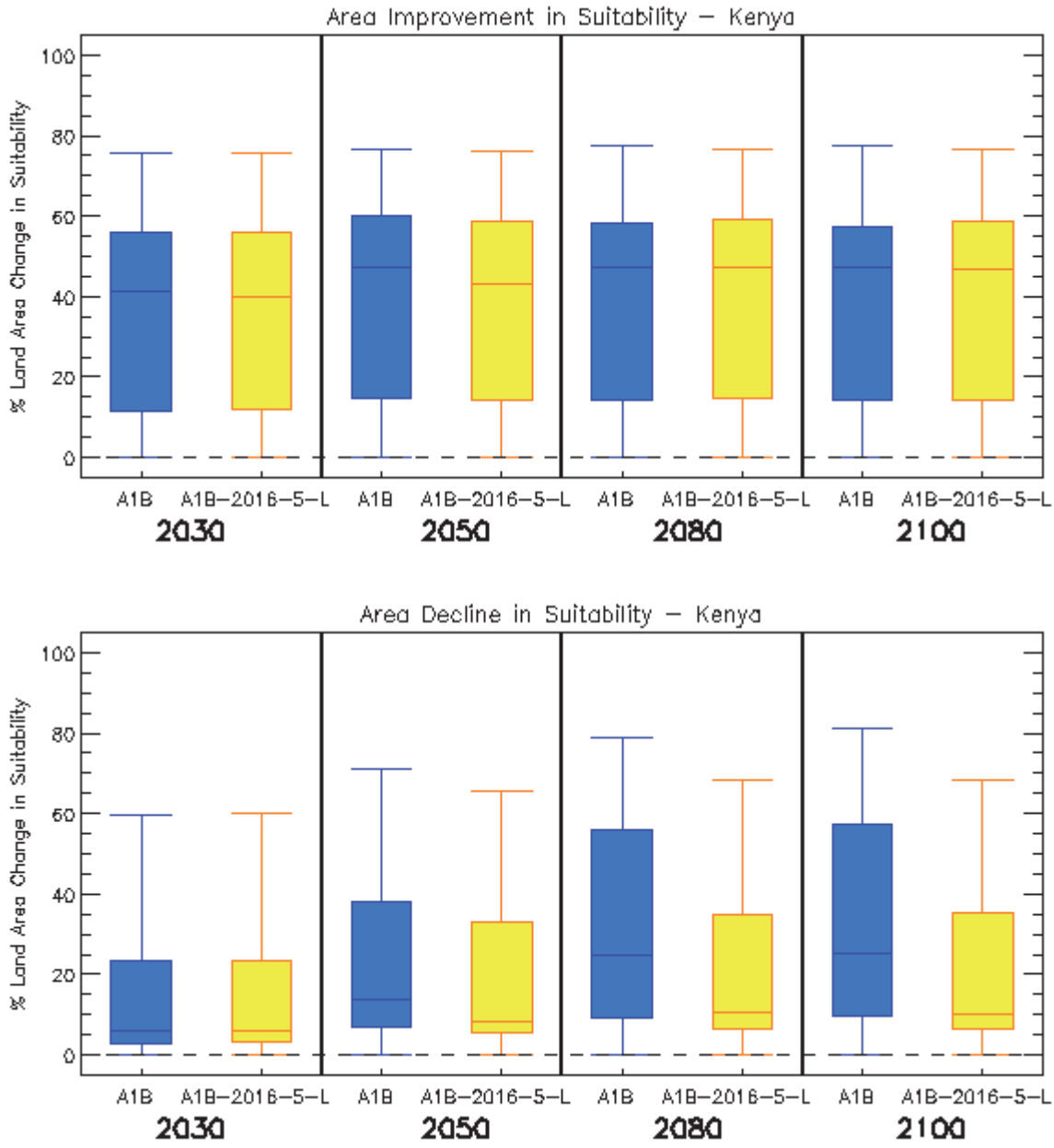

Figure 3. *Box and whisker plots for the impact of climate change on increased crop suitability (top panel) and decreased crop suitability (bottom panel) for Kenya, from 21 GCMs under two emissions scenarios (A1B and A1B-2016-5-L), for four time horizons. The plots show the 25th, 50th, and 75th percentiles (represented by the boxes), and the maximum and minimum values (shown by the extent of the whiskers).*

Food security

Headline

Several studies suggest that food security in Kenya could be threatened by climate change. One study shows that future local food production within Kenya may not be able to meet food demands. This, coupled with Kenya's inability to purchase more foods from outside through trade, means that more efforts are needed to combat hunger in terms of future actions (such as food aid and development programs). Climate change also has the potential to have major effects on national kilocalorie availability and child malnourishment.

Supporting literature

Introduction

Food security is a concept that encompasses more than just crop production, but is a complex interaction between food availability and socio-economic, policy and health factors that influence access to food, utilisation and stability of food supplies. In 1996 the World Food Summit defined food security as existing 'when all people, at all times, have physical and economic access to sufficient, safe and nutritious food to meet their dietary needs, and their food preferences are met for an active and healthy life'.

As such this section cannot be a comprehensive analysis of all the factors that are important in determining food security, but does attempt to assess a selection of the available literature on how climate change, combined with projections of global and regional population and policy responses, may influence food security.'

Assessments that include a global or regional perspective

According to the FAO's Food Security Country profiles (FAO, 2010) a moderately high proportion (20-34%) of Kenya's population are currently undernourished.

Climate change studies

Moreover, a number of global studies point towards a negative outlook for the impact of climate change on food security in Kenya. The most recent of these is presented by Wu et al. (2011) who simulated crop yields with the GIS-based Environmental Policy Integrated Climate (EPIC) model. These simulations were combined with crop areas simulated by a

crop choice decision model to calculate total food production and per capita food availability across the globe, which was used to represent the status of food availability and stability. The study focussed on the SRES A1 scenario and applied climate change simulations for the 2000s (1991–2000) and 2020s (2011–2020). The climate simulations were performed by MIROC (Model for Interdisciplinary Research on Climate) version 3.2., which means the effects of climate model uncertainty were not considered. Downscaled population and GDP data from the International Institute for Applied Systems Analysis (IIASA) were applied in the simulations. Wu et al. (2011) show that both per capita food availability and Kenya's capacity to import food could decrease between 2000 and 2020. Local food production within Kenya may not be able to meet food demands and this coupled with Kenya's populations' inability to purchase more foods from outside through trade, means that more efforts are needed to combat hunger in terms of future actions (such as food aid and development programs), according to Wu et al. (2011) .

A global analysis of food security under climate change scenarios for the 2050s by Falkenmark et al. (2009) considered the importance of water availability for ensuring global food security. The study presents an analysis of water constraints and opportunities for global food production on current croplands and assesses five main factors:

1) how far improved land and water management might go towards achieving global food security,

2) the water deficits that would remain in regions currently experiencing water scarcity and which are aiming at food self-sufficiency,

3) how the water deficits above may be met by importing food,

4) the cropland expansion required in low income countries without the needed purchasing power for such imports, and

5) the proportion of that expansion pressure which will remain unresolved due to potential lack of accessible land.

Similar to the study presented by Wu et al. (2011), there is no major treatment of modelling uncertainty; simulations were generated by only the LPJml dynamic global vegetation and water balance model(Gerten et al. 2004) with population growth and climate change under the SRES A2 emission scenario. Falkenmark et al. (2009) summarise the impacts of future improvements (or lack thereof) in water productivity for each country across the globe and

show that this generates either a deficit or a surplus of water in relation to food water requirements in each country. These can be met either by trade or by horizontal expansion (by converting other terrestrial ecosystems to crop land). The study estimated that in 2050 around one third of the world's population will live in each of three regions: those that export food, those that import food, and those that have to expand their croplands at the expense of other ecosystems because they do not have enough purchasing power to import their food. The simulations demonstrated that Kenya could have to expand their croplands by 2050, which is broadly in agreement with the negative outlook presented for Kenya by Wu et al. (2011).

The International Food Policy Research Institute (IFPRI) have produced a report and online tool that describes the possible impact of climate change on two major indicators of food security; 1) the number of children aged 0-5 malnourished, and 2) the average daily kilocalorie availability (Nelson et al., 2010, IFPRI, 2010)**.** The study considered three broad socio-economic scenarios; 1) a 'pessimistic' scenario, which is representative of the lowest of the four GDP growth rate scenarios from the Millennium Ecosystem Assessment GDP scenarios and equivalent to the UN high variant of future population change, 2) a 'baseline' scenario, which is based on future GDP rates estimated by the World Bank and a population change scenario equivalent to the UN medium variant, and 3) an 'optimistic' scenario that is representative of the highest of the four GDP growth rate scenarios from the Millennium Ecosystem Assessment GDP scenarios and equivalent to the UN low variant of future population change. Nelson et al. (2010) also considered climate modelling and emission uncertainty. The study applied two GCMs, the CSIRO GCM and the MIROC GCM, and forced each GCM with two SRES emissions scenarios (A1B and B1). They also considered a no climate change emissions scenario, which they called 'perfect mitigation' (note that in most other climate change impact studies that this is referred to as the baseline). Estimates for both indicators of food security from 2010 to 2050, for Kenya, are presented in Table 10 and Table 11. Figure 4 displays the effect of climate change, calculated by comparing the 'perfect mitigation' scenario with each baseline, optimistic and pessimistic scenario. Figure 5 and Figure 6 show how the changes projected for Kenya compare with the projections for the rest of the globe (IFPRI, 2010). The results highlight that Kenya is already one of the most food insecure countries on the globe, in line with the findings of FAO(2011). Moreover, whilst under the baseline and pessimistic scenarios, average kilocalorie availability and number of malnourished children increase and decrease respectively, from 2010 to 2050; the pessimistic scenario is associated with large decreases and increases respectively. Furthermore, for both indicators of food security, climate change has a discernible effect,

relative to the no climate change scenario (perfect mitigation) in 2050. For instance, by 2050, climate change is attributable for a decline of up to 14% in kilocalorie availability and an increase of up to 85% in child malnourishment, relative to in the absence of climate change. Within the global context, kilocalorie availability remains low in 2050 (Figure 5) and child malnourishment remains high (Figure 6), which suggests Kenya could continue to face food security issues in 2050.

Scenario	2010	2050
Baseline CSI A1B	1960	2326
Baseline CSI B1	1968	2363
Baseline MIR A1B	1933	2221
Baseline MIR B1	1956	2311
Baseline Perfect Mitigation	2010	2573
Pessimistic CSI A1B	1957	1657
Pessimistic CSI B1	1965	1684
Pessimistic MIR A1B	1929	1574
Pessimistic MIR B1	1942	1615
Pessimistic Perfect Mitigation	2006	1834
Optimistic CSI A1B	1986	2706
Optimistic CSI B1	1991	2726
Optimistic MIR A1B	1956	2563
Optimistic MIR B1	1968	2621
Optimistic Perfect Mitigation	2033	2964

Table 10. *Average daily kilocalorie availability simulated under different climate and socioeconomic scenarios, for Kenya (IFPRI, 2010).*

Scenario	2010	2050
Baseline CSI A1B	1.51	0.81
Baseline CSI B1	1.5	0.78
Baseline MIR A1B	1.53	0.91
Baseline MIR B1	1.51	0.83
Baseline Perfect Mitigation	1.47	0.62
Pessimistic CSI A1B	1.51	1.69
Pessimistic CSI B1	1.5	1.65
Pessimistic MIR A1B	1.54	1.81
Pessimistic MIR B1	1.52	1.75
Pessimistic Perfect Mitigation	1.47	1.46
Optimistic CSI A1B	1.49	0.45
Optimistic CSI B1	1.48	0.44
Optimistic MIR A1B	1.51	0.54
Optimistic MIR B1	1.5	0.5
Optimistic Perfect Mitigation	1.45	0.29

Table 11. *Number of malnourished children (aged 0-5; millions) simulated under different climate and socioeconomic scenarios, for Kenya (IFPRI, 2010).*

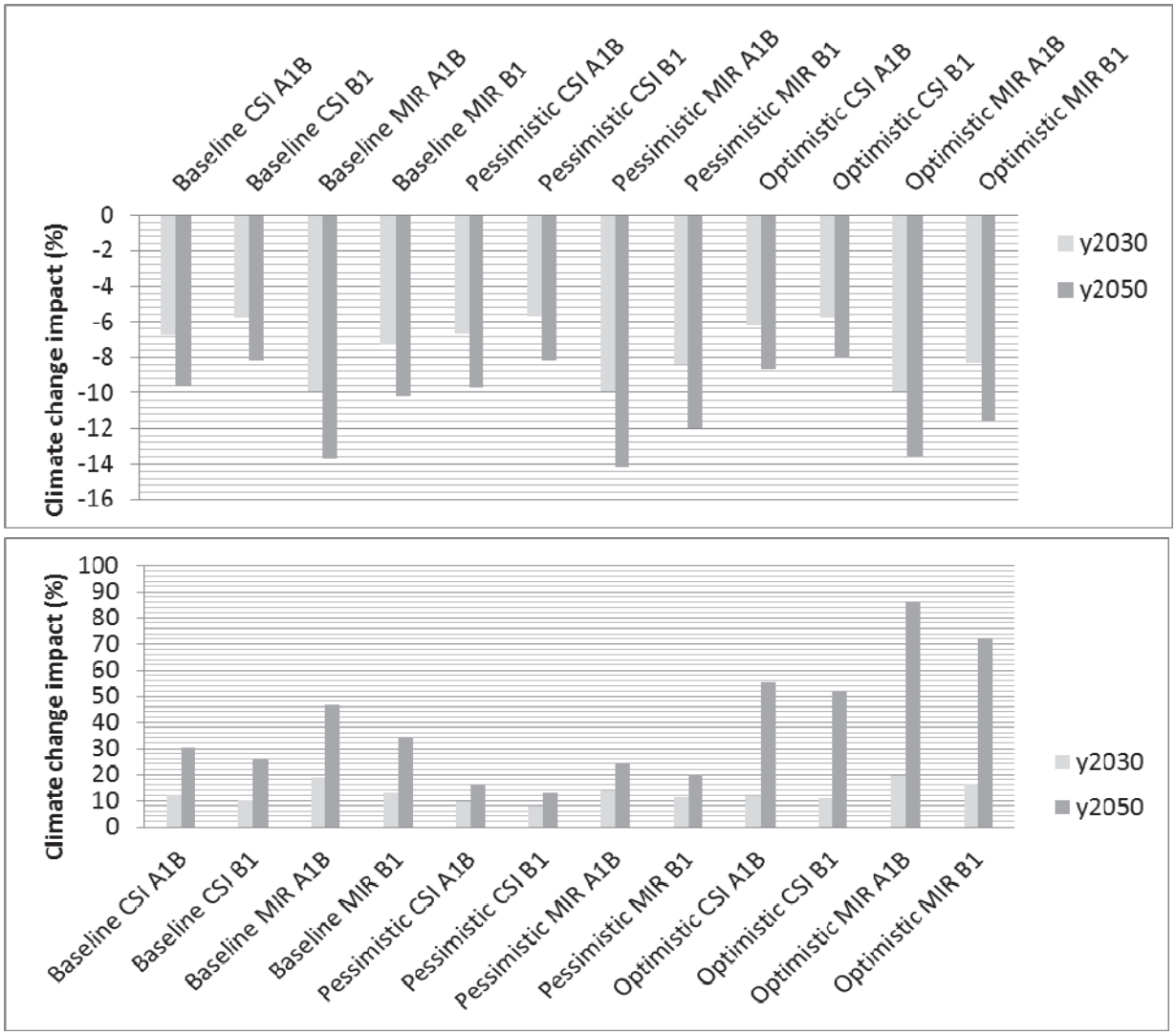

Figure 4. *The impact of climate change on average daily kilocalorie availability (top panel) and number of malnourished children (bottom) (IFPRI, 2010).*

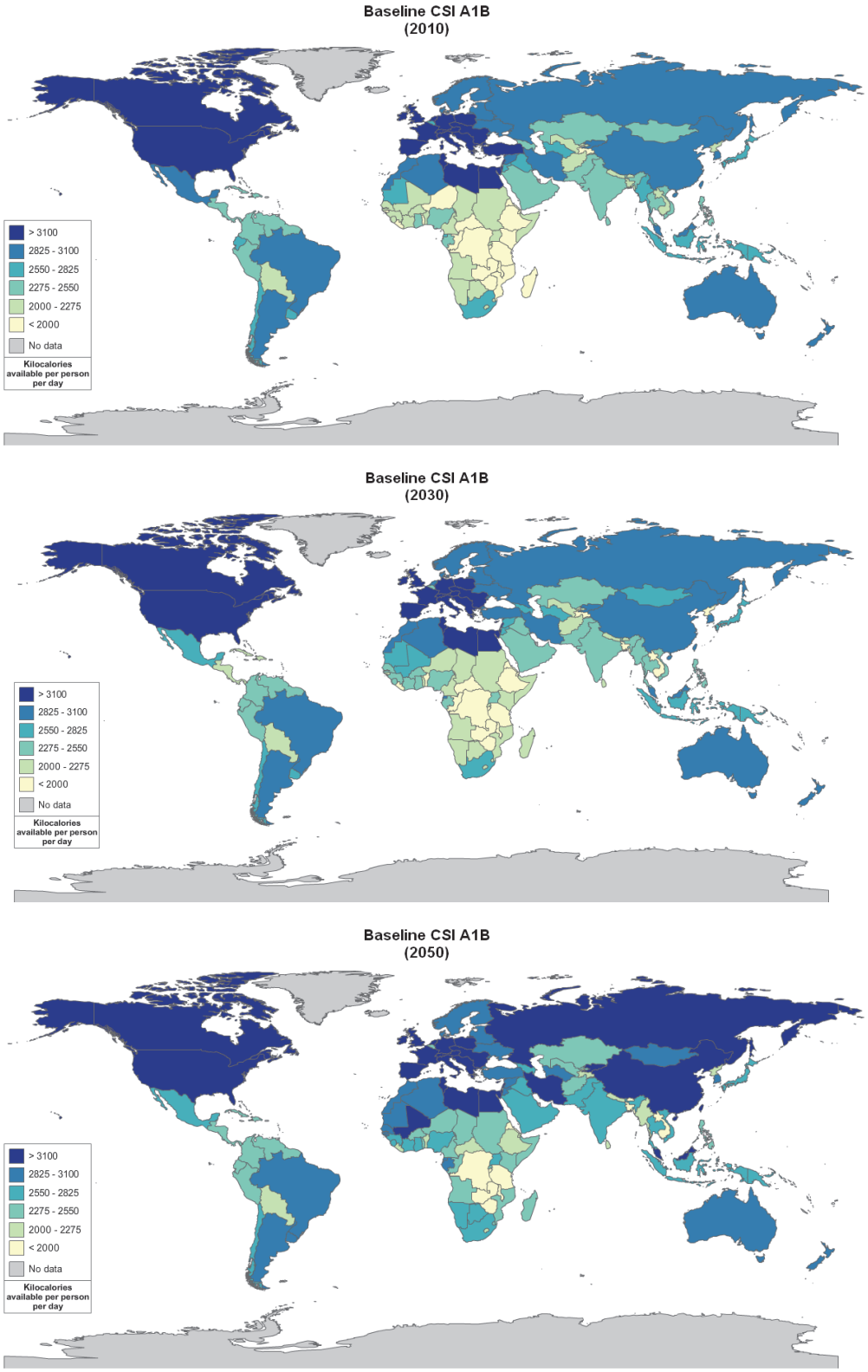

Figure 5. *Average daily kilocalorie availability simulated by the CSIRO GCM (CSI) under an A1B emissions scenario and the baseline socioeconomic scenario, for 2010 (top panel), 2030 (middle panel) and 2050 (bottom panel). Figure is from IFPRI (2010). The changes show the combination of both climate change and socio-economic changes.*

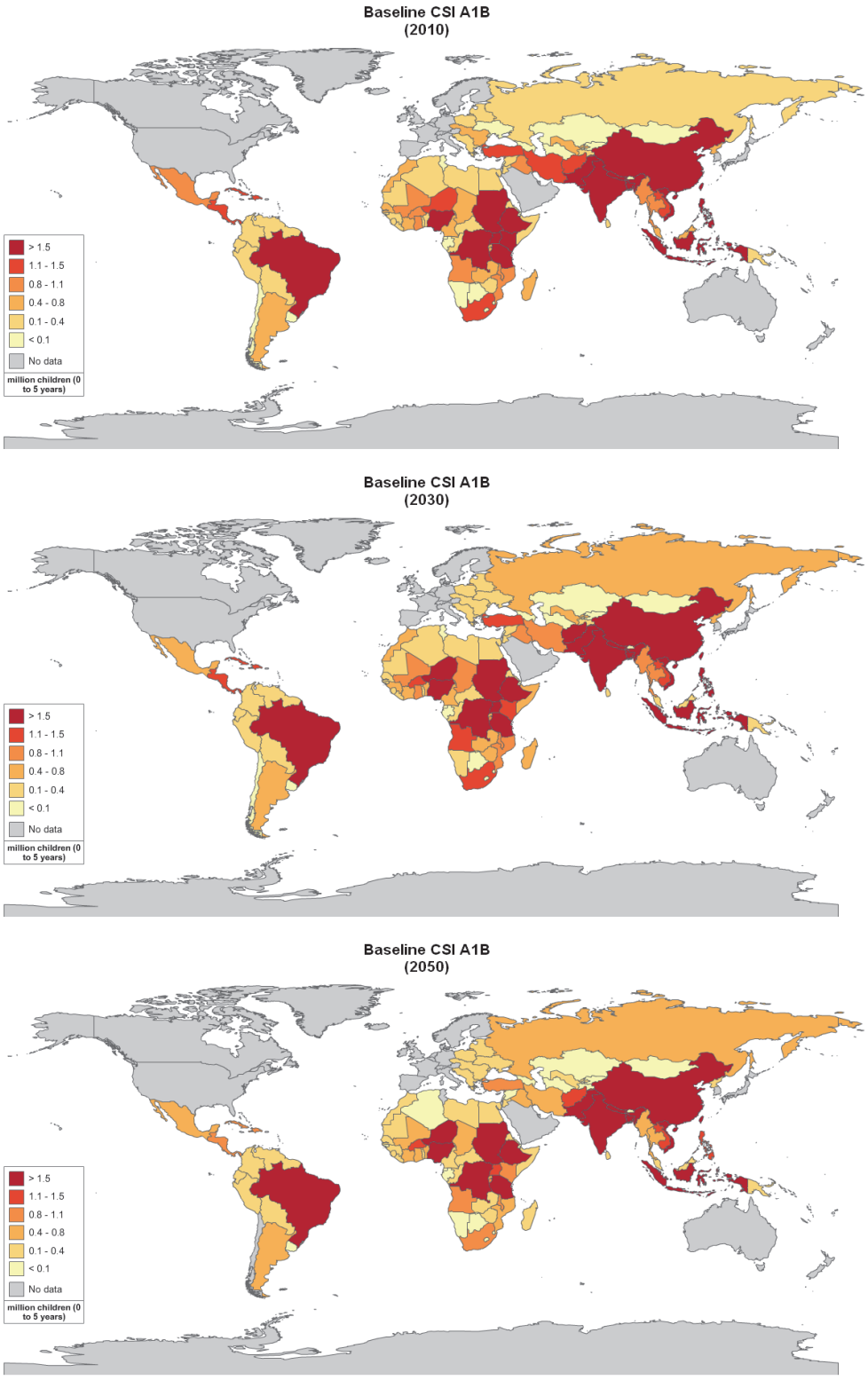

Figure 6. *Number of malnourished children (aged 0-5; millions) simulated by the CSIRO GCM (CSI) under an A1B emissions scenario and the baseline socioeconomic scenario, for 2010 (top panel), 2030 (middle panel) and 2050 (bottom panel). Figure is from IFPRI (2010). The changes show the combination of both climate change and socio-economic changes.*

It is important to note that up until recently, projections of climate change impacts on global food supply have tended to focus solely on production from terrestrial biomes, with the large contribution of animal protein from marine capture fisheries often ignored. However, recent studies have addressed this knowledge gap (Allison et al. 2009). In addition to the direct affects of climate change, changes in the acidity of the oceans, due to increases in CO_2 levels, could also have an impact of marine ecosystems, which could also affect fish stocks. However, this relationship is complex and not well understood, and studies today have not been able to begin to quantify the impact of ocean acidification on fish stocks.

Allison et al. (2009) present a global analysis that compares the vulnerability of 132 national economies to potential climate change impacts on their capture fisheries. The study considered a country's vulnerability to be a function of the combined effect of projected climate change, the relative importance of fisheries to national economies and diets, and the national societal capacity to adapt to potential impacts and opportunities. Climate change projections from a single GCM under two emissions scenarios (SRES A1FI and B2) were used in the analysis. Allison et al. (2009) concluded that the national economy of Kenya presented a moderate vulnerability to climate change impacts on fisheries. In contrast, countries in Central and Western Africa (e.g. Malawi, Guinea, Senegal, and Uganda), Peru and Colombia in north-western South America, and four tropical Asian countries (Bangladesh, Cambodia, Pakistan, and Yemen) were identified as most vulnerable (see Figure 7). It should be noted, however, that results from studies that have applied only a single climate model or climate change scenario should be interpreted with caution. This is because they do not consider other possible climate change scenarios which could result in a different impact outcome, in terms of magnitude and in some cases sign of change.

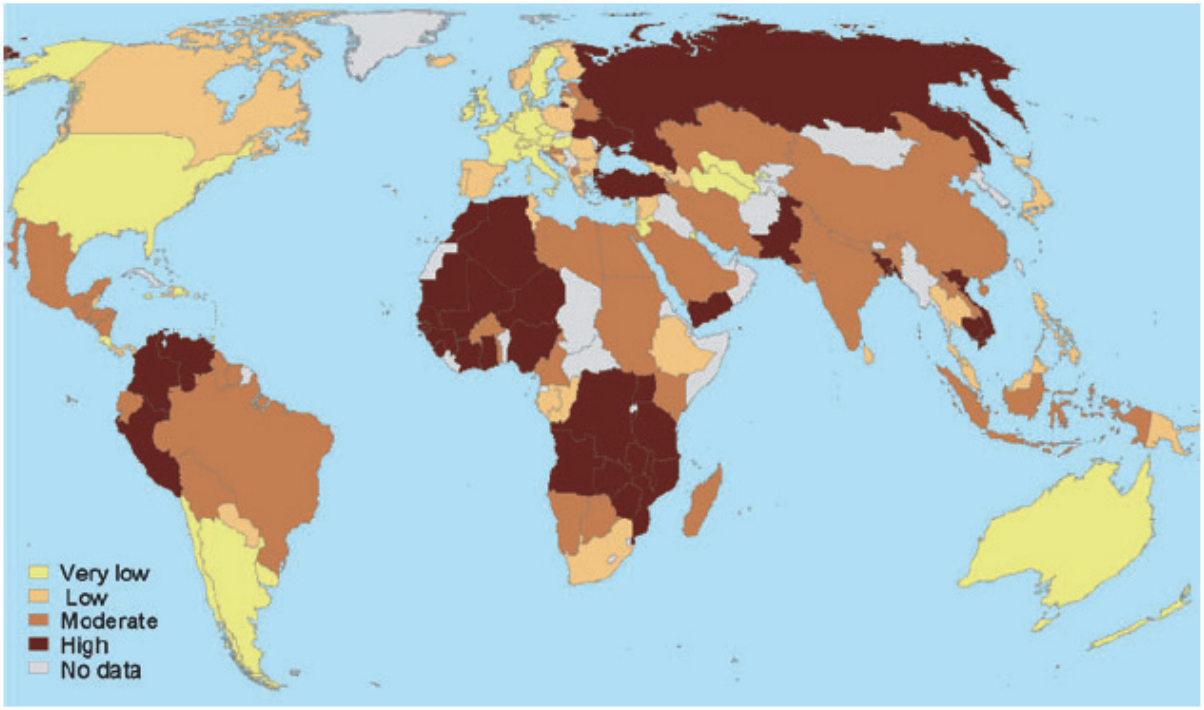

Figure 7. *Vulnerability of national economies to potential climate change impacts on fisheries under SRES B2 (Allison et al., 2009). Colours represent quartiles with dark brown for the upper quartile (highest index value), yellow for the lowest quartile, and grey where no data were available.*

National-scale or sub-national scale assessments

Included in this section are conclusions from national and sub-national studies into the spread of livestock disease, and the impact of adaptation on food security.

Recent past

Livestock products are main sources of food in semi-arid and arid lands of Kenya. While the UN stated that rinderpest (also known as cattle plague or steppe murrain; an infectious viral disease of cattle) was completely irradiated globally in 2011, past examples of this disease and its relation with climate demonstrate important sensitivities to food security in Kenya. For instance, it has been noted that rinderpest returned to East Africa after the failure of vaccine delivery programmes in 2008-2010. This failure was brought about by the return of political unrest in Sudan and continued problems in Somalia, which allowed the disease to spread within those countries and spill over into northern Kenya (ILRI-FAO, 2006). The spread was exacerbated by extended droughts that resulted in significant human and livestock migration south and west out of northern Kenya (ILRI-FAO, 2006).

Climate change studies

Recent work has highlighted the importance of adaptation for maintaining food security under climate change in Kenya. Research suggests that not only can water conservation measures have important beneficial impacts on water storage in the soil profile and hence the length of growing period under current climate conditions, they can also play a major role in helping to manage and ameliorate the impact of future climate change (Cooper et al., 2009, van de Steeg et al., 2009, Rao and Okwach, 2005).

Moreover, Schilling and Remling (2011) note that local options of adaptation to climate change in Kenya are strongly depend on the specific socio economic, cultural and geographical context. While the engagement into tourism can be an attractive source of (additional) income for the Masai in Kajiado (southern Kenya), this would be an unfeasible change of lifestyle for the Turkana in northern Kenya. Schilling and Remling (2011) also argue that it's important that the government assures the pastoralists mobility, particularly during periods of drought. That means that in South Kenya reliable agreements need to be made which enable the pastoralists and their herds to have access to pasture land inside of national parks. In the Northern part of the country agreements need to be made with the neighbouring countries Uganda, Sudan and Ethiopia to protect transnational movements and to mitigate conflicts in this region.

Water stress and drought

Headline

The IPCC AR4 noted potential increases in mean precipitation across East Africa, especially in summer, but some recent work has contradicted this, suggesting the potential for decreased rainfall over Kenya in the future. Recent analysis of Kenya's water resources has shown it is exposed to a high water security threat across its entire area. Future water availability is uncertain, with potential increases in annual runoff masking overall reductions in water availability during certain periods, while studies neglect the lack of infrastructure to store water. Large uncertainties remain, and as such, knowledge is little improved beyond that reported in the IPCC AR4.

Results from the AVOID programme for Kenya indicate that climate change generally could have a minor impact on water stress beyond 2030, based upon the majority of GCM simulations.

Supporting literature

Introduction

For the purposes of this report droughts are considered to be extreme events at the lower bound of climate variability; episodes of prolonged absence or marked deficiency of precipitation. Water stress is considered as the situation where water stores and fluxes (e.g. groundwater and river discharge) are not replenished at a sufficient rate to adequately meet water demand and consumption.

A number of impact model studies looking at water stress and drought for the present (recent past) and future (climate change scenario) have been conducted. These studies are conducted at global or national scale and include the application of global water 'availability' or 'stress' models driven by one or more climate change scenario from one or more GCM. The approaches variously include other factors and assumptions that might affect water availability, such as the impact of changing demographics and infrastructure investment, etc. These different models (hydrological and climate), assumptions and emissions scenarios mean that there are a range of water stress projections for Kenya. This section summarises findings from these studies to inform and contextualise the analysis performed by the AVOID

programme for this project. The results from the AVOID work and discussed in the next section.

Important knowledge gaps and key uncertainties which are applicable to Kenya as well as at the global-scale, include; the appropriate coupling of surface water and groundwater in hydrological models, including the recharge process, improved soil moisture and evaporation dynamics, inclusion of water quality, inclusion of water management (Wood et al. 2011) and further refinement of the down-scaling methodologies used for the climate driving variables (Harding et al. 2011).

Assessments that include a global or regional perspective

Recent Past

Recent research presented by Vörösmarty et al. (2010) describes the calculation of an '*Adjusted Human Water Security Threat'* (HWS) indicator. The indicator is a function of the cumulative impacts of 23 biophysical and chemical drivers simulated globally across 46,517 grid cells representing 99.2 million km^2. With a digital terrain model at its base, the calculations in each of the grid boxes of this model take account of the multiple pressures on the environment, and the way these combine with each other, as water flows in river basins. The level of investment in water infrastructure is also considered. This infrastructure measure (the *investment benefits factor*) is based on actual existing built infrastructure, rather than on the financial value of investments made in the water sector, which is a very unreliable and incomplete dataset. The analysis described by Vörösmarty et al. (2010) represents the current state-of-the-art in applied policy-focussed water resource assessment. In this measure of water security, the method reveals those areas where this is lacking, which is a representation of human water stress. One drawback of this method is that no analysis is provided in places where there is 'no appreciable flow', where rivers do not flow, or only do so for such short periods that they cannot be reliably measured. This method also does not address places where water supplies depend wholly on groundwater or desalination, being piped in, or based on wastewater reuse. It is based on what is known from all verified peer reviewed sources about surface water resources as generated by natural ecosystem processes and modified by river and other hydraulic infrastructure (Vörösmarty et al., 2010).

Here, the present day HWS for Kenya is mapped. The model applied operates at 50km resolution, so, larger countries appear to have smoother coverage than smaller countries, but all are mapped and calculated on the same scale, with the same data and model, and

thus comparisons between places are legitimate. It is important to note that this analysis is a comparative one, where each place is assessed *relative* to the rest of the globe. In this way, this presents a realistic comparison of conditions across the globe. As a result of this, however, some places may seem to be less stressed than may be originally considered. One example is Australia, which is noted for its droughts and long dry spells, and while there are some densely populated cities in that country where water stress is a real issue, for most of the country, *relative to the rest of the world*, the measure suggests water stress (as measured by HWS defined by Vörösmarty et al. (2010)), is not a serious problem.

Figure 8 presents the results of this analysis for Kenya. The only areas where water stress is not recorded in Kenya are in those places where no appreciable flow was recorded and so the area was not included in this analysis. High human population pressure and its associated impacts such as pollution and land degradation, have led to a severe lack of human water security, and high water stress (World Water Assessment Programme, 2006). This confirms that Kenya is a country that is currently suffering water stress.

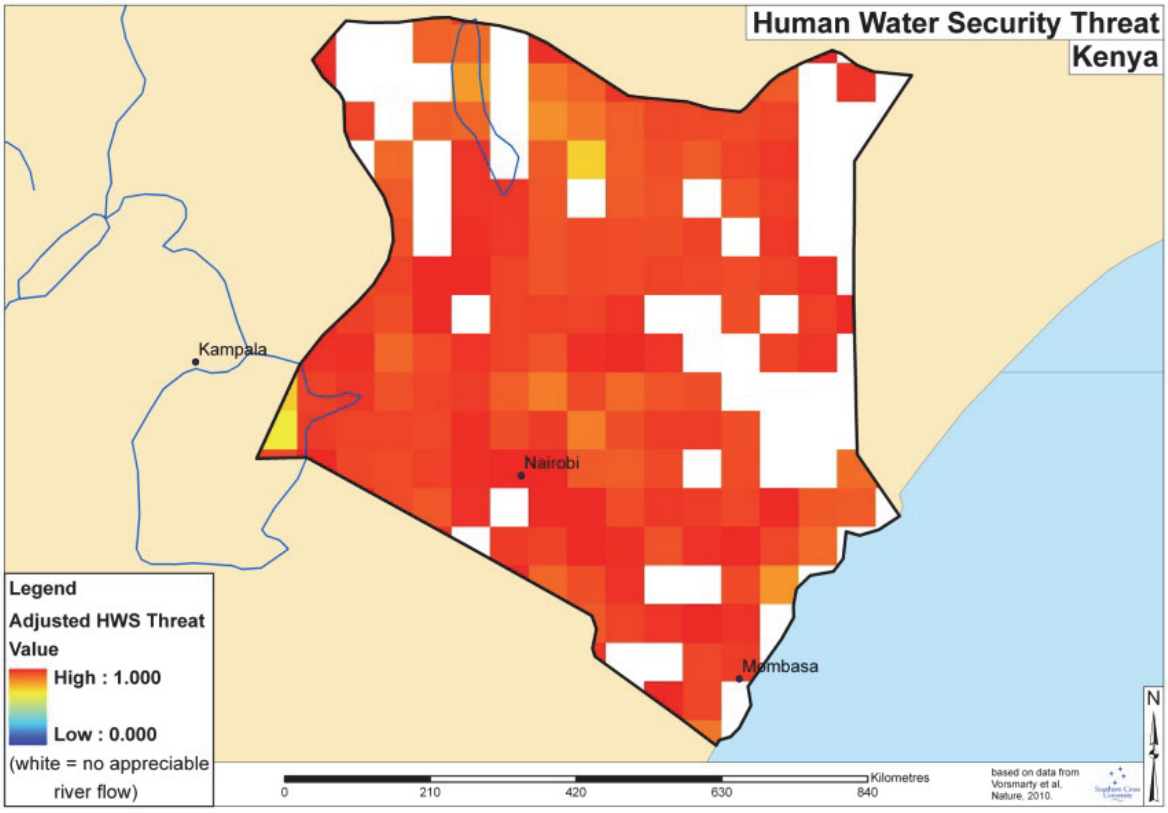

Figure 8. *Present Adjusted Human Water Security Threat (HWS) for Kenya, calculated following the method described by Vörösmarty et al. (2010).*

Climate Change Studies

Rockstrom et al. (2009) applied the LPJml vegetation and water balance model (Gerten et al. 2004) to assess green-blue water (irrigation and infiltrated water) availability and requirements. The authors applied observed climate data from the CRU TS2.1 gridded dataset for a present-day simulation, and climate change projections from the HadCM2 GCM under the SRES A2 scenario to represent the climate change scenario for the year 2050. The study assumed that if water availability was less than 1,300m^3/capita/year, then the country was considered to present insufficient water for food self-sufficiency. The simulations presented by Rockstrom et al.(2009) should not be considered as definitive, however, because the study only applied one climate model, which means climate modelling uncertainty was overlooked. The results from the two simulations are presented in Figure 9. Rockstrom et al. (2009) found that globally in 2050 and under the SRES A2 scenario, around 59% of the world's population could be exposed to "blue water shortage" (i.e. irrigation water shortage), and 36% exposed to "green water shortages" (i.e. infiltrated rain shortage). For Kenya, Rockstrom et al.(2009) found that blue-green water availability was well above the 1,300m^3/capita/year threshold at present and under climate change by 2050. However it is important to note that neighbouring countries are predicted to fall below or close to this threshold, and that national boundaries mask sub-national variation, while annual totals for water resources neglect seasonal variation and lack of storage infrastructure.

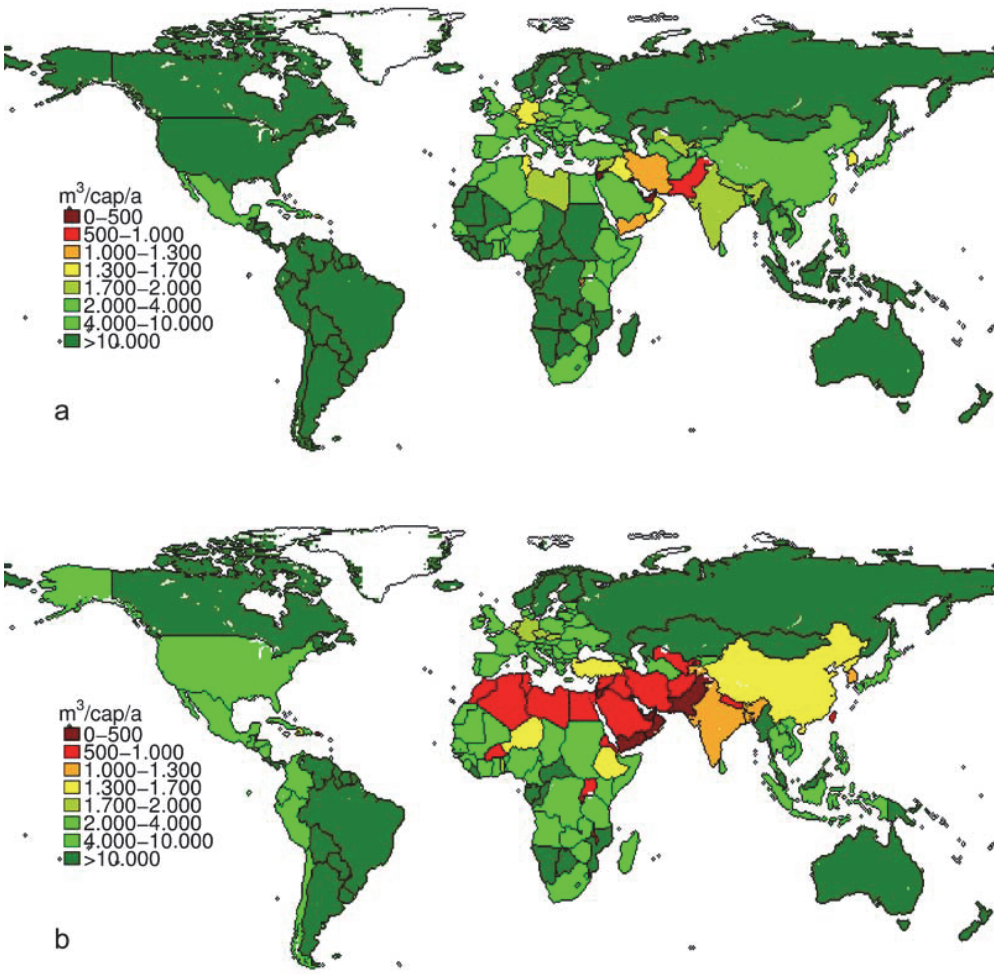

Figure 9. *Simulated blue-green water availability (m^3/capita/year) for present climate (top panel) and including both demographic and climate change under the SRES A2 scenario in 2050 (bottom panel). The study assumed that if water availability was less than 1,300m^3/capita/year, then the country was considered to present insufficient water for food self-sufficiency. The figure is from Rockstrom et al. (2009).*

Doll (2009) presents updated estimates of the impact of climate change on groundwater resources by applying a new version of the WaterGAP hydrological model. The study accounted for the number of people affected by changes in groundwater resources under climate change relative to present (1961-1990). To this end, the study provides an assessment of the vulnerability of humans to decreases in available groundwater resources (GWR). This indicator was termed the "Vulnerability Index" (VI), defined as; VI = -% change GWR * Sensitivity Index (SI). The SI component was a function of three more specific sensitivity indicators that include an indicator of water scarcity (calculated from the ratio between consumptive water use to low flows), an indicator for the dependence upon groundwater supplies, and an indicator for the adaptive capacity of the human system. Doll (2009) applied climate projections from two GCMs (ECHAM4 and HadCM3) to WaterGAP,

for two scenarios (SRES A2 and B2), for the 2050s. Figure 10 presents each of these four simulations respectively. There is variation across scenarios and GCMs but there is consensus that vulnerability is highest in the North African Mediterranean, western regions of South Africa, and north-eastern Brazil. For Kenya, the simulations projected no decreases in GWR with climate change, with the ECHAM4 GCM, but they did for the HadCM3 GCM. To this end, parts of south and eastern Kenya presented medium to high vulnerability, but the study highlights that projections of water stress in Kenya are highly uncertain, due to climate modelling uncertainty.

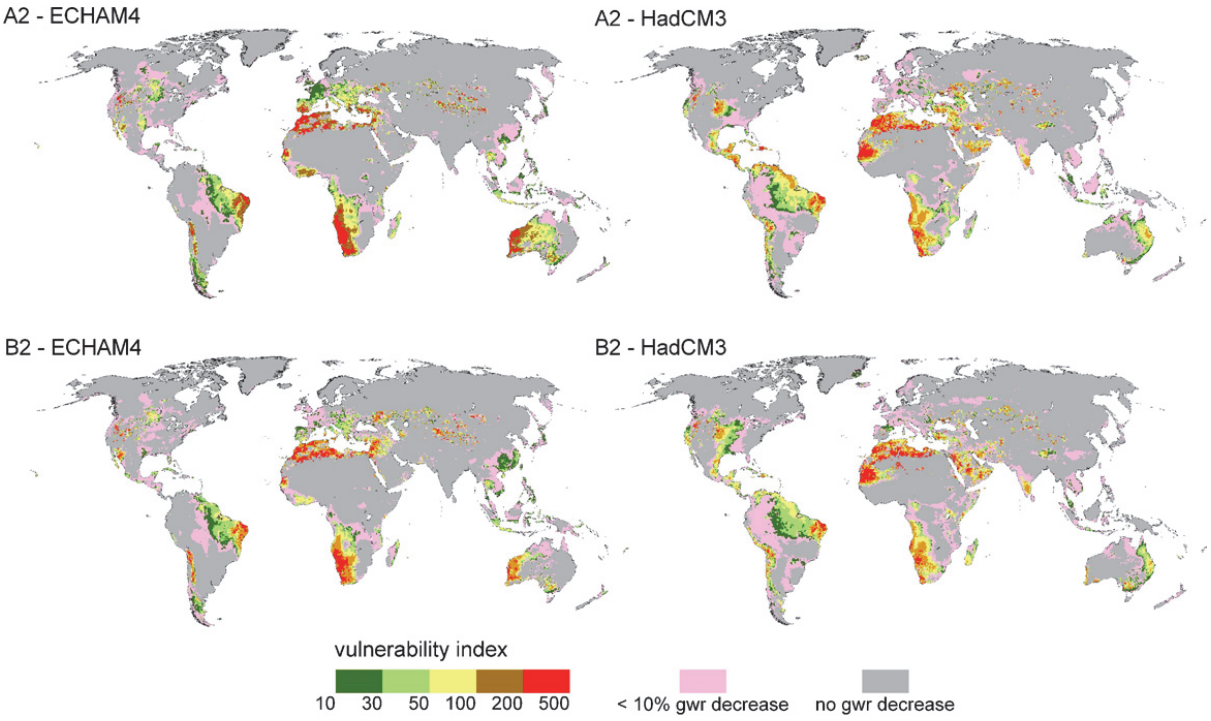

Figure 10. *Vulnerability index (VI) showing human vulnerability to climate change induced decreases of renewable groundwater resources (GWR) by the 2050s under two emissions scenarios for two GCMs. VI is only defined for areas with a GWR decrease of at least 10% relative to present (1961-1990). The figure is from Doll (2009).*

National-scale or sub-national scale assessments

Climate change studies

A report by Funk et al. (2010) highlighted the issue that recent observed rainfall tendencies have been markedly different from the results presented by the IPCC AR4 (2007a). The IPCC indicated that eastern Africa could experience a small increase in summer precipitation of 5-10%, but the work summarised by Funk et al. (2010) suggests this is unlikely. Results from Notter et al. (2007) using the NRM3 streamflow model indicate that total annual runoff will increase with climate change projections from the GCM ECHAM4 by

the period 2040-2069, but that despite this, much of the total increase will be in flood events, and that dry periods are predicted to become more severe and last longer.

There would seem an overall lack of studies post AR4 that assess the impacts of climate change on water resources in Kenya at a national or sub-national scale, despite widespread reporting of increased drought and reduced water availability in the media. Taking data from mapping of global level assessments is also problematic when data resolution and lack of visible national boundaries exists. A number of projects are aimed towards improving the adaptability of Kenya towards possible declines in water availability in the future. For example, the World Bank Adaptation to Climate Change in Arid and Semi-Arid Lands (KACCAL) project (World Bank, 2011) and the National Water Master Plan (Government of Kenya, 2007).

AVOID Programme Results

To further quantify the impact of climate change on water stress and the inherent uncertainties, the AVOID programme calculated water stress indices for all countries reviewed in this literature assessment based upon the patterns of climate change from 21 GCMs, following the method described by Gosling et al. (2010) and Arnell (2004). This ensures a consistent methodological approach across all countries and takes consideration of climate modelling uncertainties.

Methodology

The indicator of the effect of climate change on exposure to water resources stress has two components. The first is the number of people within a region with an *increase in exposure to stress*, calculated as the sum of 1) people living in water-stressed watersheds with a significant reduction in runoff due to climate change and 2) people living in watersheds which become water-stressed due to a reduction in runoff. The second is the number of people within a region with a *decrease in exposure to stress*, calculated as the sum of 1) people living in water-stressed watersheds with a significant increase in runoff due to climate change and 2) people living in watersheds which cease to be water-stressed due to an increase in runoff. It is not appropriate to calculate the net effect of “increase in exposure” and “decrease in exposure”, because the consequences of the two are not equivalent. A water-stressed watershed has an average annual runoff less than $1000m^3$/capita/year, a widely used indicator of water scarcity. This indicator may underestimate water stress in

watersheds where per capita withdrawals are high, such as in watersheds with large withdrawals for irrigation.

Average annual runoff (30-year mean) is simulated at a spatial resolution of 0.5^{o} x0.5^{o} using a global hydrological model, MacPDM (Gosling and Arnell, 2011), and summed to the watershed scale. Climate change has a "significant" effect on average annual runoff when the change from the baseline is greater than the estimated standard deviation of 30-year mean annual runoff: this varies between 5 and 10%, with higher values in drier areas.

The pattern of climate change from 21 GCMs was applied to MacPDM, under two emissions scenarios; 1) SRES A1B and 2) an aggressive mitigation scenario where emissions follow A1B up to 2016 but then decline at a rate of 5% per year thereafter to a low emissions floor (denoted A1B-2016-5-L). Both scenarios assume that population changes through the 21st century following the SRES A1 scenario as implemented in IMAGE 2.3 (van Vuuren et al., 2007). The application of 21 GCMs is an attempt to quantify the uncertainty due to climate modelling, although it is acknowledged that only one impacts model is applied (MacPDM). Simulations were performed for the years 2030, 2050, 2080 and 2100. Following Warren et al. (2010), changes in the population affected by increasing or decreasing water stress represent the additional percentage of population affected due to climate change, not the absolute change in the percentage of the affected population relative to present day.

Results

The results for Kenya are presented in Figure 11. The results show that climate change generally has a minor impact on water stress beyond 2030, based upon the majority of GCM simulations. However, some outliers suggest that up to 20% of Kenya's population could experience an increase in water stress with climate change under the A1B scenario by 2100. This confirms the important role of climate modelling uncertainty in estimates of water stress impacts for Kenya.

The results for the percentage of the population experiencing a decrease in water stress are quite unusual. The same number of models show the same result, post-2050, for both the A1B and the aggressive mitigation scenario. This signal is not necessarily a result of climate change, and could be a feature associated with the way that the model data was processed, or the fact that the driving GCMs behind the impacts model have a relatively low resolution. For this reason, these results should be treated with caution.

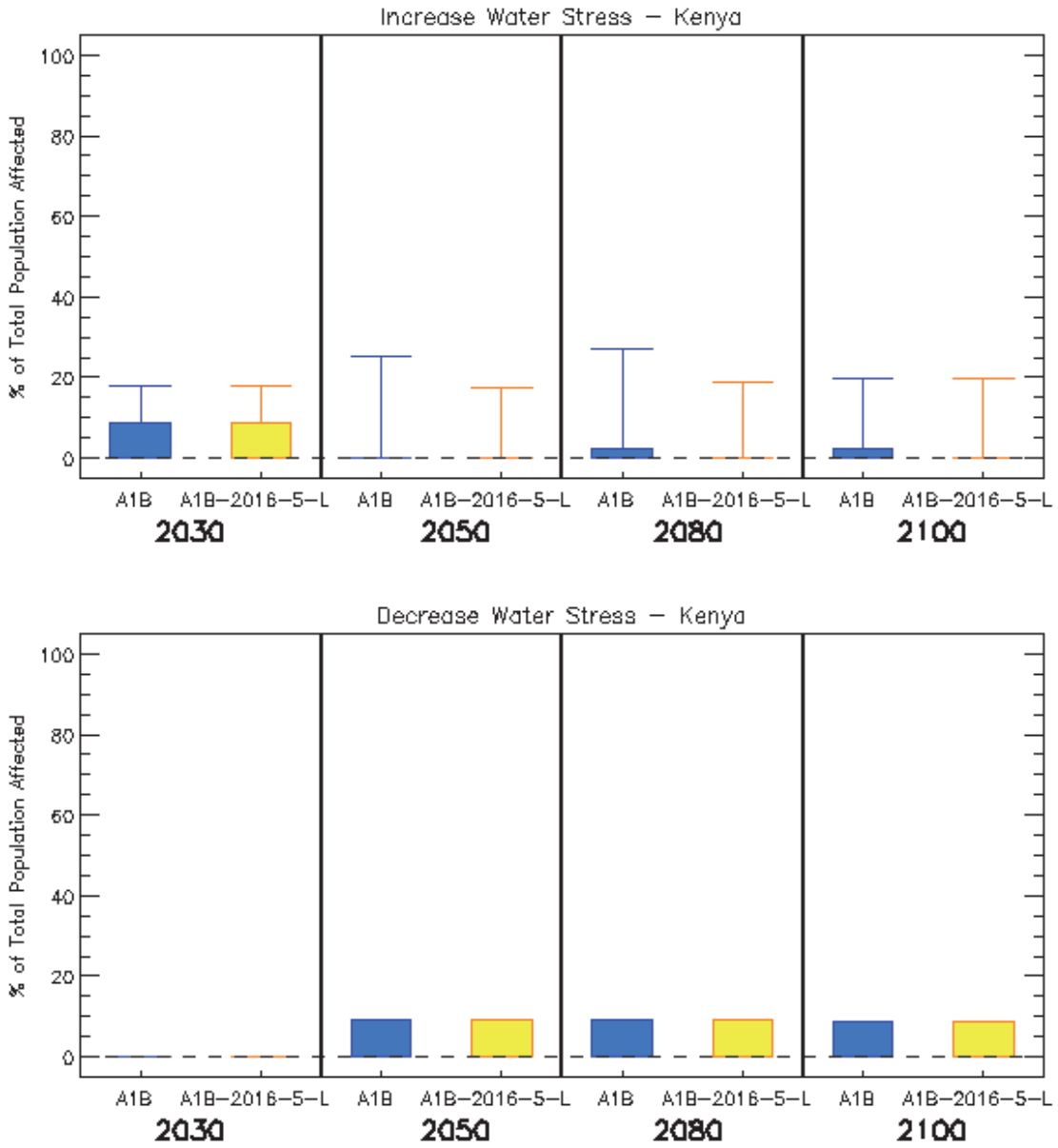

Figure 11. *Box and whisker plots for the impact of climate change on increased water stress (top panel) and decreased water stress (bottom panel) in Kenya, from 21 GCMs under two emissions scenarios (A1B and A1B-2016-5-L), for four time horizons. The plots show the 25th, 50th, and 75th percentiles (represented by the boxes), and the maximum and minimum values (shown by the extent of the whiskers).*

Pluvial flooding and rainfall

Headline

The IPCC AR4 noted potential increases in mean precipitation across East Africa, especially in summer. Some recent work has contradicted this, suggesting the potential for decreased summer rainfall over Kenya in the future. Large uncertainties remain, however, and additional assessments of the impact of future climate change on Kenyan precipitation are needed.

Supporting literature

Introduction

Pluvial flooding can be defined as flooding derived directly from heavy rainfall, which results in overland flow if it is either not able to soak into the ground or exceeds the capacity of artificial drainage systems. This is in contrast to fluvial flooding, which involves flow in rivers either exceeding the capacity of the river channel or breaking through the river banks, and so inundating the floodplain. Pluvial flooding can occur far from river channels, and is usually caused by high intensity, short-duration rainfall events, although it can be caused by lower intensity, longer-duration events, or sometimes by snowmelt. Changes in mean annual or seasonal rainfall are unlikely to be good indicators of change in pluvial flooding; changes in extreme rainfall are of much greater significance. However, even increases in daily rainfall extremes will not necessarily result in increases in pluvial flooding, as this is likely to be dependent on the sub-daily distribution of the rainfall as well as local factors such as soil type, antecedent soil moisture, land cover (especially urbanisation), capacity and maintenance of artificial drainage systems etc. It should be noted that both pluvial and fluvial flooding can potentially result from the same rainfall event.

Assessments that include a global or regional perspective

The IPCC AR4 (2007a) indicates that there is likely to be an increase in mean rainfall in East Africa. This was found to be robust across the ensemble of GCMs applied, with 18 out of 21 models projecting increased precipitation. There was limited research available at the time of publication of the IPCC AR4 on changes in precipitation extremes in the region. General results suggested an increase in high-rainfall events, in common with other regions. In East Africa, the number of extremely wet seasons was projected to increase to approximately

20%, i.e. 1 in 5 seasons could be extremely wet by the end of the 21st century under an A1B scenario, compared with 1 in 20 during the late 20th century (IPCC, 2007a). It is well known that climate models have difficulties representing some of the key processes in east African rainfall, and the spread of the CMIP3 multi-model dataset model projections is quite wide (IPCC, 2007a). Seasonal rainfall is poorly represented, and many models suggest a shift to a more El Niño-like climate, which would suggest enhanced October-November-December rainfall and an usually dry January-February in Kenya.

Funk and Brown (2009) showed that rainfall estimates from a 10-GCM ensemble constrained with observed 1980-2000 SSTs were actually anti-correlated with observed long-season rainfall totals in east Africa. A recent study by Williams and Funk (2011) shows that observations and model simulations link anthropogenic greenhouse gas and aerosol emissions with increasing Indian Ocean SSTs. This has resulted in large-scale circulation changes which have suppressed convection over tropical eastern Africa, and decreased precipitation during the March-May long-rains season.

National-scale or sub-national scale assessments

As mentioned in the section on water stress, a report by Funk et al. (2010) highlighted the issue that recent observed rainfall tendencies have been markedly different from the results presented by the IPCC AR4 (2007a). The IPCC indicated that eastern Africa could experience a small increase in summer precipitation of 5-10%, but the work summarised by Funk et al. (2010) suggests this is unlikely. Moreover, trends in Kenyan rainfall are seasonally and regionally dependent.

Fluvial flooding

Headline

A number of global-scale and catchment-scale assessments are consistent in indicating that flood magnitudes in Kenya could increase with climate change. Simulations by the AVOID programme, based on 21 GCMs, support this, with a large majority of the models showing a tendency for (sometimes very large) increases in flood risk, particularly later in the century and in the A1B scenario.

Supporting literature

Introduction

This section summarises findings from a number of post IPCC AR4 assessments on river flooding in Kenya to inform and contextualise the analysis performed by the AVOID programme for this project. The results from the AVOID work are discussed in the next section.

Fluvial flooding involves flow in rivers either exceeding the capacity of the river channel or breaking through the river banks, and so inundating the floodplain. A complex set of processes is involved in the translation of precipitation into runoff and subsequently river flow (routing of runoff along river channels). Some of the factors involved are; the partitioning of precipitation into rainfall and snowfall, soil type, antecedent soil moisture, infiltration, land cover, evaporation and plant transpiration, topography, groundwater storage. Determining whether a given river flow exceeds the channel capacity, and where any excess flow will go, is also not straightforward, and is complicated by the presence of artificial river embankments and other man-made structures for example. Hydrological models attempt to simplify and conceptualise these factors and processes, to allow the simulation of runoff and/or river flow under different conditions. However, the results from global-scale hydrological modelling need to be interpreted with caution, especially for smaller regions, due to the necessarily coarse resolution of such modelling and the assumptions and simplifications this entails (e.g. a 0.5^{o} grid corresponds to landscape features spatially averaged to around 50-55km for mid- to low-latitudes). Such results provide a consistent, high-level picture, but will not show any finer resolution detail or variability. Smaller-scale or catchment-scale hydrological modelling can allow for more local factors affecting the

hydrology, but will also involve further sources of uncertainty, such as in the downscaling of global climate model data to the necessary scale for the hydrological models. Furthermore, the application of different hydrological models and analysis techniques often makes it difficult to compare results for different catchments.

Assessments that include a global or regional perspective

Climate change studies

A global modelling study presented by Hirabayashi et al. (2008), which applied climate change projections from a single GCM under the A1B emissions scenario, suggests that between 2001 and 2030, the return period of what was a 100-year flood event in the 20th century reduces to less than 60 years in some (mostly southern) parts of Kenya. By the end of the century (2071-2100) this reduces to less than 30 years in most of the country, suggesting that the probability of extreme (and currently rare) flooding events could more than treble. The simulations by Hirabayashi et al. (2008) suggest little change in the seasonality of flooding although there is some tendency for peak flows to occur about 1 month later than currently in some parts of the country. It should be noted, however, that results from studies that have applied only a single climate model or climate change scenario should be interpreted with caution. This is because they do not consider other possible climate change scenarios which could result in a different impact outcome, in terms of magnitude and in some cases sign of change.

National-scale or sub-national scale assessments

Climate change studies

A number of local-scale modelling studies largely confirm the trends described by global-scale assessments. In the Nzoia catchment in western Kenya, Githui et al. (2009) projected an increasing likelihood of flood-like events, which was more pronounced in the 2050s than in the 2020s, and stronger under the A2 emissions scenario than under B2. In the Nyando Basin, also in western Kenya, Taye et al. (2011) projected the peak flows of the Nyando River to generally increase under both the A1B and B1 emissions scenarios. In their simulations, the magnitude of floods with a return period of 10 years increased by a factor 1.2 to 3.8. Different GCMs agreed in projecting an increase in the peak flows even though the magnitudes of change were different. These trends may be further exacerbated by land use changes that have already led to an increase in flood peak discharges and volumes by 16 and 10% respectively in this area (Olang and Furst, 2011). In a modelling study of the Upper Ewaso Ng'iro Basin (Mt. Kenya region) Notter et al. (2007) found that by the middle of

the 21st century (2040-2069) the A2 scenario could be associated with extreme flood flows at the beginning of the year, reaching a multiple of current flood flow amounts. This increase was less extreme under the B2 scenario.

AVOID programme results

To quantify the impact of climate change on fluvial flooding and the inherent uncertainties, the AVOID programme calculated an indicator of flood risk for all countries reviewed in this literature assessment based upon the patterns of climate change from 21 GCMs (Warren et al., 2010). This ensures a consistent methodological approach across all countries and takes consideration of climate modelling uncertainties.

Methodology

The effect of climate change on fluvial flooding is shown here using an indicator representing the percentage change in average annual flood risk within a country, calculated by assuming a standardised relationship between flood magnitude and loss. The indicator is based on the estimated present-day (1961-1990) and future flood frequency curve, derived from the time series of runoff simulated at a spatial resolution of 0.5°x0.5° using a global hydrological model, MacPDM (Gosling and Arnell, 2011). The flood frequency curve was combined with a generic flood magnitude–damage curve to estimate the average annual flood damage in each grid cell. This was then multiplied by grid cell population and summed across a region, producing in effect a population-weighted average annual damage. Flood damage is thus assumed to be proportional to population in each grid cell, not the value of exposed assets, and the proportion of people exposed to flood is assumed to be constant across each grid cell (Warren et al., 2010).

The national values are calculated across major floodplains, based on the UN PREVIEW Global Risk Data Platform (preview.grid.unep.ch). This database contains gridded estimates, at a spatial resolution of 30 arc-seconds (0.00833°x0.00833°), of the estimated frequency of flooding. From this database the proportion of each 0.5°x0.5° grid cell defined as floodplain was determined, along with the numbers of people living in each 0.5°x0.5° grid cell in flood-prone areas. The floodplain data set does not include “small” floodplains, so underestimates actual exposure to flooding. The pattern of climate change from 21 GCMs was applied to MacPDM, under two emissions scenarios; 1) SRES A1B and 2) an aggressive mitigation scenario where emissions follow A1B up to 2016 but then decline at a rate of 5% per year thereafter to a low emissions floor (denoted A1B-2016-5-L). Both scenarios assume that

population changes through the 21st century following the SRES A1 scenario as implemented in IMAGE 2.3 (van Vuuren et al., 2007). The application of 21 GCMs is an attempt to quantify the uncertainty due to climate modelling, although it is acknowledged that only one impacts model is applied (MacPDM). Simulations were performed for the years 2030, 2050, 2080 and 2100. The result represents the change in flood risk due to climate change, not the change in flood risk relative to present day (Warren et al., 2010).

Results

The results for Kenya are presented in Figure 12. By the 2030s, the models project a range of changes in mean fluvial flooding risk over Kenya in both scenarios, with some models projecting decreases and others increases. However, the balance is much more towards higher flood risk, with three quarters of the models projecting an increase. The largest decrease projected for the 2030s is around −20%, while the largest increase is +200%. The mean across all projections is an increase in average annual flood risk of approximately 50%.

By 2100 the balance shifts even more towards increased flood risk in both scenarios, and the difference in projections from the different models also becomes greater. Both these aspects of the results are more pronounced for the A1B scenario than the mitigation scenario. Under the mitigation scenario, a small number of models still project a lower flood risk (down to −30%), but a large majority projects increased flood risk. The mean of all projections under the mitigation scenario is an increase of 100%, but the upper projection is an increase of approximately 450%. Under the A1B scenario, most models project an increased flood risk, but still a few project a decrease (down to −30%). The largest projected increase is over 1500%, with the mean of all projections being an increase in annual average flood risk of approximately 350%.

So for Kenya, the models show a much greater tendency for increasing flood risk, particularly later in the century and particularly in the A1B scenario, with many models showing very large increases. Differences between the model projections are also greater later in the century and particularly for A1B.

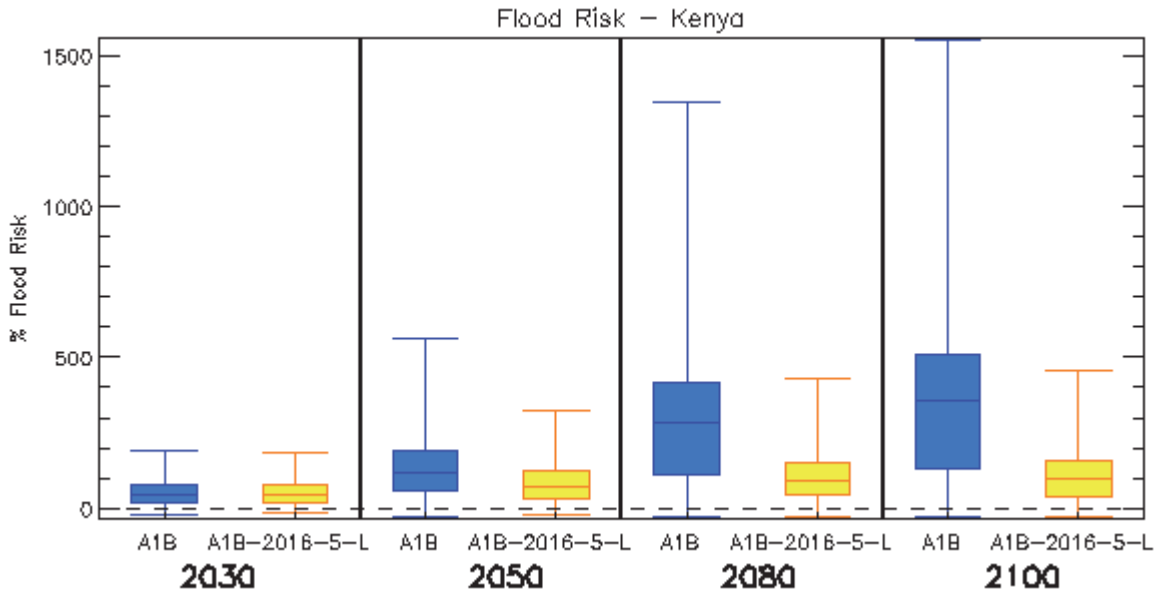

Figure 12. *Box and whisker plots for the percentage change in average annual flood risk within Kenya, from 21 GCMs under two emissions scenarios (A1B and A1B-2016-5-L), for four time horizons. The plots show the 25th, 50th, and 75th percentiles (represented by the boxes), and the maximum and minimum values (shown by the extent of the whiskers).*

Tropical cyclones

Headline

Kenya is occasionally affected by tropical cyclones moving westward from the Indian Ocean. There is considerable uncertainty in projections of overall Indian Ocean cyclone *frequency* and *intensity*, however. Furthermore, there is large uncertainty in projections of the tracks of these cyclones toward a particular country. It is therefore not possible to robustly state whether cyclone damages in Kenya may increase or decrease with climate change.

Introduction

Tropical cyclones are different in nature from those that exist in mid-latitudes in the way that they form and develop. There remains an overall large uncertainty in the current understanding of how tropical cyclones might be affected by climate change because conclusions are based upon a limited number of studies. Moreover, the majority of tropical-cyclone projections are from either coarse-resolution global models or from statistical or dynamical downscaling techniques. The former are unable to represent the most-intense storms, whereas the very patterns used for the downscaling may change in itself under climate change. To this end, caution should be applied in interpreting model-based results, even where the models are in agreement.

Assessments that include a global or regional perspective

Assessment of cyclone frequency

Tropical cyclones moving west from the Indian Ocean occasionally impact Kenya, but such storms are few and far between. Projections of changes in tropical-cyclone frequency in the Indian Ocean are currently highly uncertain, even in the sign of the change. McDonald et al. (2005) applied the Hadley Centre atmospheric model (HadAM3) at 100km resolution, driven by the sea-surface temperature (SST) and sea-ice changes from the HadCM3 GCM under the IPCC IS95a greenhouse-gas emissions scenario for the 2081-2100 time horizon. The authors compared the results of this experiment to a similar one conducted for 1979-1994, but using observed SSTs and sea-ice. The 2081-2100 time horizon showed a 45% increase in the number of tropical cyclones in the North Indian Ocean and a 10% increase in the South Indian Ocean, although only the increase in the North Indian Ocean was statistically significant at the 5% level. The authors attributed the increase in genesis to the projected SST warming in the Indian Ocean being greater than the tropics-mean SST warming. The

model also simulated reduced vertical wind shear, which is conducive to tropical cyclogenesis (cyclone formation), for much of the eastern half of the basin.

Sugi et al. (2002) conducted a similar experiment by applying the Japanese Meteorological Agency (JMA) climate model at 120km resolution and under a $2xCO_2$ emissions scenario. The model simulated a 9% increase in North Indian Ocean tropical cyclone frequencies, but a 57% decrease in the frequency of tropical cyclones in the South Indian Ocean. In a much finer-resolution timeslice experiment (experiments over a short period of time to enable ensemble simulations using reasonable amounts of computational power), Oouchi et al. (2006) applied the JMA climate model at 20km resolution, using mean SSTs and sea ice projections from the Meteorological Research Agency (MRI) GCM for the 2080-2099 time horizon under the A1B emissions scenario. The authors found that North Indian Ocean cyclones decreased in frequency by 52%, while in the South Indian Ocean they decreased in frequency by 28%. The North Indian Ocean decrease was much greater than the 30% global reduction in tropical cyclones simulated by this model. The authors concluded that the decreases were due to increased atmospheric stability in a warmer world; the model simulated a 10% increase in the dry static stability, defined as the difference in potential temperature between the 250hPa level of the atmosphere and the land surface.

In a study restricted to the Northern Hemisphere, Bengtsson et al. (2007) conducted timeslice experiments with the atmospheric component of the ECHAM5 GCM at 60km and 40km resolutions respectively. The model was driven by the SSTs and sea ice simulated by the lower-resolution version of the GCM under the A1B emissions scenario. The authors considered the 2071-2100 time horizon for the 60km simulation and 2081-2100 for the 40km simulation. The two experiments simulated a decrease in North Indian Ocean tropical cyclones, but the magnitudes varied considerably with resolution; the 60km resolution simulation showed a 26% reduction and the 40km resolution simulation showed a 52% decrease. This highlights that even when applying a single climate model, the response of Indian Ocean cyclones to climate change varies considerably.

Zhao et al. (2009) applied the 50km resolution GFDL GCM with four SST and sea ice distributions; 1) the ensemble mean from 18 GCMs, 2) the HadCM3 GCM, 3) the GFDL GCM, and 4) the ECHAM5 GCM. The SSTs distributions were for the A1B emissions scenario for the 2081-2100 time horizon. In all four experiments, the frequencies of cyclones in the North and South Indian Ocean basins decreased. In the former, the magnitudes of the decrease ranged from 2% to 25% (range across all experiments), while in the latter the

range was 13-41%, with three models simulating decreases over 30%. Zhao et al. (2009) reported very high uncertainties in the North Indian Ocean projections, however, due to the low number of observed tropical cyclones in this basin to use for a baseline climate.

Sugi et al. (2009) applied the JMA climate model, driven at 60km and 20km resolutions respectively, with SSTs and sea ice from three individual GCMs as well as the CMIP3 multi-model dataset ensemble mean, for a total of eight simulations, all under the A1B emissions scenario. The North Indian Ocean showed considerable variation in projected tropical-cyclone frequencies, with three experiments simulating large increases (30-80%), one showing little change and four demonstrating substantial decreases (12-39%). Results for the South Indian Ocean were more consistent, with six experiments simulating decreases in frequency (18-28%), one showing little change (5%) and one simulating an increase (10%).

Assessment of cyclone damages

To estimate the impact of climate change on tropical cyclone damages, Mendelsohn et al. (2011) applied four GCMs under the A1B emissions scenario and constructed a damage model to estimate the damages from each landfalling storm. The study applied the "seeding" method described by Emanuel et al. (2008), whereby cyclone-like disturbances are randomly generated in the large-scale environment simulated by a climate model under a climate change scenario. The storms can then grow or decay, as determined by the climate model's atmospheric conditions and the underlying SST. The method employed by Mendelsohn et al. (2011) separates the additional damages from the impact of climate change on tropical cyclones from the additional damages due to future economic development. This is accomplished through applying the damages from both present-day and future tropical cyclones to the projected economic conditions in 2100 (the "future baseline"). Against a future baseline of $25.3 million in damages per year in Kenya, two of the four GCMs considered by Mendelsohn et al. (2011) simulated an increase in cyclone damages; the CNRM GCM ($19.4 million increase) and the ECHAM5 GCM ($12.4 million). The other two GCMs (GFDL and MIROC) simulated virtually no change in damages.

There is therefore great uncertainty in the projections of changes in Indian Ocean cyclone frequencies and to this end little is known about how the tracks of these cyclones across the basin might be affected by climate change. It is therefore not possible to robustly quantify the impacts of climate change on tropical cyclones affecting Kenya, especially as these are relatively rare events.

National-scale or sub-national scale assessments

Literature searches yielded no results for national-scale or sub-national scale studies for this impact sector.

Coastal regions

Headline

A recent study provides new knowledge relative to the IPCC AR4, for coastal impacts in Kenya. A 10% intensification of the current 1-in-100-year storm surge combined with a 1m Sea Level Rise (SLR) could affect around 42% of coastal total land, 22% of coastal agricultural land, 32% of coastal GDP, and 39% of coastal urban areas. Research presented in the first national communication of Kenya to the Conference of the Parties to the United Nations Framework Convention on Climate Change (UNFCCC) also suggests that Kenya is highly vulnerable to SLR, and that impacts could be severe, especially in Mombasa district. However, further research is required to better quantify the effects of climate model and emissions scenario uncertainty on the magnitude of such impacts.

Supporting literature

Assessments that include a global or regional perspective

The IPCC AR4 concluded that at the time, understanding was too limited to provide a best estimate or an upper bound for global SLR in the twenty-first century (IPCC, 2007b). However, a range of SLR, excluding accelerated ice loss effects was published, ranging from 0.19m to 0.59m by the 2090s (relative to 1980-2000), for a range of scenarios (SRES A1FI to B1). The IPCC AR4 also provided an illustrative estimate of an additional SLR term of up to 17cm from acceleration of ice sheet outlet glaciers and ice streams, but did not suggest this is the upper value that could occur. Although there are published projections of SLR in excess of IPCC AR4 values (Nicholls et al., 2011), many of these typically use semi-empirical methods that suffer from limited physical validity and further research is required to produce a more robust estimate. Linking sea level rise projections to temperature must also be done with caution because of the different response times of these two climate variables to a given radiative forcing change.

Nicholls and Lowe (2004) previously showed that mitigation alone would not avoid all of the impacts due to rising sea levels, adaptation would likely be needed too. Recent work by van Vuuren et al. (2011) estimated that, for a world where global mean near surface temperatures reach around 2°C by 2100, global mean SLR could be 0.49m above present levels by the end of the century. Their sea level rise estimate for a world with global mean

temperatures reaching 4°C by 2100 was 0.71m, suggesting around 40% of the future increase in sea level to the end of the 21st century could be avoided by mitigation. A qualitatively similar conclusion was reached in a study by Pardaens et al. (2011), which examined climate change projections from two GCMs. They found that around a third of global-mean SLR over the 21st century could potentially be avoided by a mitigation scenario under which global-mean surface air temperature is near-stabilised at around 2°C relative to pre-industrial times. Under their baseline business-as-usual scenario the projected increase in temperature over the 21st century is around 4°C, and the sea level rise range is 0.29-0.51m (by 2090-2099 relative to 1980-1999; 5% to 95% uncertainties arising from treatment of land-based ice melt and following the methodology used by the IPCC AR4). Under the mitigation scenario, global mean SLR in this study is projected to be 0.17-0.34m.

The IPCC 4th assessment (IPCCa) followed Nicholls and Lowe (2004) for estimates of the numbers of people affected by coastal flooding due to sea level rise. Nicholls and Lowe (2004) projected for the Africa Indian Ocean coast region that an additional 2.2 million people per year could be flooded due to sea level rise by the 2080s relative to the 1990s for the SRES A2 scenario (note this region also includes other countries, such as Mozambique). However, it is important to note that this calculation assumed that protection standards increased as GDP increased, although there is no additional adaptation for sea level rise. More recently, Nicholls et al. (2011) also examined the potential impacts of sea level rise in a scenario that gave around 4°C of warming by 2100. Readings from Figure 3 from Nicholls et al. (2011) for the Africa Indian Ocean region suggest that less than an approximate 5 million additional people could be flooded for a 0.5 m SLR (assuming no additional protection). Nicholls et al. (2011) also looked at the consequence of a 2m SLR by 2100, however as we consider this rate of SLR to have a low probability we don't report these figures here.

A national-scale indicator of the impact of SLR on Kenya is available from a single global-scale assessment, presented by Dasgupta et al. (2009), which facilitates the comparison of impacts for Kenya with other countries across the globe. The results presented by Dasgupta et al. (2009) suggest that Kenya could suffer major negative impacts on coastal agricultural lands, GDP and urban areas. The study considered 84 developing countries with a 10% intensification of the current 1-in-100-year storm surge combined with a prescribed 1m SLR. GIS inundation models were applied in the analysis and the method means that uncertainty associated with the climate system is inherently overlooked. Nevertheless, the projections give a useful indicator of the possible impact of SLR in Kenya. Table 13 shows that whilst

274km^2 of Kenya's coastal population could be affected by SLR, which appears relatively small compared with other countries, when expressed as a proportion of the coastal total population, this is one of the highest impacts observed across the 84 developing countries investigated by Dasgupta et al. (2009) (around 40%). Also, SLR was estimated to affect around 42% of coastal total land, 22% of coastal agricultural land, 32% of coastal GDP, and 39% of coastal urban areas.

To further quantify the impact of SLR and some of the inherent uncertainties, the DIVA model was used to calculate the number of people flooded per year for global mean sea level increases (Brown et al., 2011). The DIVA model (DINAS-COAST, 2006) is an integrated model of coastal systems that combines scenarios of water level changes with socio-economic information, such as increases in population. The study uses two climate scenarios; 1) the SRES A1B scenario and 2) a mitigation scenario, RCP2.6. In both cases an SRES A1B population scenario was used. The results are shown in Table 12.

	A1B		**RCP**	
	Low	**High**	**Low**	**High**
Additional people flooded (1000s)	62.54	223.02	55.21	211.18
Loss of wetlands area (% of country's total wetland)	14.39%	24.78%	11.19%	24.54%

Table 12. *Number of additional people flooded (1000s), and percentage of total wetlands lost by the 2080s under the high and low SRES A1B and mitigation (RCP 2.6) scenarios (Brown et al., 2011).*

National-scale or sub-national scale assessments

Research presented in the first national communication of Kenya to the Conference of the Parties to the United Nations Framework Convention on Climate Change (UNFCC), notes that Kenya's coast is one of the most vulnerable to SLR across the globe (Ministry of Environment and Natural Resources, 2002), which confirms conclusions by Dasgupta et al. (2009). The Kenyan Ministry of Environment and Natural Resources (Ministry of Environment and Natural Resources, 2002) found that around 4,600ha (17% of Mombasa district) could be submerged by a 0.3m SLR, and that another 70,500ha of the district could be made uninhabitable or agriculturally unexploitable. In the Kilifi District, an estimated 0.5%

of the total land area could be submerged under a 0.3m SLR (Ministry of Environment and Natural Resources, 2002).

Country	Incremental Impact: Land Area (sq. km)	Projected Impact as a % of Coastal Total	Incremental Impact: Population	Projected Impact as a % of Coastal Total	Incremental Impact: GDP (mil. USD)	Projected Impact as a % of Coastal Total	Incremental Impact: Agricultural Area (sq. km)	Projected Impact as a % of Coastal Total	Incremental Impact: Urban Extent (sq. km)	Projected Impact as a % of Coastal Total	Incremental Impact: Wetlands (sq. km)	Projected Impact as a % of Coastal Total
Africa												
South Africa	607	43.09	48,140	32.91	174	30.98	70	34.48	93	48.10	132	46.23
Egypt	2,290	13.61	2,600,000	14.68	4,600	16.67	692	5.23	627	15.30	640	28.36
Kenya	274	41.93	27,400	40.23	10	32.05	40	22.13	9	38.89	177	52.51
Americas												
Argentina	2,400	18.03	278,000	19.52	2,240	16.42	157	9.93	313	27.47	459	11.30
Brazil	6,280	15.08	1,100,000	30.37	4,880	28.48	275	16.47	960	33.67	2,590	11.48
Mexico	9,130	29.04	463,000	20.56	2,570	21.22	310	10.89	701	18.35	1,760	52.25
Peru	727	36.69	61,000	46.90	177	46.18	5	26.92	54	42.72	20	37.91
Asia												
China	11,800	17.52	10,800,000	16.67	31,200	17.15	6,640	11.66	2,900	15.70	4,360	39.77
Rep. of Korea	902	61.73	863,000	50.48	10,600	47.86	237	66.75	335	48.15	77	78.81
India	8,690	29.33	7,640,000	28.68	5,170	27.72	3,740	23.64	1,290	30.04	2,510	32.31
Indonesia	14,400	26.64	5,830,000	32.75	7,990	38.71	4,110	26.12	1,280	33.25	2,680	26.97
Saudi Arabia	1,360	41.58	243,000	42.92	2,420	40.60	0	0.00	390	45.85	715	51.04
Bangladesh	4,450	23.45	4,840,000	16.01	2,220	19.00	2,710	17.52	433	18.30	3,890	24.29

Table 13. *The impact of a 1m SLR combined with a 10% intensification of the current 1-in-100-year storm surge. Impacts are presented as incremental impacts, relative to the impacts of existing storm surges. Each impact is presented in absolute terms, then as a percentage of the coastal total; e.g. 9.93% of Argentina's coastal agricultural land is impacted. The table is adapted from a study presented by Dasgupta et al. (2009), which considered impacts in 84 developing countries. Only those countries relevant to this review are presented here and all incremental impacts have been rounded down to three significant figures.*

References

AERTS, J., LASAGE, R., BEETS, W., DE MOEL, H., MUTISO, G., MUTISO, S. & DE VRIES, A. 2007. Robustness of sand storage dams under climate change. *Vadose Zone Journal,* 6**,** 572-580.

AINSWORTH, E. A. & MCGRATH, J. M. 2010. Direct Effects of Rising Atmospheric Carbon Dioxide and Ozone on Crop Yields. *In:* LOBELL, D. & BURKE, M. (eds.) *Climate Change and Food Security.* Springer Netherlands.

ALLISON, E. H., PERRY, A. L., BADJECK, M.-C., NEIL ADGER, W., BROWN, K., CONWAY, D., HALLS, A. S., PILLING, G. M., REYNOLDS, J. D., ANDREW, N. L. & DULVY, N. K. 2009. Vulnerability of national economies to the impacts of climate change on fisheries. *Fish and Fisheries,* 10**,** 173-196.

ARNELL, N., OSBORNE, T., HOOKER, J., DAWSON, T., PERRYMAN, A. & WHEELER, T. 2010. Simulation of AVOIDed impacts on crop productivity and food security. *Work stream 2, Report 17 of the AVOID programme (AV/WS2/D1/R17).*

ARNELL, N. W. 2004. Climate change and global water resources: SRES emissions and socio-economic scenarios. *Global Environmental Change,* 14**,** 31-52.

AVNERY, S., MAUZERALL, D. L., LIU, J. F. & HOROWITZ, L. W. 2011. Global crop yield reductions due to surface ozone exposure: 2. Year 2030 potential crop production losses and economic damage under two scenarios of O_3 pollution. *Atmospheric Environment,* 45**,** 2297-2309.

BENGTSSON, L., HODGES, K. I., ESCH, M., KEENLYSIDE, N., KORNBLUEH, L., LUO, J.-J. & YAMAGATA, T. 2007. How may tropical cyclones change in a warmer climate? *Tellus A,* 59**,** 539-561.

BETTS, R. A., BOUCHER, O., COLLINS, M., COX, P. M., FALLOON, P. D., GEDNEY, N., HEMMING, D. L., HUNTINGFORD, C., JONES, C. D., SEXTON, D. M. H. & WEBB, M. J. 2007. Projected increase in continental runoff due to plant responses to increasing carbon dioxide. *Nature,* 448**,** 1037-1041.

BROWN, S., NICHOLLS, R., LOWE, J.A. and PARDAENS, A. (2011), Sea level rise impacts in 24 countries. Faculty of Engineering and the Environment and Tyndall Centre for Climate Change Research, University of Southampton.

CHAKRABORTY, S. & NEWTON, A. C. 2011. Climate change, plant diseases and food security: an overview. *Plant Pathology,* 60**,** 2-14.

CIA 2011. World Factbook. US Central Intelligence Agency.

COOPER, P., RAO, K., SINGH, P., DIMES, J., TRAORE, P. S., DIXIT, P. & TWOMLOW, S. J. 2009. Farming with current and future climate risk: advancing a 'hypothesis of hope' for rainfed agriculture in the semi-arid tropics. *Journal of SAT Agricultural Research,* 7**,** 1-19.

DASGUPTA, S., LAPLANTE, B., MURRAY, S. & WHEELER, D. 2009. Sea-level rise and storm surges: a comparative analysis of impacts in developing countries. Washington DC, USA: World Bank.

DINAS-COAST Consortium. 2006 DIVA 1.5.5. Potsdam, Germany: Potsdam Institute for Climate Impact Research (on CD-ROM)

DOLL, P. 2009. Vulnerability to the impact of climate change on renewable groundwater resources: a global-scale assessment. *Environmental Research Letters,* 4.

DOLL, P. & SIEBERT, S. 2002. Global modeling of irrigation water requirements. *Water Resources Research*. Vol: 38 Issue: 4. Doi: 10.1029/2001WR000355

DYSZYNSKI, J., DROOGERS, P. & BUTTERFIELD, R. 2009. Climate adaptation economics. Stockholm Environment Institute: Stockholm Environment Institute.

EMANUEL, K., SUNDARARAJAN, R. & WILLIAMS, J. 2008. Hurricanes and Global Warming: Results from Downscaling IPCC AR4 Simulations. *Bulletin of the American Meteorological Society,* 89**,** 347-367.

FALKENMARK, M., ROCKSTRÖM, J. & KARLBERG, L. 2009. Present and future water requirements for feeding humanity. *Food Security,* 1**,** 59-69.

FAO. 2008. *Food and Agricultural commodities production* [Online]. Available: http://faostat.fao.org/site/339/default.aspx [Accessed 1 June 2011].

FAO. 2010. *Food Security country profiles* [Online]. Available: http://www.fao.org/economic/ess/ess-fs/ess-fs-country/en/ [Accessed 1 Sept 2011].

FISCHER, G. 2009. World Food and Agriculture to 2030/50: How do climate change and bioenergy alter the long-term outlook for food, agriculture and resource availability? *Expert Meeting on How to Feed the World in 2050.* Food and Agriculture Organization of the United Nations, Economic and Social Development Department.

FISCHER, G., VELTHUIZEN, H. V., HIZSNYIK, E. & WIBERG, D. 2009. Potentially obtainable yields in the semi-arid tropics. *Global Theme on Agroecosystems Report.* Patancheru: International Crops Research Institute for the Semi-Arid Tropics (ICRISAT).

FUNK, C.C. & BROWN, M.E. 2009. Declining global per capita agricultural production and warming oceans threaten food security. *Food Security* 1:271-289

FUNK, C., EILERTS, G., DAVENPORT, F. & MICHAELSEN, J. 2010. A Climate Trend Analysis of Kenya -August 2010. *U.S. Geological Survey Fact Sheet 2010-3074*.

GERTEN D., SCHAPHOFF S., HABERLANDT U., LUCHT W., SITCH S. 2004 . Terrestrial vegetation and water balance: hydrological evaluation of a dynamic global vegetation model *International Journal Water Resource Development* 286:249–270

GITHUI, F., GITAU, W., MUTUA, F. & BAUWENS, W. 2009. Climate change impact on SWAT simulated streamflow in western Kenya. *International Journal of Climatology,* 29**,** 1823-1834.

GORNALL, J., BETTS, R., BURKE, E., CLARK, R., CAMP, J., WILLETT, K., WILTSHIRE, A. 2010. Implications of climate change for agricultural productivity in the early twenty-first century. *Phil. Trans. R. Soc. B*, DOI: 10.1098/rstb.2010.0158

GOSLING, S., TAYLOR, R., ARNELL, N. & TODD, M. 2011. A comparative analysis of projected impacts of climate change on river runoff from global and catchment-scale hydrological models. *Hydrology and Earth System Sciences,* 15**,** 279–294.

GOSLING, S. N. & ARNELL, N. W. 2011. Simulating current global river runoff with a global hydrological model: model revisions, validation, and sensitivity analysis. *Hydrological Processes,* 25**,** 1129-1145.

GOSLING, S. N., BRETHERTON, D., HAINES, K. & ARNELL, N. W. 2010. Global hydrology modelling and uncertainty: running multiple ensembles with a campus grid. *Philosophical Transactions of the Royal Society A: Mathematical, Physical and Engineering Sciences,* 368**,** 4005-4021.

GOVERNMENT OF KENYA 2007. The State of the Environment Report (2006/7). Kenya: Government of Kenya.

HARDING, R., BEST, M., BLYTH, E., HAGEMANN, D., KABAT, P., TALLAKSEN, L.M., WARNAARS, T., WIBERG, D., WEEDON, G.P., van LANEN, H., LUDWIG, F., HADDELAND, I. 2011. Preface to the "Water and Global Change (WATCH)" special collection: Current knowledge of the terrestrial global water cycle. *Journal of Hydrometeorology*, DOI: 10.1175/JHM-D-11-024.1

HIRABAYASHI, Y., KANAE, S., EMORI, S., OKI, T. & KIMOTO, M. 2008. Global projections of changing risks of floods and droughts in a changing climate. *Hydrological Sciences Journal-Journal Des Sciences Hydrologiques,* 53**,** 754-772.

IFPRI. 2010. *International Food Policy Research Institute (IFPRI) Food Security CASE maps. Generated by IFPRI in collaboration with StatPlanet.* [Online]. Available: www.ifpri.org/climate-change/casemaps.html [Accessed 21 June 2010].

IGLESIAS, A., GARROTE, L., QUIROGA, S. & MONEO, M. 2009. Impacts of climate change in agriculture in Europe. PESETA-Agriculture study. *JRC Scientific and Technical Reports.*

IGLESIAS, A. & ROSENZWEIG, C. 2009. Effects of Climate Change on Global Food Production under Special Report on Emissions Scenarios (SRES) Emissions and Socioeconomic Scenarios: Data from a Crop Modeling Study. Palisades, NY: Socioeconomic Data and Applications Center (SEDAC), Columbia University.

ILRI-FAO 2006. The Future of Livestock in Developing Countries to 2030. *ILRI-FAO Meeting.* Nairobi, Kenya.

IPCC 2007a. Climate Change 2007: The Physical Science Basis. Contribution of Working Group I to the Fourth Assessment Report of the Intergovernmental Panel on Climate Change *In:* SOLOMON, S., QIN, D., MANNING, M., CHEN, Z., MARQUIS, M., AVERYT, K.

B., TIGNOR, M. & MILLER, H. L. (eds.). Cambridge, United Kingdom and New York, NY, USA.

IPCC 2007b. Climate Change 2007: Impacts, Adaptation and Vulnerability. Contribution of Working Group II to the Fourth Assessment Report of the Intergovernmental Panel on Climate Change. *In:* PARRY, M. L., CANZIANI, O. F., PALUTIKOF, J. P., VAN DER LINDEN, P. J. & HANSON, C. E. (eds.). Cambridge, UK.

LATIF, M. & KEENLYSIDE, N. S. 2009. El Nino/Southern Oscillation response to global warming. *Proceedings of the National Academy of Sciences of the United States of America,* 106**,** 20578-20583.

LOBELL, D. B., BURKE, M. B., TEBALDI, C., MASTRANDREA, M. D., FALCON, W. P. & NAYLOR, R. L. 2008. Prioritizing climate change adaptation needs for food security in 2030. *Science,* 319**,** 607-610.

LOBELL, D. B., SCHLENKER, W. & COSTA-ROBERTS, J. 2011. Climate Trends and Global Crop Production Since 1980. *Science*.

LUCK, J., SPACKMAN, M., FREEMAN, A., TRE¸BICKI, P., GRIFFITHS, W., FINLAY, K. & CHAKRABORTY, S. 2011. Climate change and diseases of food crops. *Plant Pathology,* 60**,** 113-121.

MCDONALD, R. E., BLEAKEN, D. G., CRESSWELL, D. R., POPE, V. D. & SENIOR, C. A. 2005. Tropical storms: representation and diagnosis in climate models and the impacts of climate change. *Climate Dynamics,* 25**,** 19-36.

MENDELSOHN, R., EMANUEL, K. & CHONABAYASHI, S. 2011. The Impact of Climate Change on Global Tropical Cyclone Damages.

MINISTRY OF ENVIRONMENT AND NATURAL RESOURCES 2002. Kenya. First national communication of Kenya to the Conference of the Parties to the United Nations Framework Convention on Climate Change (UNFCCC). Nairobi.

NELSON, G. C., ROSEGRANT, M. W., KOO, J., ROBERTSON, R., SULSER, T., ZHU, T., RINGLER, C., MSANGI, S., PALAZZO, A., BATKA, M., MAGALHAES, M., VALMONTE-SANTOS, R., EWING, M. & LEE, D. 2009. Climate change. Impact on Agriculture and Costs of Adaptation. Washington, D.C.: International Food Policy Research Institute.

NELSON, G. C., ROSEGRANT, M. W., PALAZZO, A., GRAY, I., INGERSOLL, C., ROBERTSON, R., TOKGOZ, S., ZHU, T., SULSER, T. & RINGLER, C. 2010. Food Security, Farming and Climate Change to 2050. *Research Monograph, International Food Policy Research Institute.* Washington, DC.

NICHOLLS, R. J. and LOWE, J. A. (2004). "Benefits of mitigation of climate change for coastal areas." *Global Environmental Change* **14**(3): 229-244.

NICHOLLS, R. J., MARINOVA, N., LOWE, J. A., BROWN, S., VELLINGA, P., DE GUSMÃO, G., HINKEL, J. and TOL, R. S. J. (2011). "Sea-level rise and its possible impacts given a 'beyond 4◦C world' in the twenty-first century." *Philosophical Transactions of the Royal Society A* **369**: 1-21.

NOTTER, B., MACMILLAN, L., VIVIROLI, D., WEINGARTNER, R. & LINIGER, H. P. 2007. Impacts of environmental change on water resources in the Mt. Kenya region. *Journal of Hydrology,* 343**,** 266-278.

OLANG, L. O. & FURST, J. 2011. Effects of land cover change on flood peak discharges and runoff volumes: model estimates for the Nyando River Basin, Kenya. *Hydrological Processes,* 25**,** 80-89.

OOUCHI, K., YOSHIMURA, J., YOSHIMURA, H., MIZUTA, R., KUSUNOKI, S. & NODA, A. 2006. Tropical Cyclone Climatology in a Global-Warming Climate as Simulated in a 20 km-Mesh Global Atmospheric Model: Frequency and Wind Intensity Analyses. *Journal of the Meteorological Society of Japan,* 84**,** 259-276.

PARDAENS, A. K., LOWE, J., S, B., NICHOLLS, R. & DE GUSMÃO, D. 2011. Sea-level rise and impacts projections under a future scenario with large greenhouse gas emission reductions. *Geophysical Research Letters,* 38**,** L12604.

PARRY, M. L., ROSENZWEIG, C., IGLESIAS, A., LIVERMORE, M. & FISCHER, G. 2004. Effects of climate change on global food production under SRES emissions and socio-economic scenarios. *Global Environmental Change-Human and Policy Dimensions,* 14**,** 53-67.

RAHMSTORF, S. 2010. A new view on sea level rise. *Nature Reports Climate Change,* 4**,** 44-45.

RAMANKUTTY, N., EVAN, A. T., MONFREDA, C. & FOLEY, J. A. 2008. Farming the planet: 1. Geographic distribution of global agricultural lands in the year 2000. *Global Biogeochemical Cycles,* 22**,** GB1003.

RAMANKUTTY, N., FOLEY, J. A., NORMAN, J. & MCSWEENEY, K. 2002. The global distribution of cultivable lands: current patterns and sensitivity to possible climate change. *Global Ecology and Biogeography,* 11**,** 377-392.

RAO, K. P. C. & OKWACH, G. E. 2005. Enhancing productivity of water under variable climate. International Water Management Institute.

REICHLER, T. & KIM, J. 2008. How well do coupled models simulate today's climate? *Bulletin of the American Meteorological Society,* 89**,** 303-+.

ROCKSTRÖM, J., FALKENMARK, M., KARLBERG, L., HOFF, H., ROST, S. & GERTEN, D. 2009. Future water availability for global food production: The potential of green water for increasing resilience to global change. *Water Resources Research,* 45.

SAJI, N. H., GOSWAMI, B. N., VINAYACHANDRAN, P. N. & YAMAGATA, T. 1999. A dipole mode in the tropical Indian Ocean. *Nature,* 401**,** 360-363.

SCHILLING, J. & REMLING, E. 2011. Local Adaptation and National Climate Change Policy in Kenya: Discrepancies, Options, and the Way Forward. Hamburg: Universität Hamburg.

SUGI, M., MURAKAMI, H. & YOSHIMURA, J. 2009. A reduction in global tropical cyclone frequency due to global warming. *SOLA,* 5**,** 164-167.

SUGI, M., NODA, A. & SATO, N. 2002. Influence of the Global Warming on Tropical Cyclone Climatology: An Experiment with the JMA Global Model. *Journal of the Meteorological Society of Japan,* 80**,** 249-272.

TATSUMI, K., YAMASHIKI, Y., VALMIR DA SILVA, R., TAKARA, K., MATSUOKA, Y., TAKAHASHI, K., MARUYAMA, K. & KAWAHARA, N. 2011. Estimation of potential changes in cereals production under climate change scenarios. *Hydrological Processes,*Special Issue: Japan Society of Hydrology and water resources, 25 (17), 2715-2725

TAYE, M. T., NTEGEKA, V., OGIRAMOI, N. P. & WILLEMS, P. 2011. Assessment of climate change impact on hydrological extremes in two source regions of the Nile River Basin. *Hydrology and Earth System Sciences,* 15**,** 209-222.

THORNTON, P. K., JONES, P. G., ERICKSEN, P. J. & CHALLINOR, A. J. 2011. Agriculture and food systems in sub-Saharan Africa in a 4°C+ world. *Philosophical Transactions of the Royal Society A: Mathematical, Physical and Engineering Sciences,* 369**,** 117-136.

VAN DE STEEG, J., HERRERO, M., KINYANGI, J., THORNTON, P., RAO, K., STERN, R. & COOPER, P. 2009. The influence of current and future climate-induced risk on the agricultural sector in East and Central Africa. *Sensitizing the ASARECA strategic plan to climate change.* Nairobi, Kenya: ICRISAT (International Crop Research Institute for the Semi-Arid Tropics) and ASARECA (Association for Strengthening Agricultural Research in Eastern and Central Africa).

VAN VUUREN, D., DEN ELZEN, M., LUCAS, P., EICKHOUT, B., STRENGERS, B., VAN RUIJVEN, B., WONINK, S. & VAN HOUDT, R. 2007. Stabilizing greenhouse gas concentrations at low levels: an assessment of reduction strategies and costs. *Climatic Change,* 81**,** 119-159.

VAN VUUREN, D. P., ISAAC, M., KUNDZEWICZ, Z. W., ARNELL, N., BARKER, T., CRIQUI, P., BERKHOUT, F., HILDERINK, H., HINKEL, J., HOF, A., KITOUS, A., KRAM, T., MECHLER, R. & SCRIECIU, S. 2011. The use of scenarios as the basis for combined assessment of climate change mitigation and adaptation. *Global Environmental Change,* 21**,** 575-591.

VÖRÖSMARTY, C. J., MCINTYRE, P. B., GESSNER, M. O., DUDGEON, D., PRUSEVICH, A., GREEN, P., GLIDDEN, S., BUNN, S. E., SULLIVAN, C. A., LIERMANN, C. R. & DAVIES, P. M. 2010. Global threats to human water security and river biodiversity. *Nature,* 467**,** 555-561.

WILLIAMS, A. & FUNK, C. 2011. A westward extension of the warm pool leads to a westward extension of the Walker circulation, drying eastern Africa. *Climate Dynamics***,** 1-19.

WOOD, E.F., ROUNDY, J.K., TROY, T.J., van BEEK, L.P.H., BIERKENS, M.F.P., BLYTH, E., de ROO, A., DOLL, P., EK, M., FAMIGLIETTI, J., GOCHIS, D., van de GIESEN, N., HOUSER, P., JAFFE, P.R., KOLLET, S., LEHNER, B., LETTENMAIER, D.P., PETERS-LIDARD, C., SIVAPALAN, M., SHEFFIELD, J., WADE, A. & WHITEHEAD, P. 2011. Hyperresolution global land surface modelling: Meeting a grand challenge for monitoring Earth's terrestrial water. *Water Resources Research,* 47, W05301.

WORLD BANK. 2011. *Adaptation to Climate Change in Arid and Semi-Arid Lands (KACCAL)* [Online]. Available: http://web.worldbank.org/external/projects/main?pagePK=64283627&piPK=73230&theSitePK=40941&menuPK=228424&Projectid=P091979 [Accessed September 2011].

WORLD WATER ASSESSMENT PROGRAMME 2006. 'Water: A shared responsibility' - Prepared for the 2nd UN World Water Development Report - Case Study: Kenya. *Kenya National Water Development Report.* UNESCO.

WOS. 2011. *Web of Science* [Online]. Available: http://thomsonreuters.com/products_services/science/science_products/a-z/web_of_science [Accessed August 2011].

WU, W., TANG, H., YANG, P., YOU, L., ZHOU, Q., CHEN, Z. & SHIBASAKI, R. 2011. Scenario-based assessment of future food security. *Journal of Geographical Sciences,* 21**,** 3-17.

ZHAO, M., HELD, I. M., LIN, S.-J. & VECCHI, G. A. 2009. Simulations of Global Hurricane Climatology, Interannual Variability, and Response to Global Warming Using a 50-km Resolution GCM. *Journal of Climate,* 22**,** 6653.0

Acknowledgements

Funding for this work was provided by the UK Government Department of Energy and Climate Change, along with information on the policy relevance of the results.

The research was led by the UK Met Office in collaboration with experts from the University of Nottingham, Walker Institute at the University of Reading, Centre for Ecology and Hydrology, University of Leeds, Tyndall Centre — University of East Anglia, and Tyndall Centre — University of Southampton.

Some of the results described in this report are from work done in the AVOID programme by the UK Met Office, Walker Institute at the University of Reading, Tyndall Centre — University of East Anglia, and Tyndall Centre — University of Southampton.

The AVOID results are built on a wider body of research conducted by experts in climate and impact models at these institutions, and in supporting techniques such as statistical downscaling and pattern scaling.

The help provided by experts in each country is gratefully acknowledged — for the climate information they suggested and the reviews they provided, which enhanced the content and scientific integrity of the reports.

The work of the independent expert reviewers at the Centre for Ecology and Hydrology, University of Oxford, and Fiona's Red Kite Climate Consultancy is gratefully acknowledged.

Finally, thanks go to the designers, copy editors and project managers who worked on the reports.

Met Office
FitzRoy Road, Exeter
Devon, EX1 3PB
United Kingdom

Tel: 0870 900 0100
Fax: 0870 900 5050
enquiries@metoffice.gov.uk
www.metoffice.gov.uk

Produced by the Met Office.